Summer 2010

Sediment-size analysis, nitrate monitoring, bathymetric mapping and construction of a two-dimensional hydrodynamic model of a backwater region of the Upper Mississippi River System 2008-2009

Nathan Anderson Quarderer
University of Iowa

SEDIMENT-SIZE ANALYSIS, NITRATE MONITORING, BATHYMETRIC MAPPING AND CONSTRUCTION OF A TWO-DIMENSIONAL HYDRODYNAMIC MODEL OF A BACKWATER REGION OF THE UPPER MISSISSIPPI RIVER SYSTEM 2008 – 2009

by

Nathan Anderson Quarderer

A thesis submitted in partial fulfillment
of the requirements for the
Master of Science degree in Civil and Environmental Engineering
in the Graduate College of
The University of Iowa

July, 2010

Thesis Supervisors: Adjunct Assistant Professor Douglas Schnoebelen
Professor Larry Weber

Graduate College
The University of Iowa
Iowa City, Iowa

CERTIFICATE OF APPROVAL

_____

MASTER'S THESIS

_____

This is to certify that the Master's thesis of

Nathan Anderson Quarderer

has been approved by the Examining Committee for the thesis requirement for the Master of Science degree in Civil and Environmental Engineering at the July 2010 graduation.

Thesis Committee: _____
Douglas Schnoebelen, Thesis Supervisor

_____
Larry Weber, Thesis Supervisor

_____
E. Arthur Bettis III

_____
William Eichinger

ABSTRACT

In April 2008, the non-profit organization Living Lands & Waters (LL&W) approached IIHR–Hydroscience and Engineering to assist with the preliminary scoping and assessment for the proposed dredging and restoration of the backwater region located near the confluence of the Iowa and Mississippi Rivers, commonly referred to as Boston Bay. IIHR was responsible for the measurement and analysis of relevant physical and chemical parameters including particle-size analysis of sediment cores; real-time monitoring of nitrate-nitrogen concentration of agricultural runoff entering Boston Bay; bathymetric surveying; as well as the development of a two-dimensional hydrodynamic capable of simulating the proposed dredging activity.

Particle-size analysis was achieved using the hydrometer method of sedimentation to determine the distribution of fine particles (silt and clay) while traditional sieving techniques were employed to establish the proportions of sand-sized particles. Results indicate that the sediment contained in Boston Bay consists primarily of particles with diameters in the range of 2-50 μm, what the USDA considers silt, and clay.

A real-time nitrate-nitrogen sensor was deployed at the Bay Island Drainage & Levee District pump intake from October 2008, through June 2009. The data collected, coupled with the daily maintenance logs from the pumping station, allow one to estimate that roughly 800 tons of nitrate-nitrogen were pumped into Boston Bay from the drainage district during the time period that the nitrate sensor was deployed in the field.

Bathymetric surveying took place in March, 2009. Survey results indicate that the average elevation of Boston Bay is 531.9 feet above sea level (MSL, 1912). Overall, the bay is very flat with little topographic relief except in the areas of Bell's Pocket and the pond where the drainage district pumps discharge. These areas are

much deeper than other areas of the bay, with elevations as low as 508 feet above sea level in the deepest regions.

A two-dimensional hydrodynamic model of the bay (pre- and post-dredge) was constructed using the US Bureau of Reclamation's SRH-W modeling package. Initial results indicate that dredging Boston Bay does not appear to have detrimental impacts on the existing hydrology of the study area. Model outputs reveal that dredging will create greater availability of deep-water regions, with increased areas of faster moving current. The total area of inundation will also be affected by dredging, perhaps creating ideal habitat for hardwood tree species in portions of the study area that would otherwise be wet under existing conditions. Further studies should be conducted to couple the data obtained during particle-size analysis, with the model results to help estimate the feasibility of the proposed dredging activity and lifetime of the excavated channels.

TABLE OF CONTENTS

LIST OF TABLES

LIST OF FIGURES

CHAPTER 1 – INTRODUCTION

1.1 – Backwater Regions of the Upper Mississippi River System

The Upper Mississippi River System (UMRS) is a large river ecosystem consisting of a spatially complex network of pools, channels, and backwater areas. The hydrodynamics of this system are controlled to a large extent by a series of navigation dams built in the 1930's to aid barge traffic. The reaches between the dams of the UMRS, commonly referred to as 'pools,' contain a main navigation channel connected by shallower side-channels to backwater areas (shallow lakes, wetlands, and islands). The backwaters of the UMRS are essential in supporting a variety of habitats, affording areas for nutrient processing and acting as sinks for sediment storage. Backwaters serve as an ideal habitat for various plant species, invertebrates, popular sport fishes, migratory waterfowl, shorebirds, wading birds, reptiles and amphibians, while also providing quiet places off the main channel where animals and humans alike can seek refuge (U.S. Army Corps of Engineers [USACE], 2006a).

In addition to providing suitable habitat for native plant and animal species, backwaters also act as nutrient retention mechanisms. The shallow backwaters of large river systems such as the UMRS support abundant submersed and emergent macrophyte growth with attached microbial communities and accrete anaerobic organic sediments capable of accommodating bacterial denitrification (Phipps and Crumpton, 1994; Mitsch and Day, 2006; Strauss, et al., 2006; Bukaveckas, 2007; James, et. al, 2008b).

Prior to European settlement of the Upper Mississippi River (UMR) valley, these backwater regions thrived in response to the natural ebb and flow of the main channel of the river. However, as settlers began to use the Mississippi for

transportation of goods and services, the river and the surrounding floodplain became forever altered from its natural condition. As early as 1824, the federal government initiated navigational improvements on the UMR. The work consisted of removing snags, shoals, and sandbars, excavating rock to eliminate rapids, and closing-off backwaters to confine flows to the main channel. These activities helped create adequate depths for navigation during periods of low-water flow (Chen and Simons, 1986).

Development and management of floodplain lands requires flood control, and levees have often been constructed so that flooding is nearly eliminated (Dister, et al, 1990). These activities tend to reduce or eliminate backwater habitats like side-arm channels, sloughs, oxbow lakes and inundated floodplains, replacing them with more uniform terrestrial habitats and main channel or reservoir pools (Gore and Shields, 1995). Such is the case with the UMRS where the most significant change to the river (and the floodplain backwaters) occurred after 1930 following the passage of the River and Harbor Act which authorized the construction of the lock and dam systems currently in place along with the introduction of the nine-foot (ft) navigation channel (Theiling, 1998; USACE, 2006b). While initial construction of the navigation channel produced great aquatic capacity in the newly created shallow backwater wetlands, productivity has declined as sediment from the surrounding upland regions has accumulated in backwater areas (Damberg and Davis, 1994). The lock and dam system has also stabilized water levels, eliminating the abiotic controls (i.e., flooding and drying) that had previously helped to maintain highly productive river floodplain habitats (Chen and Simons, 1986; Machesky, et al., 2005; Theiling, 1998; USACE, 2006b; Wisconsin Department of Natural Resources [DNR], 2009;).

The ecological integrity of many UMRS backwaters has continually degraded over time due to excessive amounts of sediment emanating from the basin,

tributaries, and main stem sources. This degradation is in the form of loss of depth, poor sediment quality, poor water quality, and sediment re-suspension that blocks sunlight required by aquatic plants (Bhowmik and Demissie, 1989; USACE, 2006a). Fish habitat quality has also decreased in backwater areas especially during the winter when such locations could provide refuge from harsh conditions in main channel areas (USACE, 2006a).

1.2 – Restoration of Backwater Regions

As backwater regions continue to degrade due to increasing sedimentation rates and decreased connectivity with the main river channel, careful attention must be paid to their maintenance and restoration. In 1986, Congress passed the Water Resources Development Act, recognizing the UMRS as "a nationally significant ecosystem and a nationally significant commercial navigation system" and declared that "the system shall be administered and regulated in recognition of its several purposes" (108th Congress, 1986). The WRDA authorized many ecosystem restoration projects -- including rehabilitation of degraded backwater systems -- where an attempt is made to direct biological and geohydrological processes toward an endpoint at or near pre-disturbance conditions (Gore and Shields, 1995).

One solution to the sedimentation problem in backwaters is dredging. The removal of sediment by dredging commonly consists of creating channels with fingers (dredged channels extending out away from the main dredge cut) to improve flow and aquatic habitat. The added bathymetric relief serves to provide habitat for fish species dependant on deep-water environments. The sediment spoils dredged from backwater areas can also be used to enhance aquatic areas with islands, or terrestrial areas with increased elevation which promotes the growth of hardwood tree species. (Berry and Anderson, 1986; USACE, 2006a).

Another proposed method to assist in backwater restoration techniques involves river diversion techniques which redirect flows into isolated wetlands and adjacent off-channel regions (Mitsch and Day, 2006; Lane, et al., 2003). This method has proven successful for watersheds in Illinois and Ohio where flows diverted into degraded wetlands act to revitalize deteriorating ecosystems. It has been shown that these regions can act as sinks for nitrate-nitrogen, capable of significantly reducing nitrate concentrations (Phipps and Crumpton, 1994). Similar efforts have also resulted in increased wildlife benefits including migratory bird habitat (USFWS, 2009). Studies indicate that the populations of breeding bird species have dramatically increased following wetland restoration (Hickman, 1994; O'Neal, et al., 2008).

As the practice of river restoration continues to grow, the need to develop a sound scientific basis is obvious, as evidenced by the number of working groups and policy initiatives devoted to the topic. These include the federal government (USACE, U.S. Geological Survey Long Term Resource Monitoring Program and Interagency River Science Network, USFWS), state governments, nongovernmental organizations (Nature Conservancy, National Audubon Society and American Rivers) and academia (Whol, et al, 2005). However, despite legal mandates, massive expenditures and the burgeoning industry of aquatic and riparian restoration, large river backwater systems continue to deteriorate as a result of human activity (Karr and Chu, 1999; Whol, et al, 2005).

1.3 – Purpose and Scope

As part of the broader effort to restore backwater systems of the UMRS, the non-profit organization Living Lands & Waters (LL&W) of Moline, Illinois was interested in the potential for the restoration of a 650-acre backwater in Pool 18 of

the UMRS near New Boston, Illinois. This backwater, commonly referred to as 'Boston Bay,' is located four miles downstream from Lock and Dam #17, adjacent to the confluence of the Iowa and Mississippi Rivers (Figure 1). As is the case with many backwater systems of the UMRS, Boston Bay has degraded over time due to increased sedimentation from upland watersheds, and the controlled water-surface elevation necessary to maintain successful navigation in the main channel. The Boston Bay study area had been identified by the USACE as a site of potential improvement for a backwater area and research on the hydrology and sediment of the area was needed for potential site investigation.

In an attempt to help restore the ecological integrity of Boston Bay while also providing overwintering habitat for native fish species, LL&W has proposed that certain areas of the bay be dredged. The dredged material would then be used to create a network of berms and ridges throughout the study area that would help generate the topographic diversity necessary for mast-producing trees like oak and hickory to survive in a region that experiences annual flooding (Robertson, 2008).

Before a project of this magnitude can proceed as planned, the initial scoping process required the collection and review of the relevant physical and chemical parameters including grain-size analysis of bed material obtained through sediment coring, and water quality monitoring of agricultural runoff entering Boston Bay from an adjacent agricultural drainage district. Additionally, a bathymetric survey must be conducted to obtain the existing elevation profile of the study area while also serving to calibrate a two-dimensional (2D) hydrodynamic model capable of simulating the proposed dredging activity. Collectively, these data will be used to assist interested parties as they begin to assess the feasibility of restoring Boston Bay to its pre-lock and dam condition.

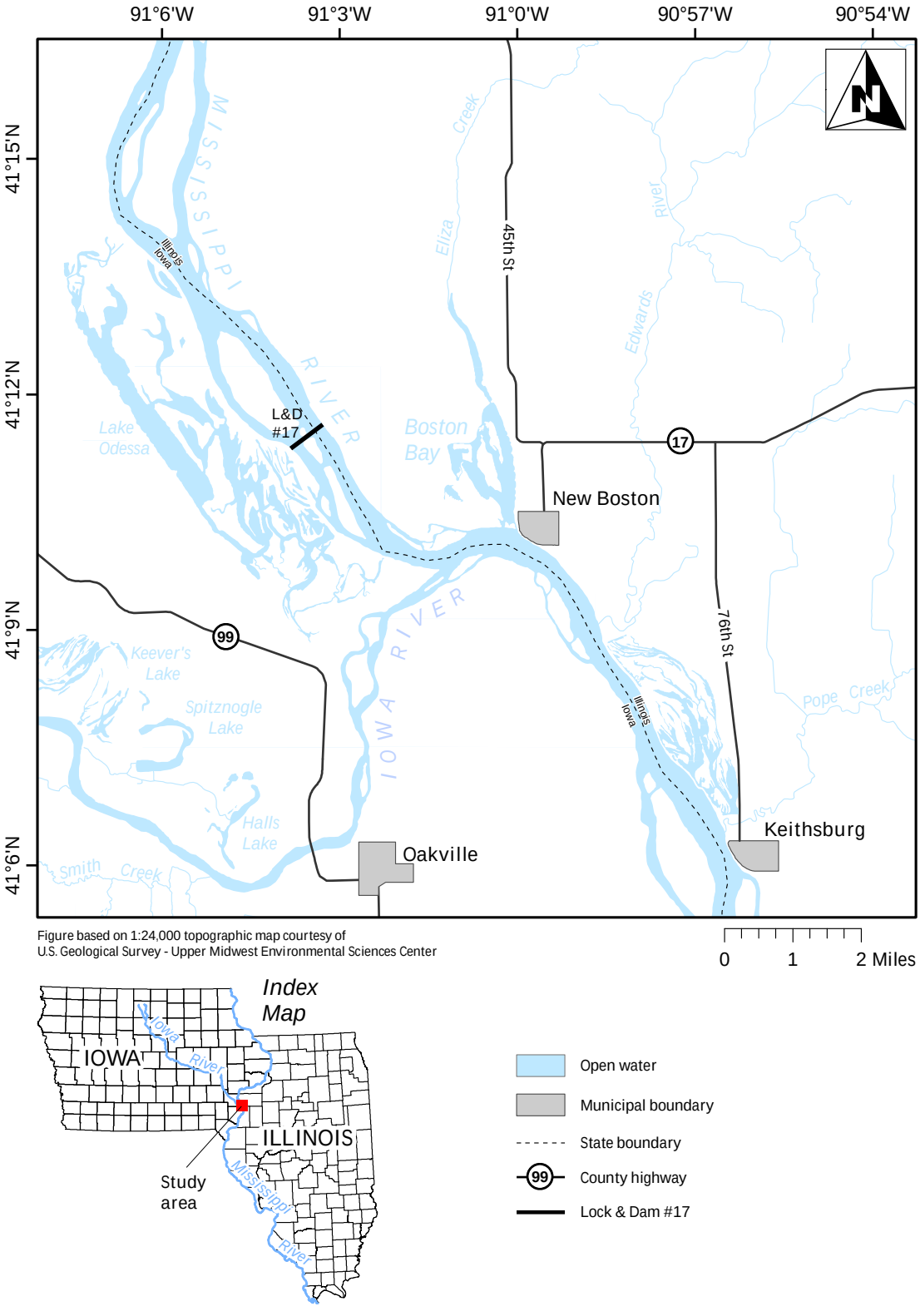

Figure 1: Map of the Boston Bay study area, adjacent to confluence of the Iowa and Mississippi Rivers.

LL&W contracted with IIHR Hydroscience and Engineering to provide the data collection, analysis and research necessary for this project. These objectives were achieved via a combination of field-data collection, laboratory analysis and computer modeling software. It is the purpose of this thesis to summarize the methods used to obtain and resolve the relevant data along with the results from each of these areas (field, laboratory and modeling).

What follows should not be viewed as the 'final say' on whether or not the proposed dredging and restoration of Boston Bay should proceed as planned. Rather, this thesis should serve as a toolbox for decision makers going forward. The results and analysis of the data collected during this project provides a template for those parties interested in pursuing similar efforts in the future. It will also help to identify the work that still needs to be done before the restoration of Boston Bay can begin.

1.4 – Study Area

Boston Bay is a 650-acre backwater area adjacent to the main channel of the Mississippi River and is not protected by manmade levees, thereby subject to annual flooding (Figure 2). With the establishment of the nine-foot navigation channel and the construction of levees in the early 1900's many of the fast-moving chutes between islands, and even the islands themselves became inundated (Iowa DNR, 2009). With the introduction of the locks and dams in the 1930's a minimum water surface elevation was mandated to allow for barge traffic, degrading habitat for plant and animal species which had adapted to a greater range of water level fluctuations (USACE, 2004 and 2006b).

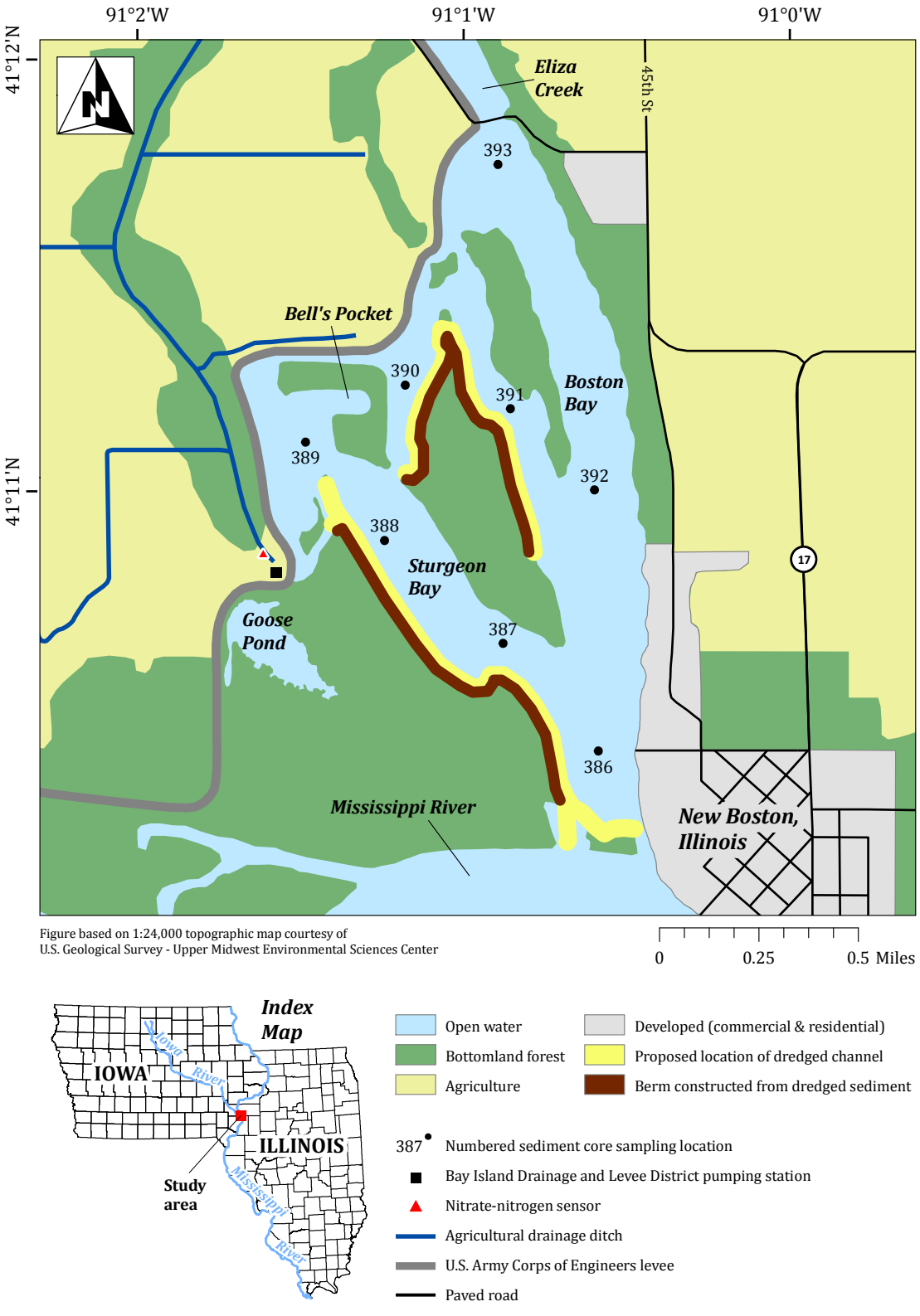

Figure 2: Map of Boston Bay study area featuring locations of proposed dredging and berm construction, along with sediment core sampling sites.

Such is the case in the region near New Boston, Illinois where the land surrounding Boston Bay is now only capable of supporting tree species that have adapted to withstand frequent flooding such as silver maple and willow (Robertson, 2008). Over time, this backwater area has also suffered from high sedimentation rates coming from the main channel of the Mississippi as well as the upland areas of the Eliza Creek watershed (Windhorn, 2002). As a result, many portions of Boston Bay become disconnected from one another during low-flow conditions. For example 'Bell's Pocket' (Figure 2), a popular location for recreational fishing is oftentimes inaccessible from the rest of the bay and can only be reached by small fishing boats and canoes (Marston, 2009; Russell, 2009; Armentrout, 2009).

The Boston Bay study area is located four miles downstream from Lock and Dam #17, and sits just across the main channel of the Mississippi from the mouth of the Iowa River (Figure 1). Water levels in the study are are highly dependent on the controlled flow conditions that exist in the Mississippi River just outside the bay. During the low-flow season that dominates late summer, fall and winter, water levels become so low that much of the bay becomes unnavigable. On the other hand, the high-flow conditions that exist during spring and early summer cause waters flowing out of the bay and into the main channel to back-up, inundating the islands and which extend into the bay. This can be seen through a comparison of aerial photographs of the study area taken during April of 2005 and August of 2008 (Figure 3). The uncontrolled flow coming from the Iowa River is also capable of contributing to the bays hydrology as witnessed after the floods of 1993 and 2008 when the water surface elevation in the bay became so high that the levees which separate the river from the Bay Island Drainage and Levee District (BIDLD) were nearly breached (Marston, 2009).

Flow conditions in Boston Bay are also dependant on the rates of inflow coming from Eliza Creek and the BIDLD (Figure 4). Eliza Creek feeds into the bay

Figure 3: Comparison of two aerial photographs of the Boston Bay study area. The photo on the left was taken in August, 2008 during the low-flow conditions that exist during late summer, fall and winter (Photo courtesy of Iowa Geographic Map Server). The photo on the right was taken during high-flow conditons in April, 2005. Much of the land to the west of the study area (marked *A*) and the vegetated islands (marked *B*) are submerged during this part of the year (photo courtesy of U.S. Geologic Survey - *Earth Explorer*).

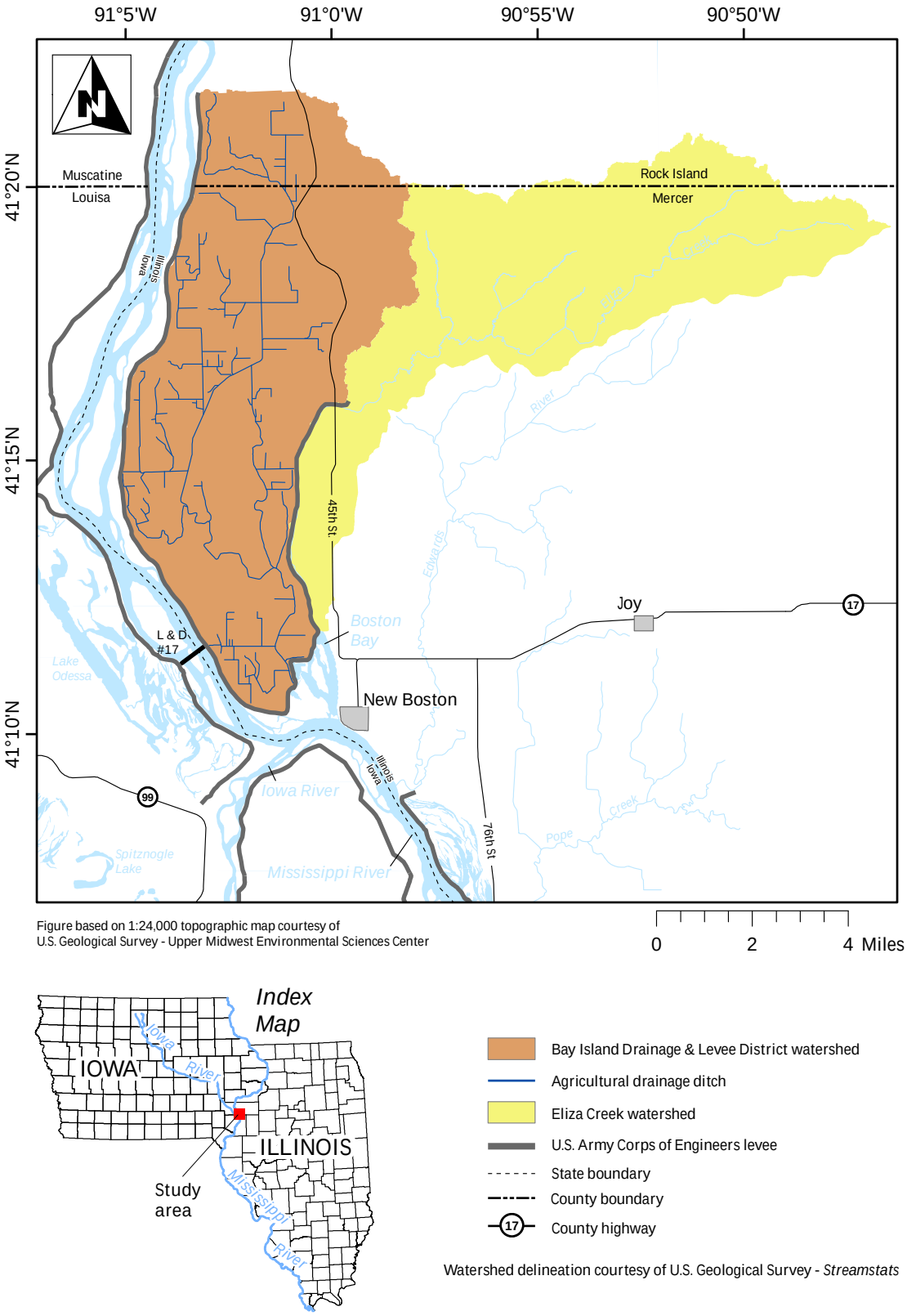

Figure 4: Map showing watersheds which empty into Boston Bay.

from the north, draining a watershed of 23,680 acres with elevations ranging from nearly 820 ft above sea level in the uplands to 530 ft in the floodplain (Windhorn, 2002; U.S. Department of Agriculture [USDA], 2004). Flows in Eliza Creek are highly variable and depend heavily on precipitation rates in the watershed. Eliza Creek is an ungaged stream but flow data collected in early June, 2009 showed flows of approximately 30 cubic feet per second (ft^3/sec). Eye-witness accounts of Eliza Creek during drought conditions estimate that water levels can be much lower (Armentrout, 2009; Marston, 2009; Russell, 2009). However, The U.S. Geological Survey (USGS) estimates that Eliza Creek is capable of handling 8,000 cubic feet per second (ft^3/s) during peak flows of a 500 year event (USGS, 2009).

In addition to receiving a steady flow from the Eliza Creek watershed, the neighboring BIDLD also pumps excess agricultural runoff into Boston Bay. The drainage district consists of nearly 24,000 acres of artificially drained farmland, and is protected from the Mississippi River by 25 miles of manmade levee (Marston, 2009) (Figure 4). While the flows entering the bay from the BIDLD vary throughout the course of a year, they are much more closely regulated than those coming from the Eliza Creek watershed. Water is pumped year-round out of the drainage district, over the levee and into Boston Bay. During the spring months or after a heavy rainfall event, all three of the drainage districts pumps are in operation, capable of discharging 265,000 gallons per minute (600 ft^3/s) (Marston, 2009). However, during the majority of the year, only two of the pumps are in use and typically discharge at a rate 200,000 gallons per minute (450 ft^3/s). The pumps are operated on an 'as needed' basis, but typically run on 8 - 10 hour cycles, three to four times a week to maintain the water table at a level that has been agreed upon by the drainage district's board of commissioners to ensure a successful growing season (Marston, 2009).

A discussion of the study area cannot exist without mentioning how the land surrounding Boston Bay has been affected by the construction of manmade features including levees, locks and dams, and the nine-foot navigation channel. As mentioned above, while wing dams and other control structures have influenced the hydrology of the UMRS, the construction of the locks and dams in the 1930's is the most significant event affecting the condition of the river and most restoration efforts attempt to alter the resulting environmental impacts (Theiling, 1998; USACE, 2006a).

Simply comparing a series of aerial photographs taken of the study area from the 1930's through 2008 with results from a survey conducted by the Mississippi River Commission in the 1890's (Figure 5) helps one to visualize how Boston Bay has changed since the introduction of the levees, locks, and dams. This figure clearly indicates that the heavily vegetated islands and peninsulas that dominated the bay in the 1890's survey map have diminished in area over time (marked *A*). Likewise comparing the aerial photograph from 2008 with those taken in 1930 and 1950, it becomes evident that the density of the vegetation has also decreased significantly (Figure 5). However, the land surrounding Goose Pond (marked *B*) appears to have experienced an increase in vegetation, presumably as a result of accelerated sedimentation rates following the construction of the locks and dams.

1.5 – Methods of Study

The analysis of Boston Bay was a multidisciplinary study that required a variety of methods to achieve the desired objectives including field data collection, laboratory analysis and computer modeling software. The methods are briefly outlined below and described in detail in each of the proceeding chapters (2 through

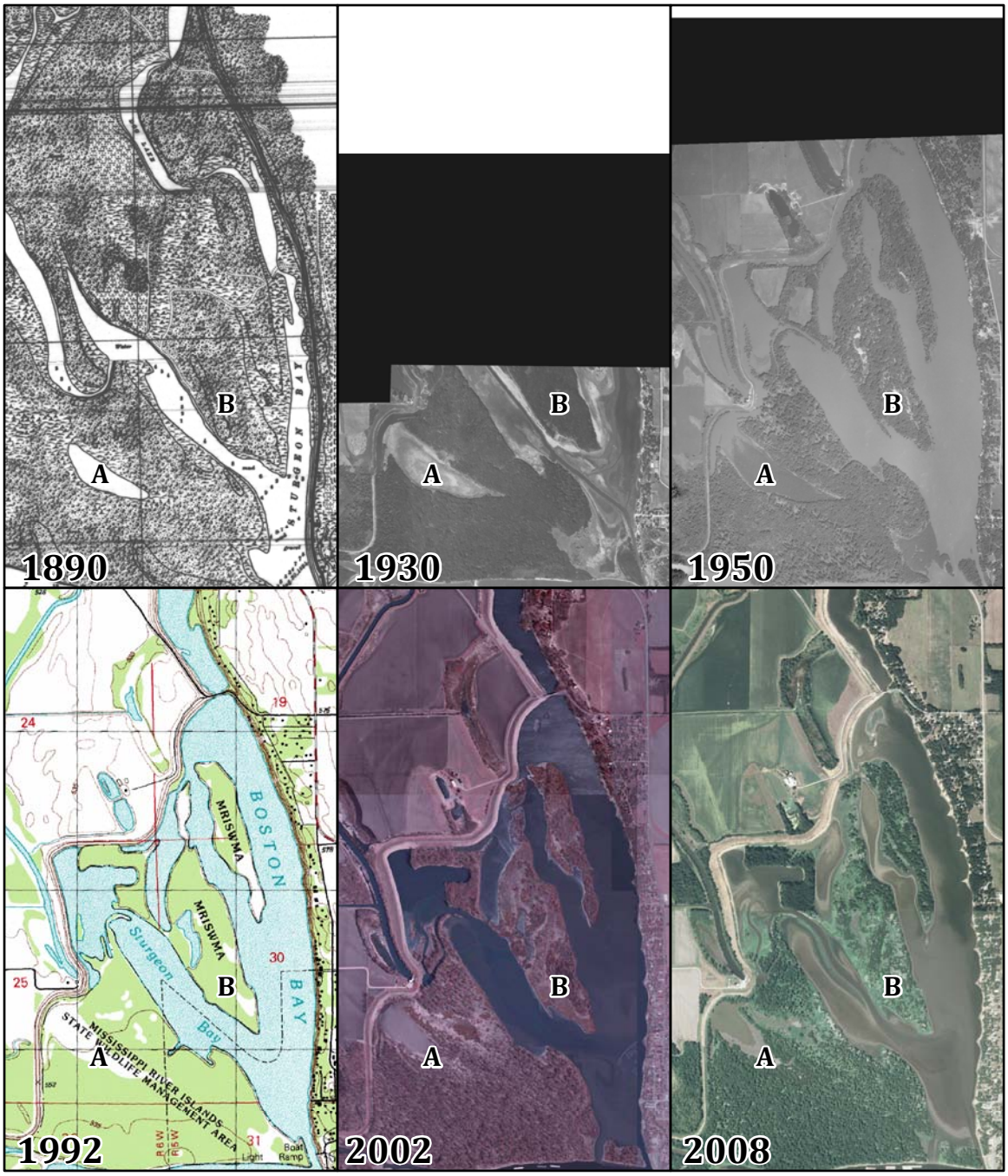

Figure 5: Map from 1890's land survey, and aerial photography of Boston Bay from the 1930's through 2008. Map courtesy of U.S. Geological Survey, *Upper Midwest Environmental Sciences Center* . Aerial photography courtesy of U.S. Geological Survey, *Earth Explorer* and Iowa Geographic Map Server . **A** indicates an area of net increased vegetation, while **B** denotes a region that has experienced a decrease in vegetation.

5). Methods include: (1) sediment sampling and grain-size analysis, (2) monitoring for nitrate-nitrogen, (3) bathymetric mapping, and (4) hydrodynamic modeling.

Eight sediment cores were obtained from the Boston Bay study area in April of 2008 and analyzed to determine soil types and characteristics of the material to be dredged. Baseline water quality monitoring of nitrate-nitrogen concentrations from the agricultural runoff water being pumped into the bay was conducted from October 2008, through June of 2009. A bathymetric survey was conducted in March 2009, using global positioning system (GPS) techniques, echo sounding equipment and a geographical information system (GIS). A two-dimensional (2D) hydrodynamic model of Boston Bay, capable of simulating the proposed dredging activity was constructed using a combination of computer modeling software and data collected in the field.

1.5.1 – Sediment Sampling and Grain-Size Analysis

Before the proposed dredging and restoration of Boston Bay can proceed, information about the relevant physical characteristics of the sediment contained within the study area were needed to better determine its suitability as potential berm-building material. Sediment cores were collected from eight locations in Boston Bay for sediment grain-size analysis (Figure 2). Initial methods of analysis included the feel test, ribbon test and soil color classification using the Munsell color chart. Dry sieving was used to determine the distribution of sands. Distributions of the finest particles (silt- and clay-size) were analyzed in the laboratory using the hydrometer method of sedimentation.

1.5.2 – Monitoring of Nitrate-Nitrogen Concentrations

In addition to restoring connectivity and creating habitat through dredging, LL&W also discussed possible methods of enhancing the quality of runoff entering the bay from the surrounding watershed, the majority of which is artificially drained for agricultural purposes. A real-time nitrate-nitrogen sensor was installed upstream from the BIDLD pumping station, continuously monitoring the concentration of nitrate-nitrogen in the agricultural runoff being pumped into the study area. The data from the nitrate monitor coupled with the daily operation logs from the pumping station allowed for the estimation of the total load of nitrate-nitrogen (in tons) entering Boston Bay via the drainage district.

1.5.3 – Bathymetric Mapping

To shed light on the elevation profile of Boston Bay, a bathymetric survey was conducted in late March of 2009. State-of-the-art hydro-acoustic survey equipment was used to assist with the data collection along with a real-time kinetic GPS navigation system. These two signals were synced through a GIS located onboard the survey vessel, resulting in over 180,000 geo-referenced elevation data points. The resulting data set can be used to generate an accurate model of the bays existing topography, while also serving as base-line data against which future surveys can be compared.

1.5.4 – Two-Dimensional Hydrodynamic Model

Finally, to better understand how the proposed dredging could potentially impact the existing flow conditions in Boston Bay, a 2D hydrodynamic model of the study area capable of simulating the proposed restoration was generated using a combination of computer modeling software packages and the results from the

bathymetric survey along with other field data measurements to serve as boundary conditions.

A series of different scenarios were simulated in an attempt to cover the range of conditions that exist in the study area throughout the course of a year. The proposed dredging activity could also be modeled by changing the hybrid mesh generated with the existing bathymetry data to reflect exactly where the dredging would occur and the berms would be placed. Results from these simulations will be used to better understand the potential environmental impacts that could result from dredging, including changes in water-surface elevation, water depth and flow velocity.

1.6 – Acknowledgements

I would first like to thank the four members of my thesis committee; Dr. E Arthur Bettis III, Dr. William Eichinger, Dr. Douglas Schnoebelen and Dr. Larry Weber for taking the time to review this thesis. The author would like to thank the Illinois State Water Survey for providing the coring boat and apparatus along with their assistance in collecting sediment core samples. Dr. John Marlin and Olivia Dorothy from the Department of Earth and Environmental Sciences at the University of Illinois at Champaign-Urbana provided significant insight into sediment-size analysis via the hydrometer method. Dr. E Arthur Bettis of the University of Iowa Geosciences Department also deserves credit for allowing access to the soils lab and equipment required for sediment-size analysis. Special recognition goes to Jeff Marston, Bay Island Drainage and Levee District, for assistance during the nitrate monitoring process, and for providing useful information about Boston Bay and the surrounding watershed. Thanks to James Rogala and Carol Lowenberg of the U.S. Geological Survey Upper Midwest

Environmental Sciences Center for providing GIS data including historical aerial photographs and results from previous bathymetric surveys. This project would not have been possible without the continued support from IIHR staff engineers – Dr. Nathan Young, Troy Lyons and Andrew Craig who helped with the bathymetric survey, and other field data collection. I will be forever grateful to my thesis advisors Dr. Douglas Schnoebelen and Dr. Larry Weber for their patience and support throughout the duration of this project. Finally, without the financial support provided by Living Lands & Waters, this project would have never met its objectives. The dedication and enthusiasm of people like Chad Pregracke and Tammy Becker, of Living Lands & Waters is unmatched. Their commitment to the Mississippi River and the rest of our Nation's waterways is truly amazing.

CHAPTER 2 – PARTICLE-SIZE ANALYSIS OF SEDIMENT CORE SAMPLES

2.1 – Background

Prior to any dredging or berm construction in Boston Bay, the physical and chemical characteristics of the existing sediment must be well understood (Bartos, 1977; Herbich, 1992; USACE, 2004; Bray, 2008). From a chemical standpoint, contaminated sediment is not an ideal candidate for berm design. Placing dredge spoils which contain harmful chemicals, including heavy metals and PCB's, on upland areas could be detrimental to human health as well as native plant and animal species (Doonze, 1990; Herbich, 2000; Bray, 2008). Additionally, treatment of contaminated sediment is a time-consuming and expensive process that should be avoided when possible (Brandon, et al, 1996).

Gaining a good understanding of the physical makeup of the sediment in Boston Bay is no less important. It is essential to know the composition of any sediment intended for use in building (Bartos, 1977; Keefe, 2005). Soils considered most suitable for wall or berm construction are those termed 'Fuller Parabola' or 'well-graded' (Minke, 2006; Keefe, 2005; Murthy, 2003). This term is used to define soils comprised of particles of many differnet diameters, having uniform distribution from coarse to fine, with no predominant particle-size as defined by the USDA soils classification scheme outlined in Table 1.

U.S. Department of Agriculture Soil Classification Scheme	
Name of Separate	**Diameter Range (μm)**
Very Coarse Sand	2000.0 – 1000.0
Coarse Sand	1000.0 – 500.0
Medium Sand	500.0 – 250.0
Fine Sand	250.0 – 100.0
Very Fine Sand	100.0 – 50.0
Silt	50.0 – 2.0
Clay	< 2.0

Table 1: USDA soil classification scheme (Day, 1965).

The lifetime of the proposed berms will be greatly increased if they are built out of soil that is easily compactable and capable of standing up to erosion. Like cement in concrete, clays, which are highly cohesive, act as a binder for all larger particles (Keefe, 2005; Minke, 2006; Bray, 2008). Samples containing high percentages of sand would not be considered appropriate berm-making material. Sands do not compact as well as clays or silts as can be shown via the 'cohesion' or 'ribbon' test, where a sediment sample is compacted between the thumb and forefinger into long, ribbon-like shapes (Minke, 2005; USDA, 1993; Thein, 1979). Clayey soils easily form ribbons, while sandy soils quickly fall apart. Ideally, the well graded soil used for berm construction would be of a clay loam, silty clay loam or loam texture, with larger aggregates (sand and gravel) evenly dispersed throughout (Keefe, 2005).

While chemical analysis was outsourced to a third party (the results of which are summarized in Appendix A), Living Lands & Waters delegated the responsibility of determining the grain-size distribution of the sediment contained within Boston Bay to IIHR, with additional support coming from the University of Iowa's Department of Geosciences and the Department of Earth and Environmental

Sciences at the University of Illinois at Champaign-Urbana. The details of this study are outlined below.

2.2 – Methods

2.2.1 – Sediment Core Collection

Sediment cores were extracted from eight locations (#'s 386 – 393) within Boston Bay, in hopes of gaining a broader understanding of the range of different sediment types covered throughout the bay, specifically in the proposed dredging locations (Figure 2). Coring was conducted by the Illinois State Water Survey (ISWS) on April 9, 2008. The cores were opened and analyzed on the following day at the ISWS office in Peoria, Illinois. Initially, cores were photographed, measured (length) and described using the touch method and a Munsell color chart.

Samples, two centimeters (cm) in thickness, were taken every 20 cm down the length of the core. Those samples found to be within the same horizon (determined visually) were combined into a single sample. This was done in hopes of obtaining a good representation of each horizon, while also cutting down on the amount of time spent doing analysis. Samples were numbered according to their core number (#386 - 393, as assigned by ISWS), and their depth within the core (sample #386-3 being from deeper reaches of core #386 than sample #386-1).

2.2.2 – Sediment-Size Distribution

Although many methods of performing particle-size analysis (PSA) exist, the hydrometer method was chosen to determine the percentages of silt and clay, while traditional dry sieving was used to find the distribution of sands. These methods were chosen because of their relatively easy learning curve when compared to other, more robust, methods like the pipette or x-ray attenuation (Sedigraph)

methods. While the claim that, with a hydrometer, 'the colloidal content of a soil can be estimated quite accurately in only 15 minutes' (Bouyoucos, 1926) might be a bit of an exaggeration, it is true that performing PSA using a hydrometer and traditional sieving techniques is much less time consuming than other means of grain-size analysis.

2.2.2.1 – Distribution of Silt and Clay

Like other methods of sediment-size analysis based on the rate at which particles settle in a given fluid, the hydrometer method depends fundamentally on Stokes' Law,

$$v = \frac{X^2 g(\rho_s - \rho_L)}{18\eta} \qquad (1)$$

(Day, 1965), which describes the rate v at which spherical particles with a diameter X and density ρ_s settle in a liquid with density ρ_L and viscosity, η. Here, g is equal to the acceleration due to gravity. Hydrometer analysis begins once sediment and water has been thoroughly mixed, after which sediment begins to settle out of the water column, obeying Stokes' Law. The density of the sediment-water suspension depends on the concentration and specific gravity of the sediments present in the mixture. If the water-soil mixture is allowed to stand, soil particles begin settling out of suspension, decreasing the density of the mixture. The hydrometer measures the density of the suspension at a known depth below the surface (Sawyer, 2008).

Perhaps the most straightforward method for determining particle fractionation from hydrometer readings is through a graphical representation (Day 1965). Measured particle diameter X (microns), a function of settling time t (minutes), is calculated using Equation 1 (Stokes' Law), which can be re-written as:

$$X = \frac{\theta}{t^{1/2}}\ ,\ \text{where}\ \theta = 1000\left[\frac{30\eta h}{g(\rho_s - \rho_L)}\right] \qquad (2)$$

(Day, 1965). The sedimentation parameter *(θ)* is dependent on the depth at which the hydrometer bulb is immersed in the suspension *(h),* and is variable during the settling process. If *h* is set equal to the distance from the center of the hydrometer bulb (in centimeters) to the surface of the suspension, a relationship between *h* and hydrometer reading *(R)* is established, making θ a function of *R* (Table 2) (Day, 1965).

R	θ	R	θ	R	θ
-5	50.4	11	46.4	27	41.9
-4	50.1	12	46.2	28	41.6
-3	49.9	13	45.9	29	41.3
-2	49.6	14	45.6	30	41
-1	49.4	15	45.3	31	40.7
0	49.2	16	45	32	40.4
1	48.9	17	44.8	33	40.1
2	48.7	18	44.5	34	39.8
3	48.4	19	44.2	35	39.5
4	48.2	20	43.9	36	39.2
5	47.9	21	43.7	37	38.9
6	47.7	22	43.4	38	38.6
7	47.4	23	43.1	39	38.3
8	47.2	24	42.8	40	38
9	47	25	42.5	41	37.7
10	46.7	26	42.2	42	37.4

Table 2: Values of sedimentation parameter *(θ)* used to calculate particle diameter *(X)* from hydrometer readings *(R)* (Day, 1965).

The concentration of the suspension *(c)* (grams/liter) can be calculated by subtracting the 'blank' sample reading *(R_L)* (obtained during hydrometer calibration, described below) from the recorded hydrometer reading *(R)*. From this, the summation percentage of each particle size (*P)* is calculated using Equation 3

$$P = 100(c/c_o) \qquad (3)$$

(Day, 1965), where c_0 is mass of the oven-dried soil sample in grams per liter of suspension.

Finally, a plot of summation percentage *(P)* versus particle size *(X)* can be constructed, with a logarithmic scale used for particle-size (Figure 6). The curve is plotted cumulatively with each grain size including all fine components (Minke, 2006). Percentage of sand, silt and clay can be inferred by interpolating from the curve at different values of *X* (2 μm, 50 μm, etc). Interpreting the graph plotted in Figure 6, one would conclude that this particular summation curve is representative of a sediment sample comprised of 4% sand, 49% silt and 47% clay and would be classified as 'silty clay.'

This result is obtained by first noting where the curve in Figure 6 crosses the boundary between silt and clay ($X = 2\mu m$) marked *A*. Finding the corresponding percentage value by simply reading off the y-axis, one see's that this sample contains 47% clay. To determine the percentage of silt, locate where the curve crosses the boundary between sand and silt ($X = 50\mu m$) marked *B*. Find the corresponding percentage value (96%) and subtract from it the clay percentage (47%) to calculate the percentage of silt which, for the case in Figure 6, is 49%. Sand percentage is found by subtracting the sum of the silt and clay percentages from 100.

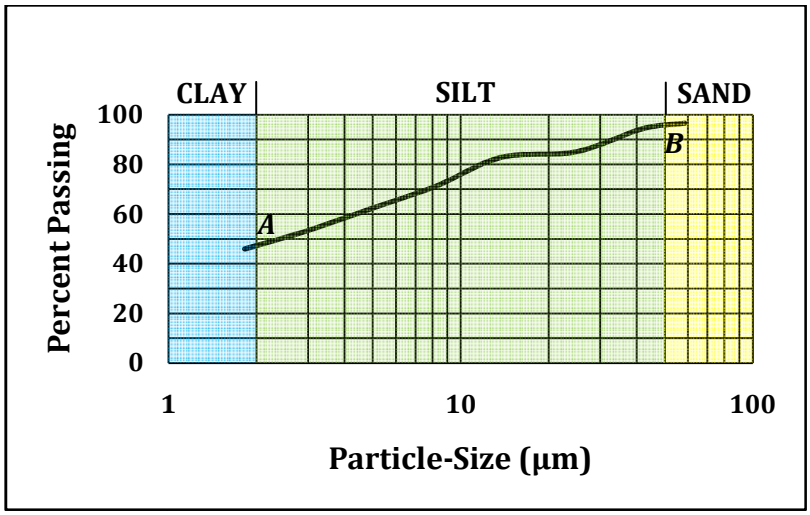

Figure 6: Summation curve for a sediment sample comprised of 4% sand, 49% silt and 47% clay.

2.2.2.2 – Distribution of Sand

While the hydrometer method is perfectly appropriate for determining percentages of finer particles like silt and clay, it is not a useful tool for ascertaining the quantity of coarse sediment (sand and gravel) contained within a soil sample. Therefore, it was decided that the traditional dry sieving method of grain size analysis be applied to the handful of core samples that contained high amounts (greater than 50%) of material with diameters larger than 50 microns.

The idea behind sieving is simple, but consistency is required to obtain accurate results. Samples must first be treated to assure that aggregates of fine-grained sediment not affect the final results (Day, 1965). This is achieved by placing a sample in a #325 sieve capable of passing particles with diameter smaller than 50 microns and thoroughly washing it with distilled water. After the samples have been allowed to dry, they are weighed and poured into a series of stacking 8-inch diameter sieves, each equipped with a wire mesh capable of passing particles of a given size. The chance that a particle passes through a sieve opening is highly

dependent upon the shape and orientation of the particle, thus requiring prolonged shaking. This can be achieved through a mechanized shaking device, such as the Ro-Tap sieve shaker. Despite the advantages that such equipment can provide, it is often not possible for sieving to be continued to 'completion' as is often prescribed (Day, 1965).

Once the shaking process is finished, the contents of each sieving pan is weighed and the percentages of sand, from very coarse to very fine, can be determined by dividing the mass remaining in each pan by the total mass of the original sample. Plots, similar to the summation curves used to determine percentages of fine sediment can be generated using the data collected during sieving to determine the distribution of sands.

2.3 – Analysis and Results

2.3.1 – Silt and Clay Size Analysis

Analysis closely followed the methodology outlined by Day (1965). An HB Instrument Co. soil analysis hydrometer was chosen for its ability to take readings over a large range of concentrations (-5 to 60 grams/liter), which meets ASTM standards. To properly calibrate the hydrometer, 10 milliliters (mL) sodium hexametaphosphate ('Calgon') was added to a sedimentation tube that was filled the rest of the way with distilled water to bring the final volume to one liter (L). The hydrometer was placed into this solution and a 'blank' reading was taken and recorded as R_{L1}. This process was repeated again on the second day of data collection, this time recorded as R_{L2}. Temperature of the blank solution was also recorded at the start of each day readings were taken. Data collected during calibration is summarized in Table 3.

Date	R_{L1} (g/L)	R_{L2} (g/L)	T_1 (°C)	T_2 (°C)
5/12/2008	1	1	20	20
5/13/2008	1	1	20	20

Table 3: Hydrometer and temperature readings on blank sample,obtained during hydrometer calibration.

Cores were treated on an individual basis with samples taken from each horizon. After the samples were allowed to dry overnight, 40 (±0.5) grams from each sample, capable of passing a sieve with a two millimeter (mm) opening, were weighed and placed in a 200 mL beaker. 50 mL of distilled water was added to each sample, along with 10 mL of hydrogen peroxide (H_2O_2) and 10 mL sodium acetate ($C_2H_3NaO_2$) to aid in the removal of soluble salts, iron oxides and organic compounds including carbonates. This solution was then placed on a heating element, and allowed to digest for two hours.

Proper fractionation and PSA depends on sufficient dispersal of soil particles in the water column (Day, 1965). That is, the soil particles must be thoroughly separated from one another and suspended in an aqueous solution. To properly disperse the particles, 50 mL Calgon was added to each sample, resulting in a strong electrical repulsion force between individual soil components which disperses flocculated clays, and acts to break-up larger aggregates composed of smaller particles (Keefe, 2005). Finally, samples were placed on a reciprocating shaker and allowed to mix for five hours.

Following pretreatment the samples were placed into sedimentation tubes, which were then filled to the one liter mark with distilled water. As stated above, hydrometer readings cannot be taken until the sediment is thoroughly mixed into the water column. This was accomplished via several long, slow, upward strokes with a plunger. The hydrometer was then placed into the suspension, and a reading

was taken at 30 seconds, after which the hydrometer was removed from the sedimentation tube. This reading was recorded as R_5. This process was repeated after 1, 3, 10, 30, 90, and 720 minutes with careful attention paid so as not to disturb the mixture each time the hydrometer was placed into the suspension. These readings were recorded as R_1, R_3, R_{10}, etc (Table 4). Once the hydrometer readings were complete, the contents of the sedimentation tubes were emptied, and filtered through a #325 sieve capable of passing particles smaller than 50 microns. The remaining sample was then dried and sand percentages were determined via traditional sieving methods as will be described in greater detail below.

Once all the hydrometer readings were taken and recorded, Stokes' Law was used to determine particle diameter (microns) based on settling time and hydrometer readings (Equation 2). However, careful attention needs to be paid to the value of the sedimentation parameter (θ) used in this expression. Equation 2 assumes that the viscosity (η) is of water at 30 °C, with a value of 0.008 Poise. As outlined in Table 3, this was not the case during the two days over which hydrometer readings were recorded. Rather, the temperature of the blank sample was only 20 °C, and θ must be multiplied by the correction factor $(\eta_{20}/\eta_{30})^{1/2}$, where η_{20} is the viscosity of water at 20 °C (0.01 Poise). This ratio of viscosities is 1.118.

Summation percentage was calculated using the oven-dry weight of the sediment sample (c_0) and the hydrometer readings (R) (Equation 3). Finally plots of summation percentage (P) versus particle diameter (X) were generated (Figures 7 - 11), as exemplified using Figure 6. From these curves, one can easily determine the distribution of sand, silt and clay as outlined above. These results have been summarized in Table 5

Core #	Mass (g)	$R_{.5}$	R_1	R_3	R_{10}	R_{30}	R_{90}	R_{720}
386-1	40.5	34	33	31	26	22	18	14
386-2	40.1	43	42	40	36	30	25	18
386-3	40.6	42	41	39	36	32	28	20
387-1	40.8	40	39	37	33	30	26	19
387-2	41.0	42	41	40	38	34	31	23
387-3	40.6	43	42	38	37	32	28	21
388-1	40.8	40	39	37	33	29	25	19
388-2	40.7	40	37	34	27	23	20	16
388-3	40.9	42	41	41	37	34	29	21
388-4	40.3	20	16	13	11	10	9	8
388-5	40.7	32	31	28	23	20	17	13
389-1	40.8	24	23	21	17	16	13	6
389-2	40.3	38	36	34	30	25	21	8
389-3	40.7	42	41	40	37	34	30	17
390-1	40.5	36	34	34	32	31	27	22
390-2	40.5	30	29	28	25	23	22	19
391-1	31.6	32	31	30	28	26	23	17
391-2	41.3	35	33	30	27	24	20	17
391-3	41.6	7	6	6	5	5	5	5
392-1	40.4	41	40	39	36	32	29	19
392-2	41.9	25	24	22	17	16	13	7
392-3	40.6	6	5	5	5	4	4	4
392-4	40.3	4	4	3	3	3	3	3
393-1	40.7	32	31	30	23	22	21	12
393-2	40.3	28	27	25	23	22	17	14
393-3	41.2	5	5	4	4	3	3	3
393-4	40.6	6	6	6	6	5	5	4
393-5	40.7	4	4	3	3	3	3	3

Table 4: Mass (grams) and hydrometer readings (R),measured in grams/liter, for each core sample, taken at 0.5, 1, 3,10, 30, 90 and 720 minutes.

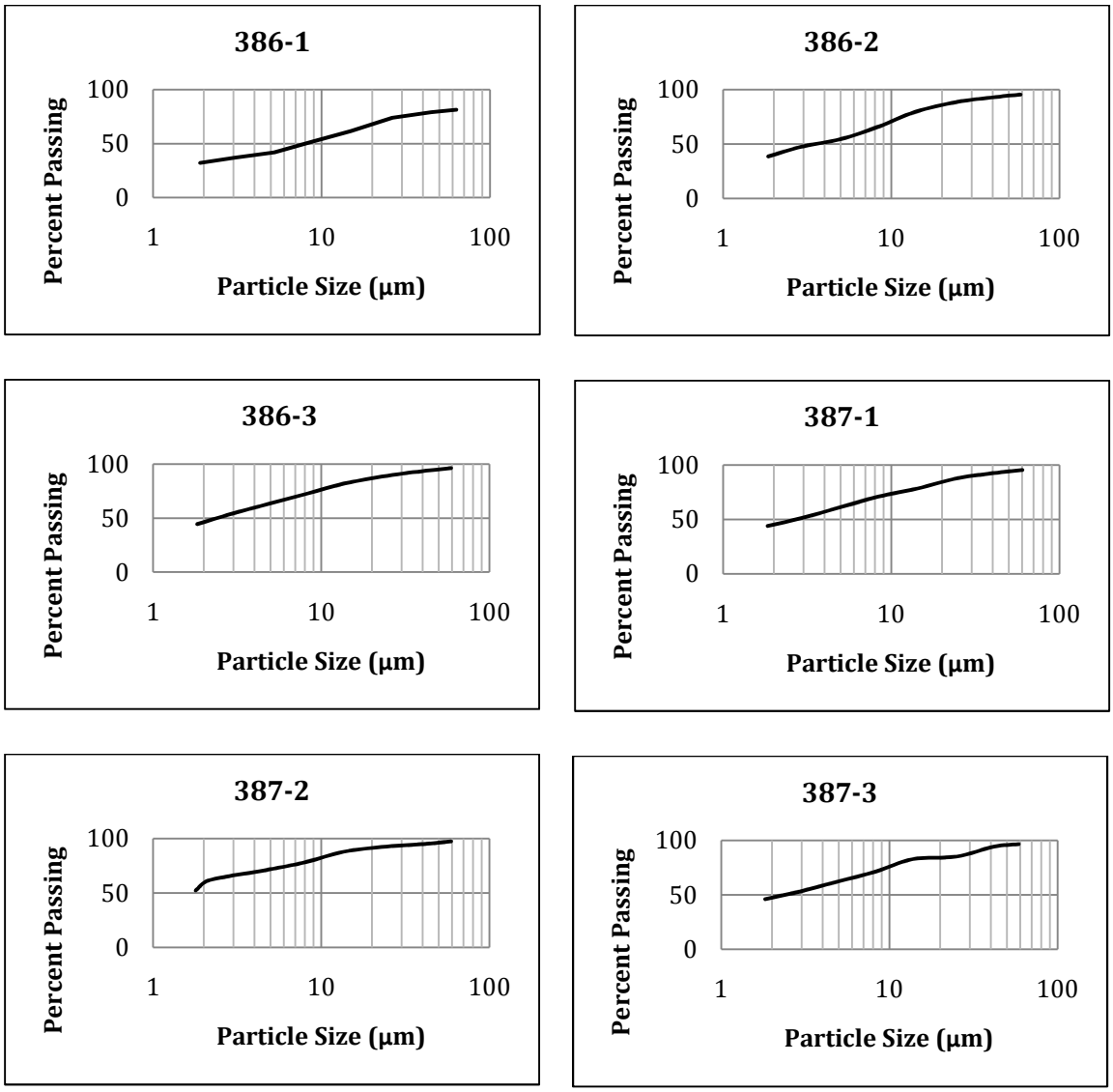

Figure 7: Summation curves for cores #386 and #387. Particle size (µm) is plotted along the x-axis, using a logarithmic scale. Summation percentage is plotted along the y-axis.

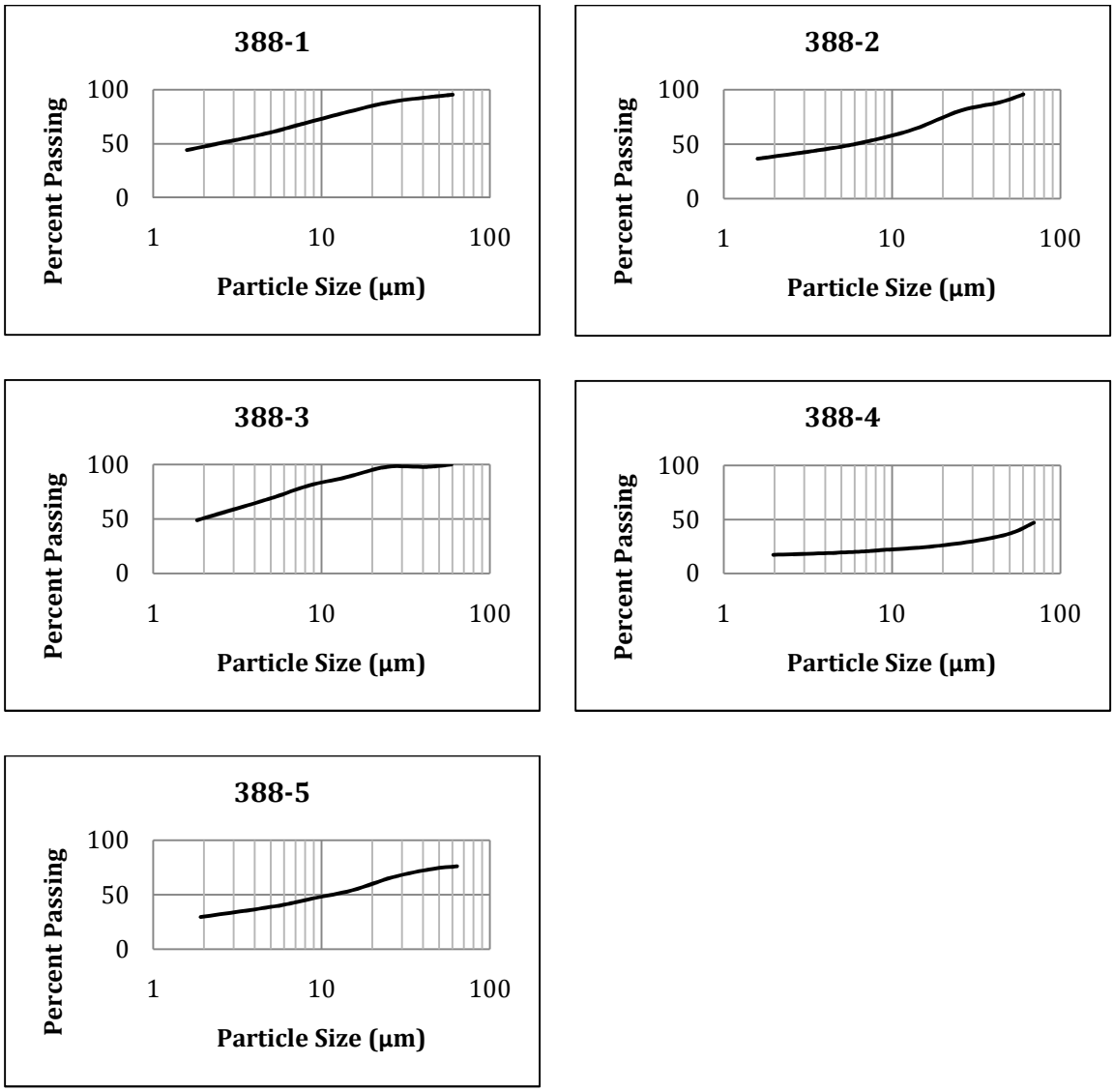

Figure 8: Summation curves for core #388. Particle size (µm) is plotted along the x-axis, using a logarithmic scale. Summation percentage is plotted along the y-axis.

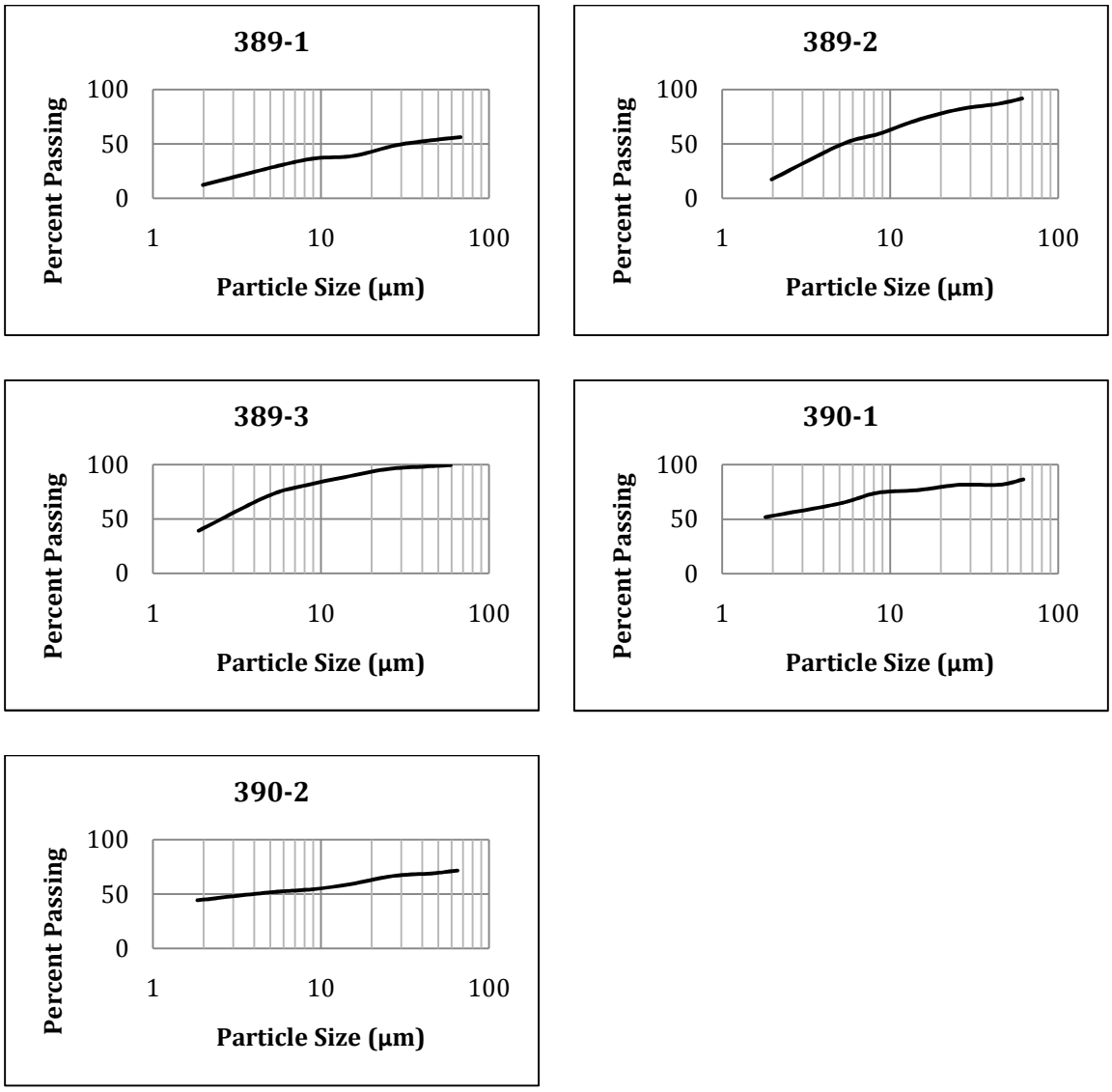

Figure 9: Summation curves for cores #389 and #390. Particle size (µm) is plotted along the x-axis, using a logarithmic scale. Summation percentage is plotted along the y-axis.

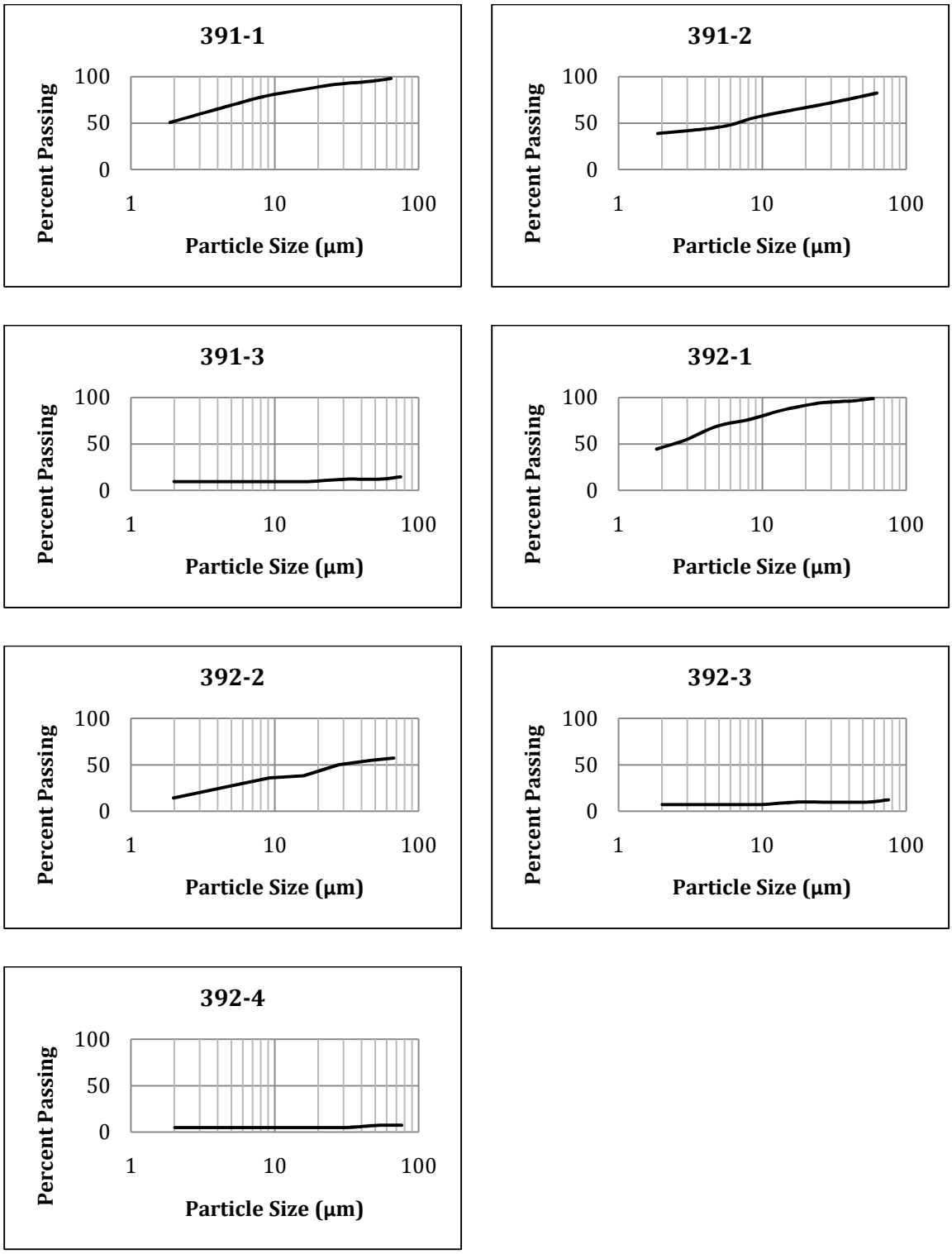

Figure 10: Summation curves for cores #391 and #392. Particle size (µm) is plotted along the x-axis, using a logarithmic scale. Summation percentage is plotted along the y-axis.

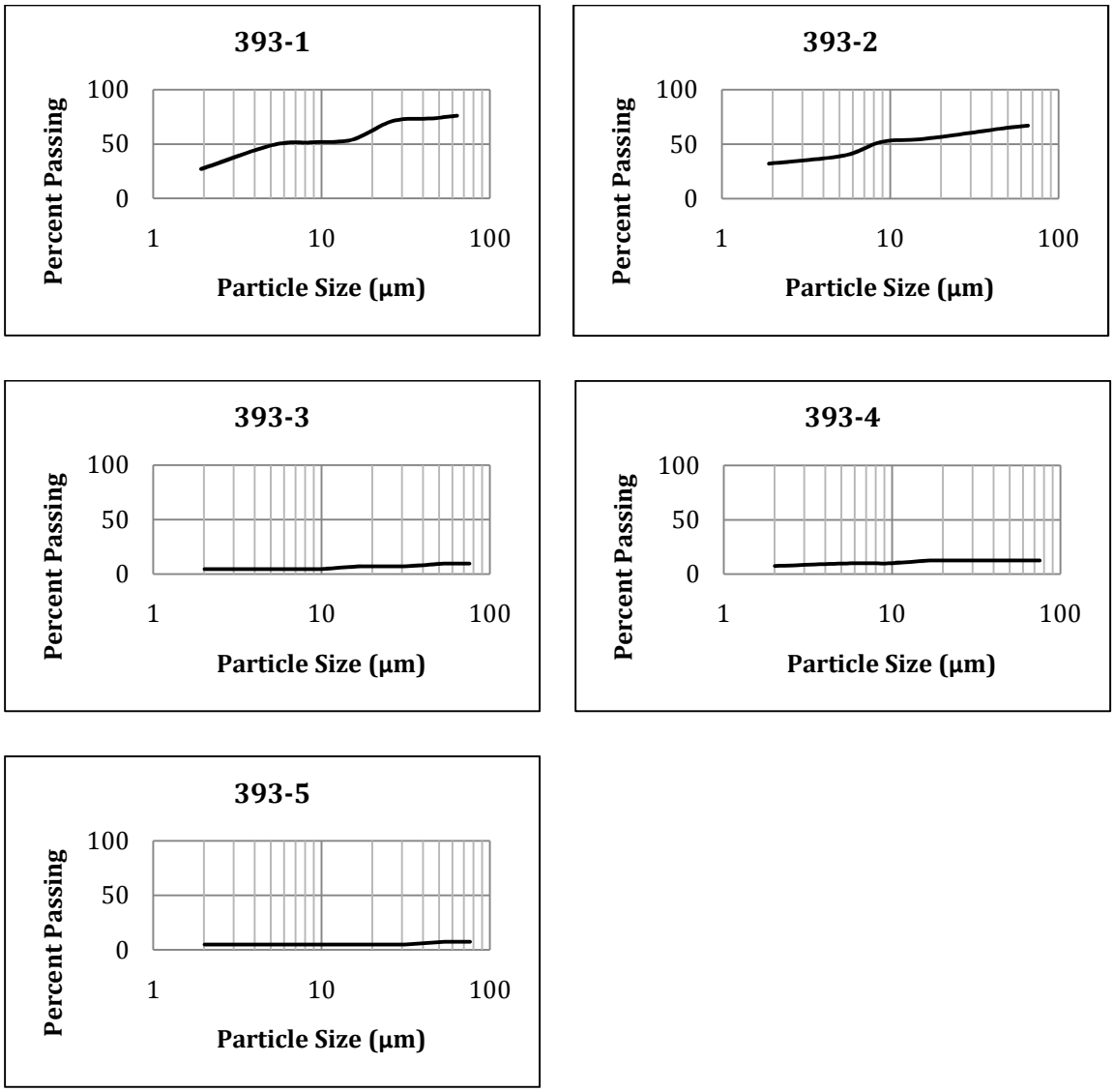

Figure 11: Summation curves for core #393. Particle size (µm) is plotted along the x-axis, using a logarithmic scale. Summation percentage is plotted along the y-axis.

Core #	% Sand	% Silt	% Clay	Texture
386-1	20.00	48.00	32.00	SiCL
386-2	8.00	52.00	40.00	SiCL
386-3	7.00	65.00	28.00	SiC
387-1	9.00	49.00	42.00	SiC
387-2	6.00	43.00	60.00	C
387-3	7.00	50.00	43.00	SiC
388-1	8.00	44.00	48.00	SiC
388-2	10.00	51.00	39.00	SiCL
388-3	1.00	49.00	50.00	SiC
388-4	61.00	21.00	18.00	SL
388-5	25.00	45.00	30.00	CL
389-1	45.00	41.00	14.00	L
389-2	11.00	70.00	19.00	SiL
389-3	1.00	58.00	41.00	SiC
390-1	18.00	27.00	55.00	C
390-2	30.00	28.00	42.00	C
391-1	5.00	43.00	52.00	SiC
391-2	18.00	41.00	41.00	SiC
391-3	88.00	2.00	10.00	LS
392-1	5.00	52.00	43.00	SiC
392-2	43.00	40.00	17.00	L
392-3	89.00	3.00	8.00	S
392-4	92.00	6.00	2.00	S
393-1	26.00	47.00	27.00	L
393-2	35.00	32.00	33.00	CL
393-3	91.00	4.00	5.00	S
393-4	88.00	5.00	7.00	LS
393-5	93.00	2.00	5.00	S

Table 5: Results from hydrometer analysis performed on sediment samples from Boston Bay. Percentages of sand, silt and clay found using the hydrometer method of grain-size analysis. Texture determined using the USDA soil texture triangle (Figure 13) (C=Clay, Si=Silt, S=Sand, L=Loam).

2.3.2 – Sand Size Analysis

A brief review of the results from the hydrometer analysis reveals that seven of the 28 samples contain greater than 50% sand (#'s 388-4, 391-3, 392-3, 392-4, 393-3, 393-4, and 393-5). What remained after hydrometer analysis from each sample was placed in a #325 sieve capable of passing particles smaller than 50 microns. The samples were rinsed with distilled water to remove any aggregates of fine sediment.

To accurately determine the break-down of different sand sizes in these samples, each was dried, re-weighed and emptied into a set of stacking sieves. Five sieving pans were placed on top of an impermeable pan, each allowing particles of a given size to freely pass through them. The particle size, USDA classification and sieve number are listed in Table 6. The sieves were placed in a mechanized Ro-Tap sediment shaker, and allowed to shake for 10 minutes, after which the contents of each sieve pan were emptied into a small dish and re-weighed. These results have been summarized in Tables 7-8.

Particle Size (μm)	USDA Classification	Sieve #
2000 - 1000	Very Coarse Sand (VCoS)	18
1000 - 500	Coarse Sand (CoS)	35
500 - 250	Medium Sand (MS)	60
250 - 100	Fine Sand (FS)	140
100 - 50	Very Fine Sand (VFS)	325

Table 6: Sizes of sand components, with their USDA classification and respective sieve number.

Sample #	Total Mass (g)	Sieve Opening (mm)	Indiv. Mass (g)	% Retained	Class
388-4	25.043	2	0.244	0.97	VCoS
		1	0.901	3.60	CoS
		0.5	7.709	30.78	MS
		0.25	12.32	49.20	FS
		0.1	3.796	15.16	VFS
		0.05	0.087	0.35	Si
391-3	10.38	2	0.434	4.18	VCoS
		1	0.812	7.82	CoS
		0.5	2.419	23.30	MS
		0.25	3.611	34.79	FS
		0.1	2.817	27.14	VFS
		0.05	0.288	2.77	Si
392-3	57.54	2	4.829	8.39	VCoS
		1	3.423	5.95	CoS
		0.5	12.587	21.88	MS
		0.25	31.809	55.28	FS
		0.1	4.424	7.69	VFS
		0.05	0.469	0.82	Si
392-4	71.13	2	5.362	7.54	VCoS
		1	19.773	27.80	CoS
		0.5	20.774	29.21	MS
		0.25	21.486	30.21	FS
		0.1	3.55	4.99	VFS
		0.05	0.189	0.27	Si

Table 7: Results of sieving to determine distribution of sands for samples 388-4, 391-3, 392-3 and 392-4 (VCos = Very Coarse Sand; CoS =Coarse Sand; MS = Medium Sand; FS = Fine Sand; VFS = Very Find Sand; Si = Silt).

Sample #	Total Mass (g)	Sieve Opening (mm)	Indiv. Mass (g)	% Retained	Class
393-3	47.15	2	4.517	9.58	VCoS
		1	1.197	2.54	CoS
		0.5	5.954	12.63	MS
		0.25	26.097	55.35	FS
		0.1	8.279	17.56	VFS
		0.05	1.106	2.35	Si
393-4	67.39	2	13.089	19.42	VCoS
		1	18.058	26.80	CoS
		0.5	18.075	26.82	MS
		0.25	10.49	15.57	FS
		0.1	7.323	10.87	VFS
		0.05	0.352	0.52	Si
393-5	78.92	2	3.595	4.56	VCoS
		1	12.817	16.24	CoS
		0.5	20.894	26.47	MS
		0.25	28.711	36.38	FS
		0.1	10.595	13.42	VFS
		0.05	2.311	2.93	Si

Table 8: Results of sieving to determine distribution of sands for samples 393-3, 393-4 and 393-5 (VCos = Very Coarse Sand; CoS =Coarse Sand; MS = Medium Sand; FS = Fine Sand; VFS = Very Find Sand; Si = Silt).

Once the fractionation of sand components was complete, the percentages of particles retained in a given sieve were plotted against the size of the sieve opening (millimeters), resulting in a plot that contains information similar to that found using the gradation curves obtained following the hydrometer analysis (Figure 12).

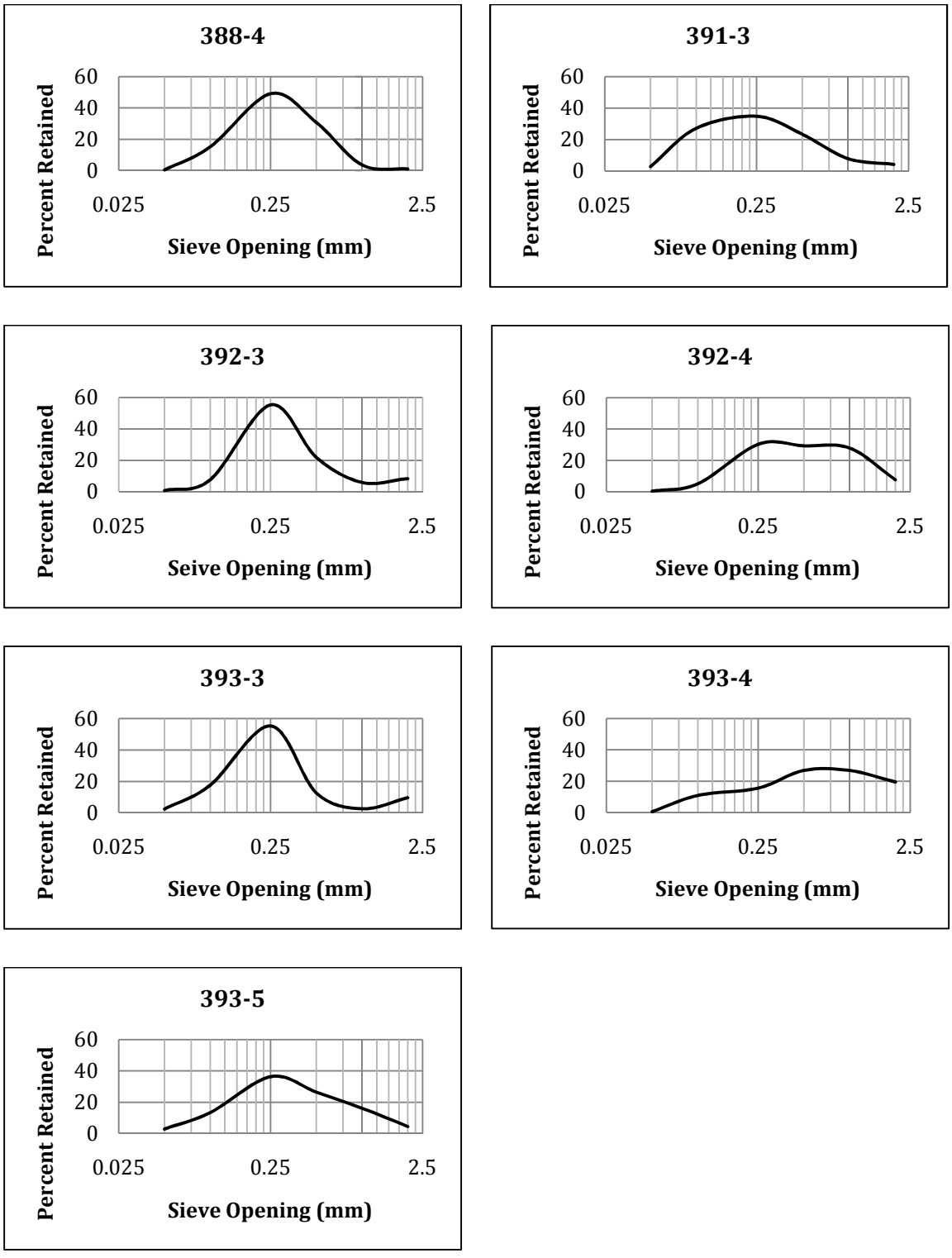

Figure 12: Gradation curves for samples containing >50% sand, obtained via sieving. Percent retained is plotted on the y-axis, with sieve opening size (mm) plotted on the x-axis.

For example, a brief glance at the curve for core sample #388-4 reveals that the majority of the sand components are in the 0.10 – 0.25 mm range, were retained in the #140 sieve, and would be best described as 'fine sand.' Similar arguments hold for the other samples that underwent particle-size analysis via sieving.

2.4 – Discussion

Particle-size analysis of core samples provided much insight into the physical characteristics of the sediment contained within Boston Bay. The eight sediment cores consisted of particles that were predominantly silt- and clay-sized (2 – 50 μm) with two cores (# 392 and 393) displaying significant amounts of sand near their bottoms. The results of this analysis are easily displayed in a ternary diagram, similar to the texture triangle used by the USDA (Figure 13).

The results of the hydrometer analysis indicate that the majority of the sediment found in Boston would classify as 'silt' with the summation curves (Figures 7 - 11) being indicative of sediment which is predominantly fine-grained (Venkatramaiah, 2006). These results closely match those obtained immediately following the opening of the cores via the touch method and cohesion test. Samples analyzed using dry sieving consisted primarily of particles with diameters in the range of 0.10 – 0.25 millimeters (mm), and would be considered 'fine sand.'

Samples taken near the location of proposed dredging (cores #387-389) are almost entirely made up of a silt-clay structure, and may contain large amounts of sediment from farm runoff pumped into the bay via the BIDLD. Analysis of sediment samples taken from within the drainage district would be necessary to help validate this hypothesis.

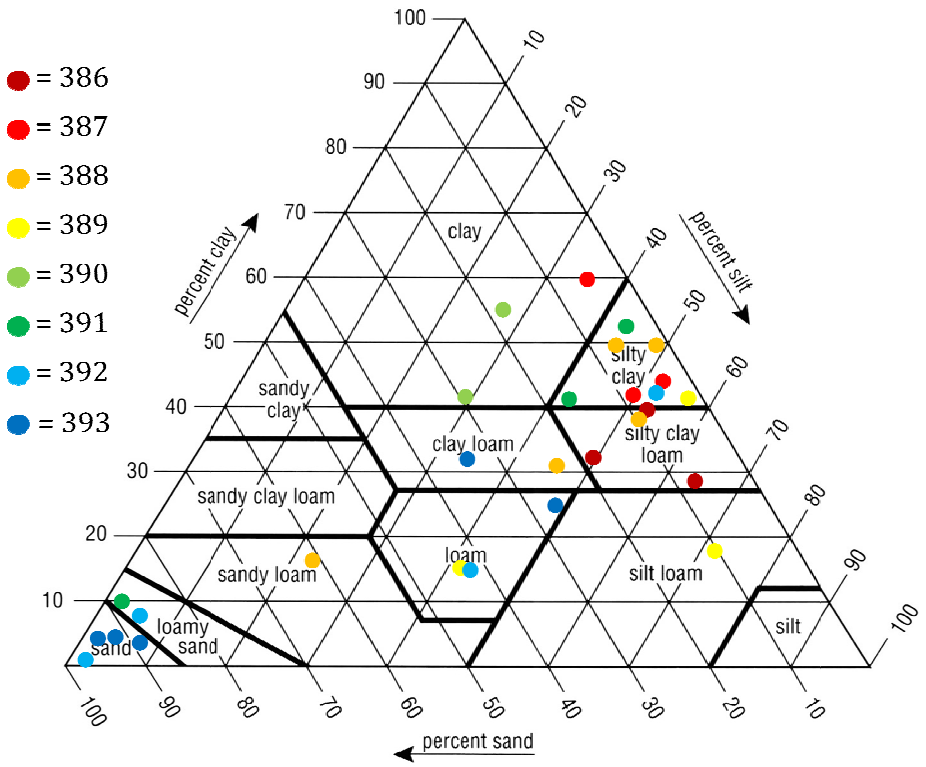

Figure 13: USDA soil texture triangle. Colored dots indicate particle-size distribution of samples taken from Boston Bay.

As it stands, the majority of these samples does not qualify as 'well-graded' and would need to be amended with coarse-grained sediment if it is to be used for engineering purposes. Soils containing high percentages of silt and mud are highly unstable, and will oftentimes transform into a 'quick' when saturated. These soils are highly susceptible to erosion and a process known as piping, where the formation of small, sub-surface tunnels undermines the soils stability (Bray, 2008). Further analysis of the engineering properties of these samples should be conducted including determination of water content, shear strength, bulk density, void ratio, porosity and other geotechnical parameters through methods such as the 'slump test' (USACE, 2004).

While silt- and clay-sized particles make up the majority of the sediment in Boston Bay, close attention should also be paid to the samples containing higher percentages of sand. The gradation curves obtained via sieve analysis indicate that fine-sand components (.10 – .25 mm) appear to dominate. Cores #391-393, taken near the confluence of the bay with Eliza Creek, which empties into Boston Bay from the North, contained the highest levels of sand near their bottoms. Core #393 especially, contained significant amounts of sandy material, possibly due to its proximity to the levee which is covered with sand (Figure 2). Again, further testing is required.

Perhaps what is more interesting about core #393 lies in its potential to shed light into sedimentation rates that exist in Boston Bay. If the hypothesis that the sandy material near this cores bottom-reaches is indeed from the levee, then the silt and clay that have collected on top of the sandier layers, could have been deposited only after the construction of the levees (1930's). A quick measure of the amount (depth) of finer sediment layered on top of the sand, coupled with the construction date of the levee would allow one to make a rough estimate of the rate at which sediment is being deposited at that particular location in the Boston Bay study area.

Taken on an individual basis, sediment-size tended to trend downwards with decreasing core depth. That is, larger particles were generally observed near the bottoms of the cores with finer particles located nearer the cores top. However, this was not the case for every sediment core sample. Core #386, located near the confluence of Boston Bay with the Mississippi River (Figure 2) exhibited the opposite trend. The sample taken from the upper-most horizon of this core contained 20% sand, whereas the lower horizons were composed of only seven and 8% sand respectively (Table 5). Core #389, taken near the outlet of the Bay Island pumping station (Figure 2) exhibited a similar trend with the upper horizon consisting of 45% sand, and the bottom layer only containing 1%. Further studies

into the flow conditions at these locations may be required to explain these anomalies.

Finally, it should be noted that the results from this study closely match data collected during extensive soil surveys of Mercer County, Illinois conducted in 1925 and 2004 (Smith, 1925; USDA, 2004). According to the Soil Survey of Mercer County, Illinois (2004) the land surrounding Boston Bay contains soils that are primarily Fluvaquents (loam), with significant amounts of Coloma sand located on the eastern shore of the bay. The survey also found that the islands and peninsulas that extend into Boston Bay contain soils which consist primarily of Blake-Beaucoup Complex , a silty clay loam (USDA, 2004) (Figure 14).

While such agreement is reassuring, a closer look at the results from the soil survey conducted in 2004 reveals insight into the suitability of such soils as building materials which may be a cause for some concern. Fluvaquents, Blake-Beaucoup Complex and Coloma sands all present severe limitations when used in the construction of embankments, dikes and levees according to the survey (USDA, 2004). The report sites ponding, seepage and piping as reasons why such soils serve as poor candidates for building material. If this is indeed the case, successful construction of berms using the sediment dredged out of Boston Bay would likely require that the dredged sediment be amended with additional, coarse-grained, material and that significant time for dewatering be provided. Further, site-specific, analysis will be required to determine the suitability of the sediment contained within Boston Bay, especially in the proposed dredging locations, as a construction material.

The data obtained during grain-size analysis of sediment found within Boston Bay is only one piece of a much larger puzzle. Close attention must also be paid to the results from chemical analysis, tests to determine the engineering and geotechnical properties of dredged material, as well as information about

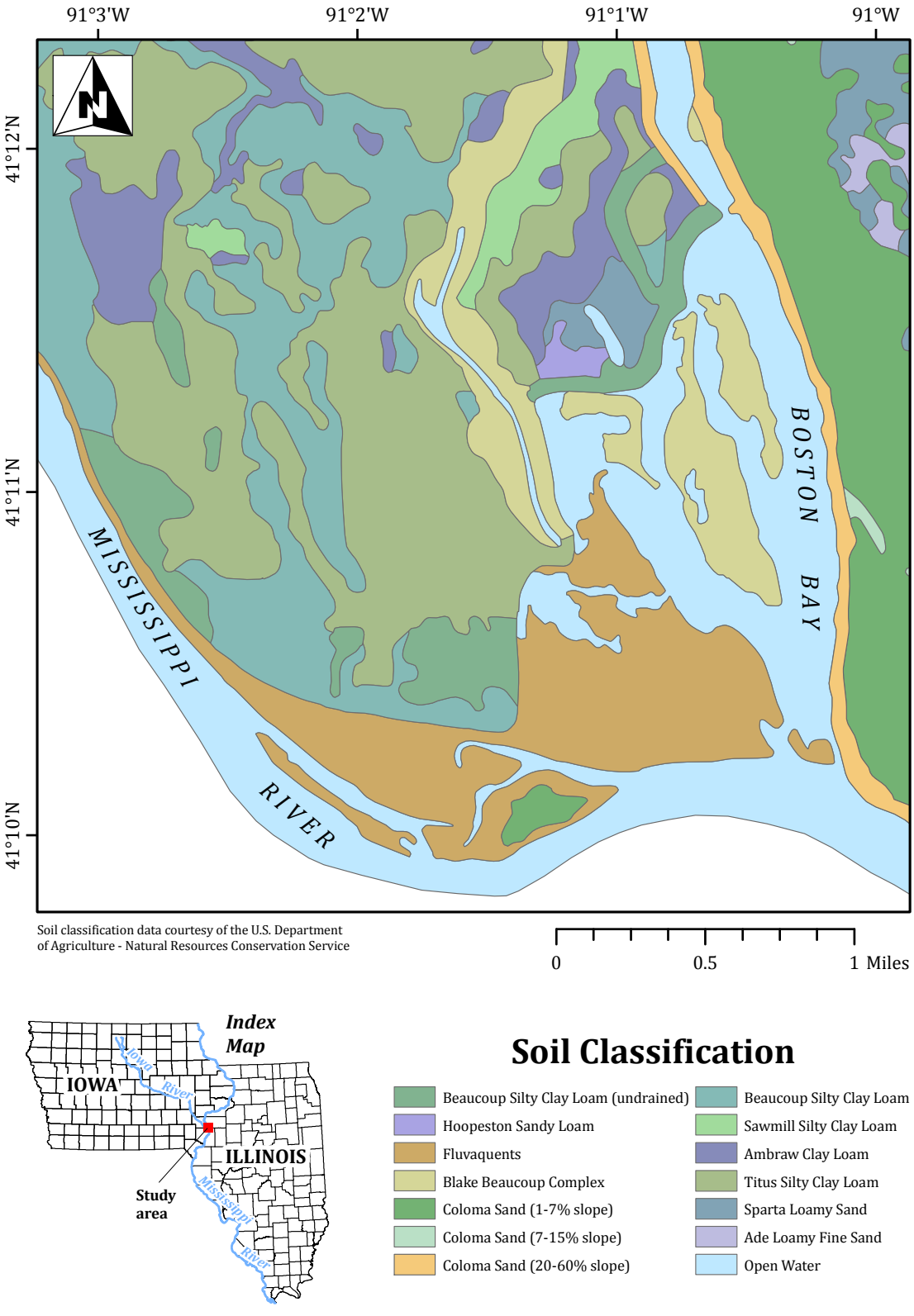

Figure 14: Map displaying results from soil survey of Mercer County, Illinois (USDA, 2004).

sedimentation rates and erosion control practices in the surrounding watersheds. These data, taken together, will serve as a useful tool for decision makers as the proposed dredging of Boston Bay moves forward.

CHAPTER 3 – NITRATE MONITORING OF AGRICULTURAL RUNOFF

3.1 – Background

Since 1985, researchers have been mapping an area off Louisiana's Gulf coast commonly referred to as the 'Dead Zone.' Aptly named, the waters in this region annually exhibit dissolved oxygen concentrations lower than 2 milligrams per liter (mg/L) beginning in early spring and lasting until temperatures begin to decrease in late fall. This condition, termed 'hypoxia,' represents the threshold below which the majority of marine life cannot exist (Leming and Stuntz, 1984; Renaud, 1986; Goolsby and Battaglin, 2000; Rabalais, et al, 1999, 2002). According to findings published in 2000 by the National Science and Technology Council's Committee on Environmental and Natural Resources (CENR), while it is possible for such conditions to occur naturally, the overwhelming scientific evidence points to excessive loads of nitrogen (resulting from human activity) coming from the Mississippi-Atchafalaya drainage basin coupled with hydrologic and climatic factors as the main contributors to the onset and duration of the hypoxic conditions existing in the northern Gulf of Mexico (Vitousek, et al, 1997; CENR, 2000; Mississippi River/Gulf of Mexico Watershed Nutrient Task Force, 2004; Ribaudo, et al, 2005).

Increased levels of nitrogen, primarily in the form of nitrate, can lead to enhanced productivity of phytoplankton algae, a process known as 'eutrophication,' which will ultimately sink to the deeper reaches of the Gulf if not otherwise incorporated into the food web (Rabalais, et al, 1999; CENR, 2000; Beecher, et al, 2001; Mississippi River/Gulf of Mexico Watershed Nutrient Task Force, 2001; Landers, 2008; Conley, et al, 2009). This extra organic material is decomposed by bacteria, a process that consumes large amounts of dissolved oxygen. When the rate at which decomposing microbes use oxygen exceeds the replenishment rate, oxygen concentrations begin to decrease. As the dissolved oxygen content of northern Gulf

waters continues to diminish during the spring and summer months, marine organisms eventually begin migrating to more hospitable regions of the Gulf. Those creatures not capable of escaping hypoxic waters will eventually die, decreasing marine biodiversity, degrading ecosystem services and impacting local community's dependant on the shrimp and fishing industry (Schoonover and Muller, 2002; Osterman, et al, 2006; Booth and Campbell, 2007; Withgott and Brennan, 2007).

Like many estuaries, density differences in the water column off Louisiana's Gulf coast lead to stratification in early spring, with limited mixing between the warm, fresh, nutrient-rich water from the Mississippi River layered above the cold, salty waters of the Gulf. Strongly stratified waters, like those which exist in the Gulf of Mexico oftentimes require heavy winds or even hurricanes to aid in the mixing process. Without such assistance, stratification will remain until late summer or early fall when temperatures begin to decrease and the density of the fresh surface-waters approach that of the submerged salt water (Rabalais, et al, 1996; CENR, 2000). This layering inhibits the deeper waters, where the majority of decomposition occurs, from receiving a steady supply of oxygen from the atmosphere, further exacerbating hypoxic conditions (Wiseman, et al, 1997; Potash and Phosphate Institute, 1999; Laine, et al, 2007).

As mentioned above, human alterations to the Mississippi-Atchafalaya River Basin (MARB) including channelization of streams and rivers, construction of levees to aid in flood control, artificial drainage of wetlands capable of acting as nitrogen sinks, and application of nitrogen-based fertilizer to agricultural lands all contribute to the increased delivery rate of nitrogen-rich waters to the Gulf (Mitsch, et al, 2001, 2005). It is estimated that during the last 200 years, 35 million acres of wetlands existing in the MARB have been artificially drained to aid in agricultural practices (CENR, 2000). Ohio, Indiana, Iowa and Illinois alone have seen roughly 80 percent of their original wetlands drained (Mitsch and Day, 2006). Additionally, many of the

wetlands and backwaters not drained for farming purposes were eventually isolated from the main channel of the Mississippi River following the construction of the locks, dams and levees in the 1930's, thus limiting their role as productive nutrient filters (Phipps and Crumpton, 1994; Mitsch and Day, 2006; Strauss, et al, 2006; Bukaveckas, 2007).

Furthermore, the increased application rate of nitrogen-based fertilizer to the heavily farmed watersheds of the MARB significantly adds to the load of nitrate-nitrogen entering the Gulf. Research indicates that nitrogen fertilizer application experienced significant expansion between the 1950s and 1980s when nitrogen inputs to the Gulf more than tripled and crop harvest increased by about 2.4 times (Goolsby, et al, 1999; CENR, 2000; Goolsby and Battaglin, 2000). Altogether, agricultural sources are thought to contribute to 74 percent of the nitrate and 65 percent of the total nitrogen carried by the Mississippi River to the Gulf of Mexico (Withgott and Brennen, 2007; Landers, 2008). Agricultural runoff, along with atmospheric deposition of nitrogen would fall under the category of 'nonpoint' source pollution, which, as of 2008, was thought to be responsible for 78 percent of the nitrogen loading to the Gulf. The other 22 percent coming from 'point' sources like industrial manufacturing facilities and municipal wastewater treatment plants (Landers, 2008; Mississippi River/Gulf of Mexico Watershed Nutrient Task Force, 2008)

While anthropogenic alterations contributing to the heightened levels of nitrogen loading to the Gulf of Mexico exist all throughout the MARB, findings indicate that the principle sources of nitrate leading to Gulf hypoxia reside in the Upper Mississippi River Basin (UMRB), above the confluence with the Ohio River (Alexander, et al, 2008, Landers, 2008). Watersheds in the UMRB that are heavily farmed and artificially drained by sub-surface tile lines are thought to be the major contributors to the hypoxic conditions that exist in the Gulf of Mexico (CENR, 2000;

USGS, 2000; Randall and Mulla, 2001; Keeney, 2002; Tomer, 2003). It is estimated that 56 percent of the total nitrate load transported to the Gulf enters the Mississippi River above the Ohio River, primarily in the form of agricultural runoff coming from the intensely cultivated, unnaturally drained watersheds of southern Minnesota, Indiana, Iowa and Illinois (Goolsby, et al, 1999; CENR, 2000).

3.2 – Methods

3.2.1 – Measurement of Nitrate Concentration

The Bay Island Drainage and Levee District (BIDLD) is just one of the many artificially drained agricultural watersheds in the UMRB described above. Located along Illinois' western border with the Mississippi River, this 24,000 acre drainage district is protected from flooding by 25 miles of manmade levee and contains nearly 500 acres of drainage ditches (Marston, 2009) (Figure 4). Agricultural runoff is pumped year-round out of the district, over the levee, and into Boston Bay before entering the flows of the Mississippi and eventually the Gulf of Mexico.

In June of 2008, Living Lands & Waters (LL&W) decided to include water quality enhancement as another piece to the proposed restoration of Boston Bay. Specifically, LL&W was interested in reducing the concentration of nitrate-nitrogen in the waters entering Boston Bay via the BIDLD. Different ideas, including nutrient retention ponds, and augmentation of the dissolved oxygen levels in the drainage ditch upstream from the pump intake were explored, but none were ever implemented.

At the request of LL&W, IIHR installed a Nitratax real-time nitrate-nitrogen sensor at the drainage district's pump intake in October of 2008 to monitor the concentration of nitrate-nitrogen entering Boston Bay via the drainage district (Figure 2). This was done in hopes of establishing a baseline dataset that could be

used to help determine the most appropriate methods for improving the quality of runoff being pumped into Boston Bay. Data was collected around the clock, from October 21, 2008 until June 3, 2009.

Following installation, the nitrate sensor was wired to a Hach sc1000 data logger located inside the pumping station. The data logger was linked to a laptop computer where results were easily downloaded as a text file. It was decided that readings would be recorded every half-hour to help conserve the data logger's memory, and cut down on analysis. On multiple occasions turbidity, organic content and nitrate concentration became high enough that the sensors range of measurement was exceeded, resulting in a noisy data set which had to be clarified during post-processing. The data collected during this exercise have been displayed as a series of plots of nitrate concentration versus time.

3.2.2 – Estimate of Nitrate Load

Taken on its own, the data collected with the nitrate sensor tells us little more than the concentration of nitrate-nitrogen at one particular spot in a much larger watershed. However, if nitrate concentration is coupled with information about the discharge from the Bay Island pumping station, then it is possible to estimate the total load of nitrate-nitrogen coming into Boston Bay via the drainage district. Daily maintenance logs for the three pumps operated by the drainage district contain information about when the pumps are turned on and off, as well as the speed n (rpm) at which the pumps are operating. Given the maximum capacity that the pumps are capable of performing (Q_1, n_1), the pump affinity law

$$\frac{Q_1}{Q_2} = \frac{n_1}{n_2} \qquad (4)$$

(Mays, 2005) is used to calculate pump discharge Q when operating at other, known values of n. For example, Pump #2 is capable of discharging 100,000 gallons per minute (Q_1) when operating at a speed of 1,210 rpm (n_1) (Marston, 2009). If, as is often the case, the speed is turned down to 1,060 rpm (n_2), the pump discharges at 87,600 gallons per minute (Q_2) as found using Equation 4. The specifications for each pump are summarized in Table 9.

Pump #	Maximum Speed (rpm)	Maximum Discharge (gal/min)
1	1,530	100,000
2	1,210	100,000
3	1,210	65,000

Table 9: Specifications for each pump at the Bay Island Drainage and Levee District pumping station, including maximum pump speed (n) and discharge (Q) (Marston, 2009).

Once pump discharge is calculated, the total volume of water being pumped into Boston Bay can be found by simply multiplying pump discharge by total operating time, which can then be converted to mass of nitrate-nitrogen by multiplying by the nitrate concentration. Continuing with this idea, an estimate of the total load of nitrate-nitrogen entering Boston Bay from the drainage district is easily obtained by summing the product of nitrate concentration, discharge, and pump operating time over the duration of time the sensor was deployed in the field (Equation 5).

$$\sum C[NO_3^-]Q\frac{n'}{n}t \qquad (5)$$

Here nitrate concentration ($[NO_3^-]$) is measured in mg/L, maximum discharge (Q) is given gallons per minute (gal/min) and time (t) is in minutes. The fraction (n'/n) represents the ratio of the speed at which the pump runs once the engine has been turned down as delegated by the pump station engineer (n') to the maximum pump speed (n), both in rpm. The constant C must be included to account for the conversion of the discharge in gal/min to L/min and has a value of 3.785. The resulting expression gives a value for total load of nitrate in milligrams, which can easily be converted to pounds or tons. An example of this calculation can be found in the Appendix.

3.3 – Analysis and Results

3.3.1 – Concentration of Nitrate-Nitrogen

The data obtained from the nitrate-nitrogen sensor is perhaps most easily displayed as a series of plots of nitrate concentration versus time (Figures 15 – 21). For the sake of consistency, data collected during the end of October, 2008 and at the beginning of June, 2009 were excluded as these did not represent complete data sets collected over an entire month of sensor deployment. Rather, only the data collected from November 1, 2008 through May 31, 2009 was reported in this thesis.

From these figures, one can easily see a correlation between nitrate concentration and precipitation events, as indicated by sudden spikes in the data set (see December, February, March, April and May). The abrupt increases in measured nitrate concentration during the month of May, 2009 (Figure 21) shows direct correspondence with rainfall events occurring in the general vicinity of the nitrate

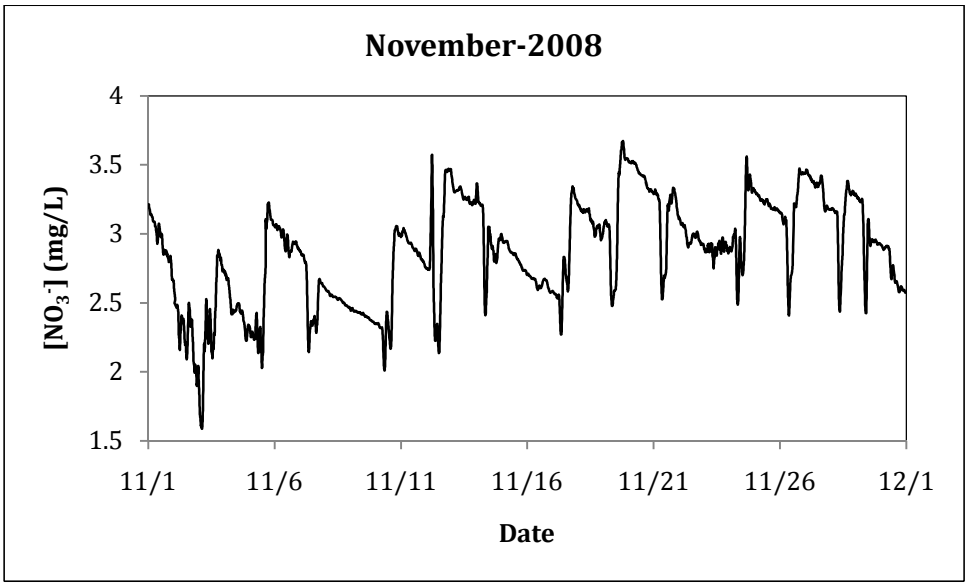

Figure 15: Nitrate-nitrogen concentration of agricultural runoff entering Boston Bay via the Bay Island Drainage and Levee District for the month of November, 2008.

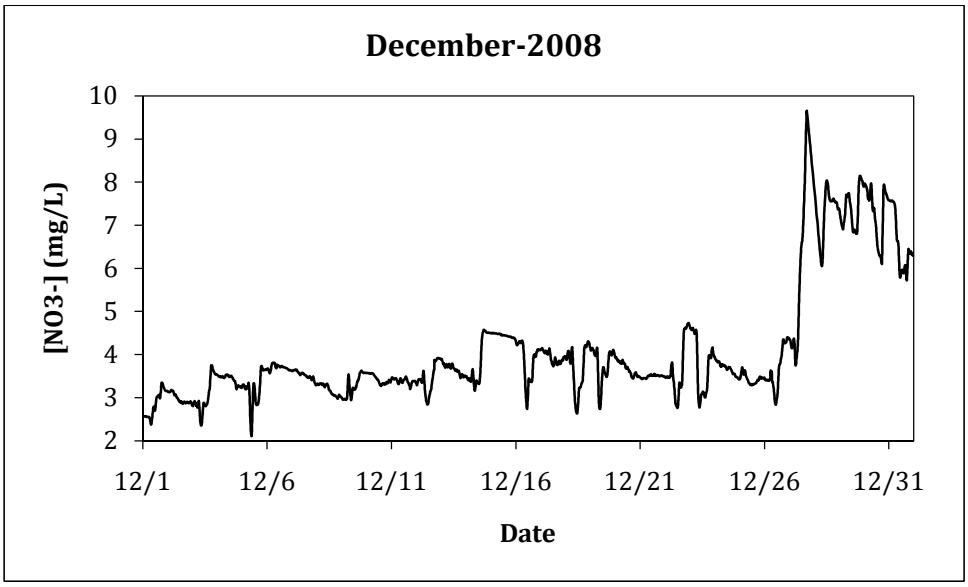

Figure 16: Nitrate-nitrogen concentration of agricultural runoff entering Boston Bay via the Bay Island Drainage and Levee District for the month of December, 2008.

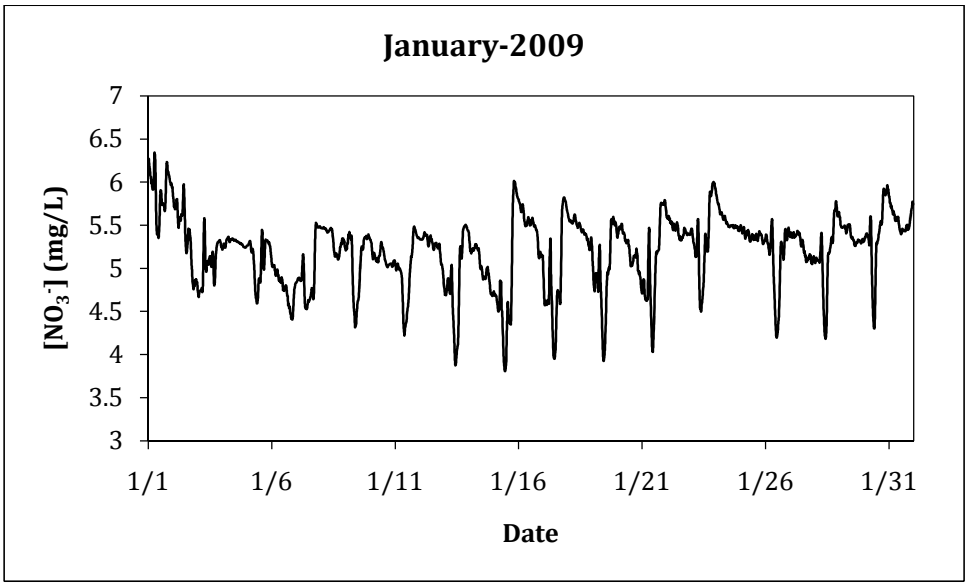

Figure 17: Nitrate-nitrogen concentration of agricultural runoff entering Boston Bay via the Bay Island Drainage and Levee District for the month of January, 2009.

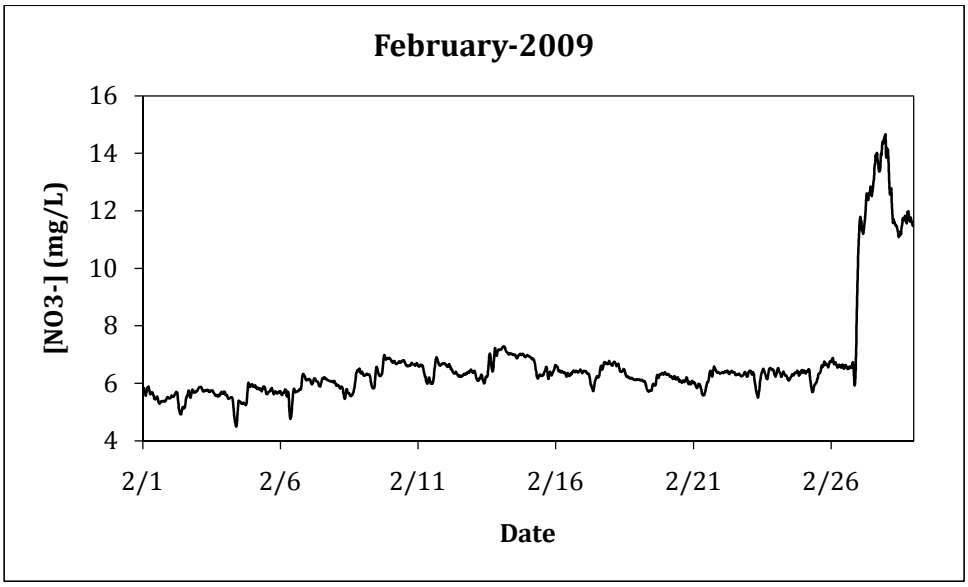

Figure 18: Nitrate-nitrogen concentration of agricultural runoff entering Boston Bay via the Bay Island Drainage and Levee District for the month of February, 2009.

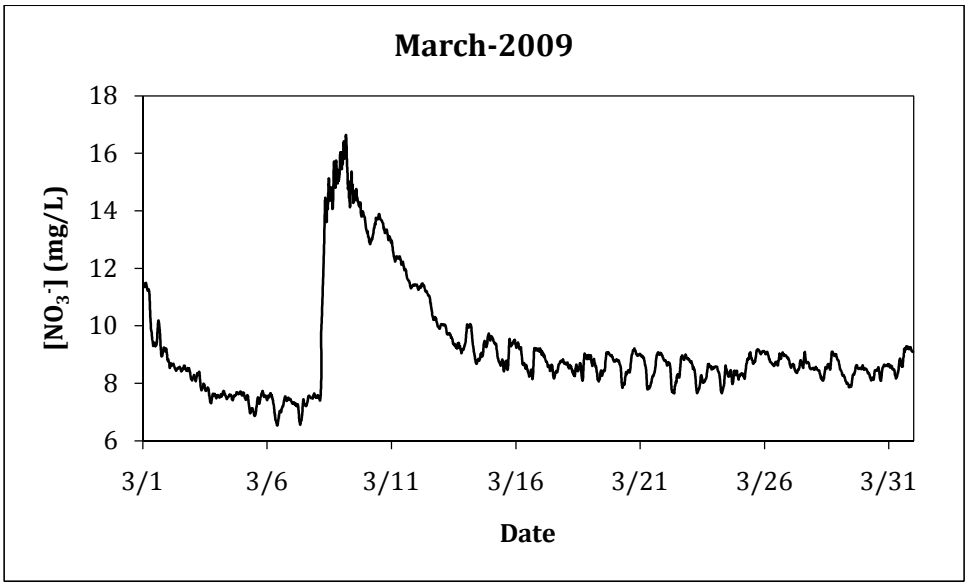

Figure 19: Nitrate-nitrogen concentration of agricultural runoff entering Boston Bay via the Bay Island Drainage and Levee District for the month of March, 2009.

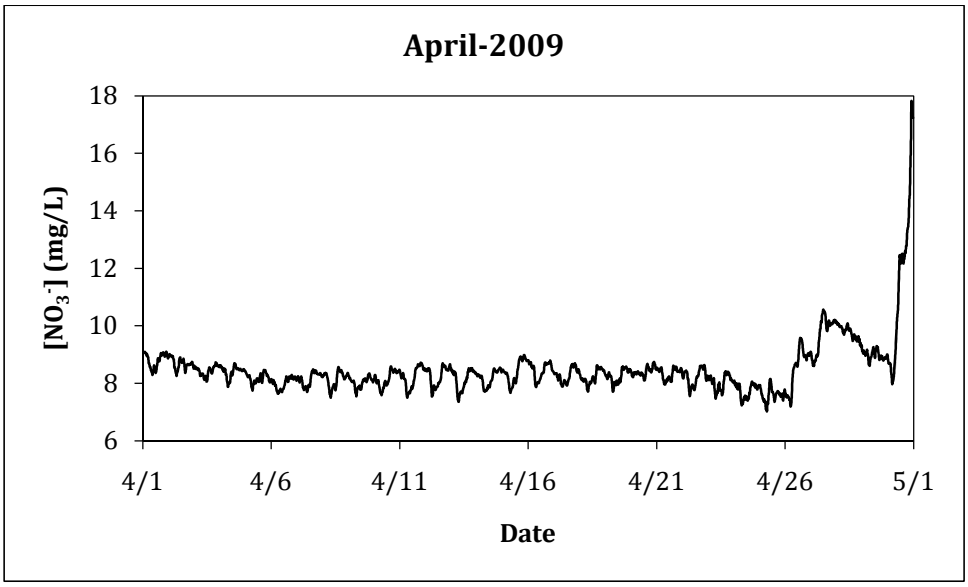

Figure 20: Nitrate-nitrogen concentration of agricultural runoff entering Boston Bay via the Bay Island Drainage and Levee District for the month of April, 2009.

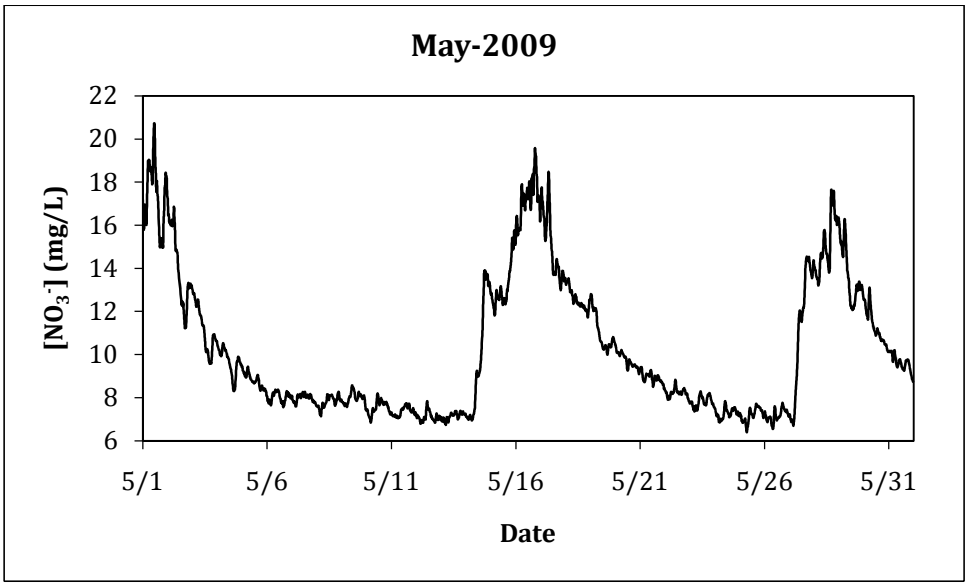

Figure 21: Nitrate-nitrogen concentration of agricultural runoff entering Boston Bay via the Bay Island Drainage and Levee District for the month of May, 2009.

sensor on April 30, May 14 and May 27, 2009 as reported by the BIDLD rain gauge (Marston, 2009). Other research has indicated that fertilizer runoff may quickly enter bodies of water following storms and heavy rainfall, greatly increasing nutrient concentrations in streams and rivers of the Midwest (Schnoebelen, et al, 1999; Kalkhoff, et al, 2000; Beecher, et al, 2001).

It is also evident that measured nitrate concentrations tend to exhibit seasonal variations, as evidenced by the upward trends in nitrate concentration during the spring season (March/May) as compared with those measured during the fall (November). Agricultural runoff from watersheds of the Midwest typically possess larger concentrations of nitrate in the spring as a result of fertilizer application and rainfall events, capable of mobilizing large amounts of nitrate to drainage networks and streams (Castillo, et al, 2000; Schnoebelen, et al, 2003). On the other hand, reduced nitrate concentrations are generally observed during the summer growing season and fall months as plants use nitrogen-based fertilizer

while runoff and rainfall amounts decrease (Roberts and Marsh, 1987; Schnoebelen, et al, 1999, 2003; Kalkhoff, et al, 2000; Beecher, et al, 2001; James, et al, 2008a). Similarly, aquatic vegetation in the form of algae act to process much of the nitrate entering rivers and streams during this part of the year, resulting in algal blooms and a decrease in measured nitrate concentrations (Isenhart and Crumpton, 1989; Sorenson, et al, 1999; Porter, et al, 2000).

Given that the nitrate monitor was only deployed during the first three days of June, 2009 little can be said about observed trends in nitrate concentration of the agricultural runoff being pumped into Boston Bay during summer months, other than the average nitrate concentration over those three days was 7.794 mg/L, and is lower than the average nitrate concentration observed during the spring months (March/May). Averages for each full month that the nitrate sensor was deployed in the field were calculated and have been displayed in Table 10, with May exhibiting the highest average nitrate concentration, and November experiencing the lowest concentration with 10.271 and 2.867 mg/L, respectively.

Month	Average (mg/L)
Nov.	2.867
Dec.	4.028
Jan.	5.212
Feb.	6.624
March	9.181
April	8.478
May	10.271

Table 10: Monthly averages of nitrate-nitrogen concentration observed in the drainage ditch upstream from the Bay Island Drainage and Levee pump intake.

In general, the nitrate concentration of the agricultural runoff entering Boston Bay from the neighboring drainage district was observed to be much lower on average during late fall and winter when compared to the concentrations measured during spring. The highest measured nitrate concentrations occurred during the spring, with a maximum value of 20.738 mg/L being observed on May 1, 2009 following a heavy rainfall event on the previous day. This is over two times the 10 mg/L maximum contaminant level (MCL) established by the U.S. Environmental Protection Agency for drinking water (1986), and could have detrimental effects to humans and livestock (Bruning-Fann and Kaneene, 1993; Knobeloch, et al, 2000; Sturgul and Kelling, 2003). Conversely, the minimum nitrate concentration measured during this study was observed on November 3, 2008 with a value of 1.586 mg/L.

3.3.2 – Total Nitrate-Nitrogen Load

According to the pumping stations daily maintenance logs, the Bay Island Drainage and Levee District pumped over 7,800,000,000 gallons of agricultural runoff into Boston Bay during the time period over which nitrate concentrations were being monitored. Additionally, the three pumps operated by the drainage district ran for a total of 4,280.5 hours during this study (Marston, 2009). Carrying out the calculation described above (using Equation 5) for the duration of time the monitor was deployed in the field while paying close attention to when the pumps were in operation one finds that 7.1998×10^{11} mg, or 1,587,267 pounds of nitrate-nitrogen was pumped into Boston Bay via the neighboring drainage district.

Dividing this figure by the total acreage of the drainage district (24,000 acres) a value of 66.136 lbs/acre is obtained. This seems reasonable as farmers in this watershed typically apply nitrogen-based fertilizer at an annual rate of roughly 100 lb/acre (Marston, 2009). Clearly this estimate would represent a lower limit, as

the nitrate sensor was not deployed for an entire year, and no data exists from early June through mid-October. However, since nitrate concentrations in agricultural runoff are typically much lower during this part of the growing season, as mentioned earlier, one is justified in assuming that this estimate is within the ballpark of the actual value.

3.3.3 – Other Observed Trends

In addition to monitoring the concentration and estimating the total load of nitrate being pumped into Boston Bay other, more subtle, trends in the dataset collected during this process were also explored in further detail. A quick glance at Figures 15-21 reveals that the measured concentration of nitrate-nitrogen is heavily dependent on the speed at which the flow is moving past the sensor (i.e. whether or not the pumps are running). Figure 22 clearly indicates a strong relationship between nitrate concentration and pump operation. Concentration of nitrate-nitrogen rapidly decreases immediately after the pumps have been turned on (represented with a vertical dotted line) and then gradually begin to increase again once the pumps have stopped operating (represented with a vertical dashed line).

Nitrate-nitrogen concentrations eventually level out until the pumps are tuned on again, and the cycle repeats itself. This trend seems to disagree with work done by others who have shown that nitrate concentrations tend to increase with increasing flow velocity (Horng-Guang, 1996). Since no data exists about the speed that water flows past the monitor, a relationship between nitrate-nitrogen concentration and flow velocity cannot be deduced at this time. However, it is clear that the measured concentration of nitrate-nitrogen is highly sensitive to whether or not the pumps are running.

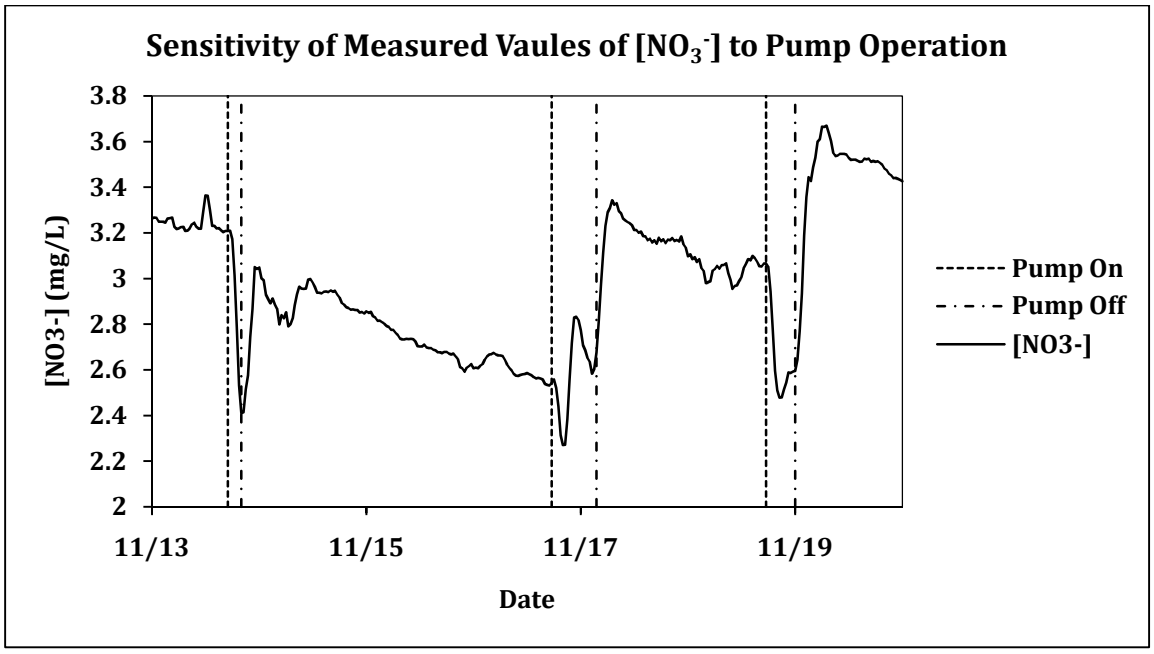

Figure 22: Plot highlighting the sensitivity of measured values of nitrate-nitrogen concentration to pump operation for the week of 11/13 - 11/20, 2008. Dotted lines indicate the times that pumps are turned 'On' - dashed lines represent when the pumps are turned 'Off.'

There is another interesting trend in the data set which occurs only when the pumps are not in operation. A closer look at the plots of nitrate-nitrogen concentration versus time (Figures 15-21) indicates that while the pumps are turned off, nitrate-nitrogen concentrations tend to slowly decrease with time at a relatively constant rate. As an example, Figures 23 and 24 show that, during the month of November, nitrate-nitrogen concentrations decreased at an average rate of 0.1667 mg L^{-1} day^{-1} during periods when the pumps were not in operation (Table 11). November is not a special case, as similar trends are observed each time the pumps are turned 'off.' This may be a measure of the rate of denitrification (the process whereby nitrate is reduced to nitrite and eventually nitrogen gas) by microorganisms living just beneath the sediment-water interface as this is where significant nitrogen removal is thought to occur (Seitzinger, 1988; Saunders, 2001)

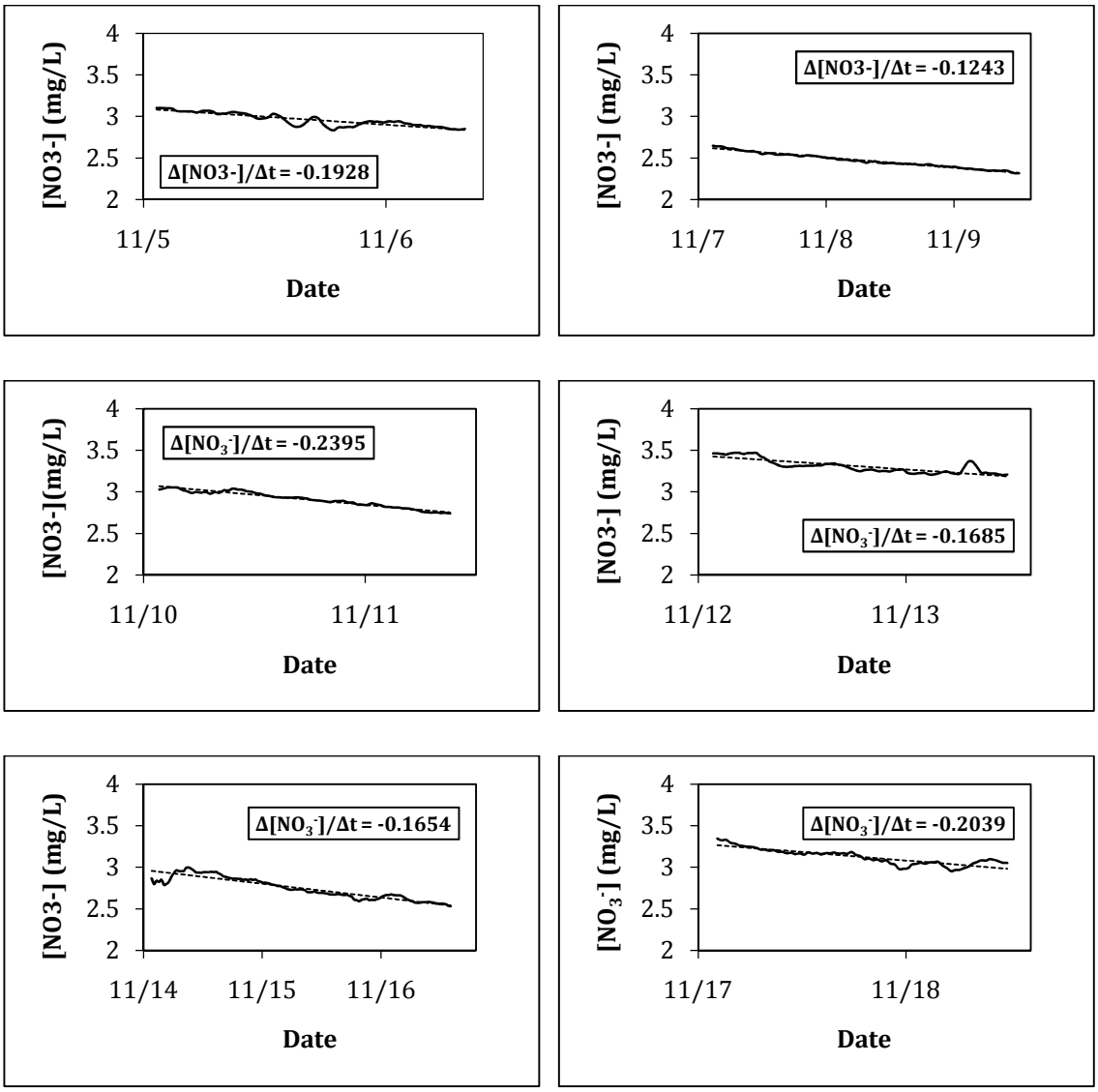

Figure 23: Curves displaying the rate (mg_{NO3-} L^{-1} D^{-1}) at which nitrate-nitrogen concentration decreases with time while the Bay Island Drainage and Levee Districts pumps are not operating (11/5 – 11/18). Here, concentration of nitrate-nitrogen (mg/L) is plotted on the y-axis, while the date is plotted along the x-axis. Trendline is dashed.

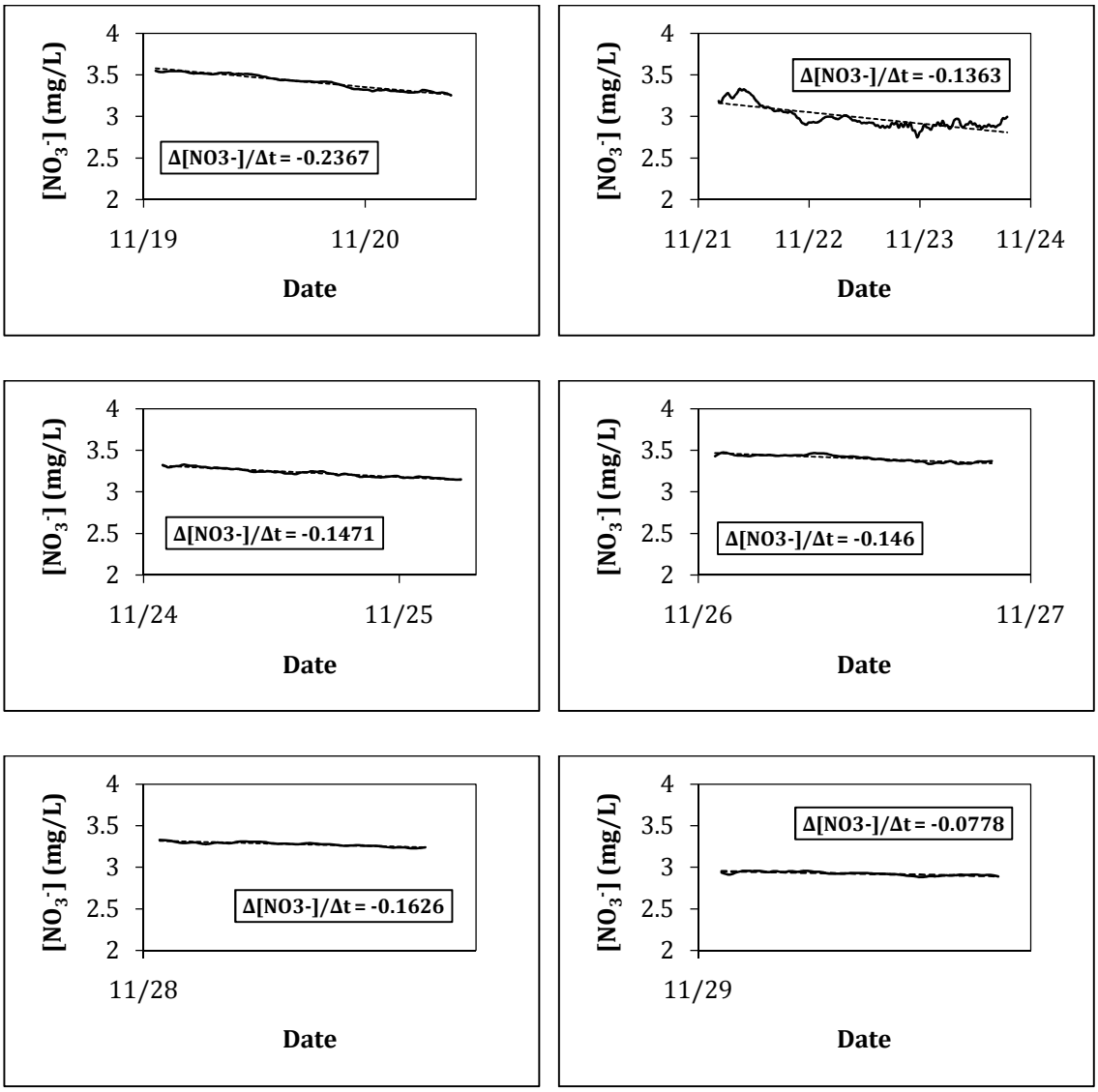

Figure 24: Curves displaying the rate (mg_{NO3-} L^{-1} D^{-1}) at which nitrate-nitrogen concentration decreases with time while the Bay Island Drainage and Levee Districts pumps are not operating (11/19 – 11/29). Here, concentration of nitrate-nitrogen (mg/L) is plotted on the y-axis, while the date is plotted along the x-axis. Trendline is dashed.

Date	$\Delta[NO_3^-]/\Delta t$ (mg L^{-1} d^{-1})
11/5 - 11/6	-0.1928
11/7 - 11/9	-0.1243
11/10- 11/11	-0.2395
11/12 - 11/13	-0.1685
11/14 - 11/16	-0.1654
11/17 - 11/18	-0.2039
11/19 - 11/20	-0.2367
11/21 - 11/24	-0.1363
11/24 - 11/25	-0.1471
11/26 - 11/27	-0.146
11/28	-0.1626
11/29	-0.0778
Average	-0.1667
Standard Dev.	0.0464

Table 11: Rate that nitrate-nitrate concentrations change with time during periods when pumps at the Bay Island Drainage and Levee District are not in operation (November, 2008).

and the monitor is positioned only a few inches above the boundary layer. Further investigation is required to test this hypothesis.

3.4 – Discussion

Unfortunately it was not possible to deploy the nitrate monitor at the Bay Island pumping station for an entire year. However, this exercise reveals many valuable applications for monitoring nitrate-nitrogen levels of artificially drained farm runoff. If other drainage districts in the Upper Mississippi River basin adopted

similar monitoring practices, identifying those watersheds that would benefit the most from best management practices (BMPs) to help reduce nitrate loading would be a much easier task.

The careful targeting of programs to areas of higher pollutant loadings could enhance the effectiveness of conservation programs designed to reduce nitrate loading to the Mississippi River (and ultimately the Gulf of Mexico) such as the Conservation Reserve Program (CRP) and the Wetlands Reserve Program (WRP) (CENR, 2000; Mississippi/River Gulf of Mexico Watershed Nutrient Task Force, 2001; Landers, 2008, National Resources Conservation Service, 2009). Targeting USDA conservation programs to areas of higher nutrient and sediment loadings can lead to BMPs for control of runoff containing sediment and nutrients being implemented on lands that are the primary sources of nonpoint pollutants and major contributors to the hypoxic conditions existing in the Gulf of Mexico (CENR, 2000; National Research Council, 2008).

As mentioned above, agricultural runoff is grouped into the category of non-point source pollution because the potential pollutants originate over large, diffuse areas and the exact point of entry into water bodies cannot be precisely identified. Non-point sources of pollution are particularly problematic in that it is difficult to capture and treat the polluted water before it enters a stream (Smith, et al., 2003). Treatment of such nonpoint source pollution is made even more difficult when one takes into account the fact that nitrate levels in agricultural runoff are not regulated by the Federal Water Pollution Control Act, popularly referred to as the Clean Water Act (1972) (Landers, 2008). This is especially troubling when viewed in the context of Gulf hypoxia as recent estimates claim that 78 percent of the nitrate-nitrogen entering the Gulf of Mexico comes in the form of agricultural, nonpoint, pollution (Landers, 2008; Mississippi River/Gulf of Mexico Watershed Nutrient Task Force, 2008).

The Bay Island Drainage and Levee District, and the runoff it discharges into Boston Bay, presents a unique opportunity to effectively treat nonpoint pollution before entering the Mississippi River. While most agricultural runoff enters streams and rivers over large, diffuse areas, the runoff being discharged into Boston Bay from the drainage district enters through one single location via three large pipes (Marston, 2009). That being said, the drainage district and its pumping station could technically be viewed as a 'point' source polluter, and could be addressed using traditional 'end-of-pipe' treatment methods. Strategically placed treatment wetlands like those described by Mitsch (2005, 2006) might be a practical solution to help reduce concentrations of nitrate-nitrogen in the waters of Boston Bay before they join the flows of the Mississippi River, ultimately contributing to the larger issue of Gulf Hypoxia.

The data set obtained during this study will undoubtedly provide LL&W and other interested parties with vital information, should they choose to explore options to improve the water quality of Boston Bay in the future.

CHAPTER 4 – BATHYMETRIC MAPPING

4.1 – Backgound

Restoration efforts which involve dredging should include in their planning and design process a detailed analysis of the physical, chemical, biological and geological properties of the proposed site location (Herbich, 1992; Bray, 2008). It is equally important to incorporate bathymetric surveying of the study area into the early phases of the project (USACE, 1998; Bray, 2008). Given the fact that many dredging activities involve contract payments based on a cost-per-unit-volume of sediment removed, an accurate understanding of the existing bathymetry of the project area is vital to properly determining payment for services rendered (Herbich, 1992; USACE, 1998). Such surveys are also commonly conducted during and after dredging projects to monitor progress, and supplement final contract acceptance (USACE, 1998)

Dredging activity will undoubtedly lead to alterations of the flow conditions in the project area resulting from the reshaping of the existing bathymetry (Herbich, 1992). These changes in flow may have an effect on sedimentation patterns which will, in turn, impact the bathymetry once again. This cycle of physical changes can only occur following the initial perturbation of the existing bathymetry (Bray, 2008). Again, surveying should be performed both before and after dredging takes place to accurately analyze the resulting environmental effects which depend heavily on the conditions of the study area prior to the start of the project (Gayman, 1978; Herbich, 1992; Smith, 1995; USACE, 1998; Bray, 2008; Sarretta, et al, 2009).

Preliminary bathymetric mapping is also helpful in assisting with other comparative studies used to determine sedimentation and erosion rates (Foyle and Norton, 2006; Smith, et al, 2007; Linhart and Lund, 2008), designing hydrodynamic models (Maa, et al, 2001; Wagner and Mueller, 2001; Huizinga, 2008), long-term

monitoring of offshore dredged material disposal facilities (Holcombe, et al, 1997; Fredette and French, 2004; Lepland, et al, 2009) and developing relationships between water level (stage), area and volume for wetlands, lakes and reservoirs (Haag, et al, 2005; Wilson and Richards, 2006). Surveys conducted to assist with such efforts provide a collection of baseline data against which future work can be compared (Sherwood, et al, 1990; DeWitt, et al, 2007; Linhart and Lund, 2008).

In a similar effort, the initial analysis conducted in response to the proposed restoration of Boston Bay included a detailed study of the physical and chemical properties of the study area, as well as a survey to determine the existing bathymetry of the bay. The results of the survey will be used in the design stages of the planned dredging activity as well as help with the construction of a numerical model capable of simulating the planned restoration. Data collected during the survey will serve as the baseline that future studies of Boston Bay will be compared against when determining sedimentation and erosion rates, developing relationships between stage and volume, or assessing contract payment.

4.2 – Methods

4.2.1 - Data Collection

The bathymetric survey of Boston Bay was conducted over a two day period on March 30 and 31, 2009 by IIHR research staff and engineers. Bathymetric data were collected over all navigable areas of the bay through the use of a survey-grade, single-beam fathometer for water-depth data, while a real-time kinetic global positioning system (RTK GPS) was used to collect corresponding horizontal position and elevation data. Survey transects were spaced roughly 150 ft apart, with higher density data collection occurring in areas of greater interest. The data sets were

then integrated using a hydrographic surveying software package and used to create a bathymetric surface of the study area.

Measurements of elevation taken during this survey are referenced to a temporary benchmark located on the northeast corner of the handicapped boat ramp at New Boston, Illinois with an elevation of 547.146 ft, mean sea-level datum of 1912 (MSL 1912), measured using differential GPS survey techniques. This was done to compensate for the fact that no benchmarks with known elevation exist within close proximity to the study area.

Water-depth data were collected by employing an Odom Hydrotrac HT100 single-beam echo sounder with a 200 kilohertz (kHz) transducer, capable of reporting depth measurements with an accuracy of +/- 0.4 inches according to manufacturer specifications (Odom Hydrographic Systems, 2007). Such a device determines water depth by measuring the elapsed time an acoustic pulse takes to travel from the bottom of the transducer to the bed material and back (Kress, et al, 2005; Wilson and Richards, 2006).

Travel time (t) for an acoustic pulse depends on the speed of sound in water (v) and the distance (D) between the face of the transducer and the bed material. After some rearrangement this relationship can be expressed as follows:

$$D = 1/2vt \qquad (6)$$

The distance (D) in Equation 6 corresponds to the measured water depth and, when added to the known distance between the water surface and the face of the transducer, the overall water depth is determined.

The echo-sound equipment was mounted to hang over the port (left) side of the survey vessel; an 18 ft, tunnel-hull, Polar Kraft equipped with a 60 horsepower, Mercury, four-stroke engine. The boat typically traveled at a speed of

three to five miles per hour, with the echo-sounder emitting five acoustic pulses every second. The resulting water-depth data set consisted of a high density of points (1 ft spacing) along survey lines, with larger gaps (150 ft) between survey cross sections (Figure 25).

Horizontal and vertical coordinates of the water-depth data collected with the echo-sounder were determined using RTK GPS techniques achieved using a Trimble R8 global navigation satellite system (GNSS). This equipment consists of a base station set up over the temporary benchmark described above and a mobile rover unit mounted on an antenna positioned directly above the echo-sounder, capable of measuring horizontal and vertical position with centimeter accuracy (Trimble Navigation Limited, 2009). Position corrections are sent from the base station to the mobile unit correcting for errors induced by satellite-clock errors and atmospheric delays (Conaway and Moran, 2004; Hornewer and Flynn, 2008).

The data sets from the echo-sounder and the RTK GPS survey equipment were streamed in real-time to a laptop computer stored onboard the survey vessel containing the hydrographic surveying software package Hypack 2008. This software integrates the data streams from the various components into a single data file, with each device referenced by a unique identification code and the data time-stamped to the nearest millisecond (DeWitt, et al, 2007). The water-depth values are easily converted to bed elevations by subtracting from the measured elevation of the RTK GPS antenna the sum of the known distance from the antenna to the transducer and the measured depth. The resulting data were exported from Hypack as an x, y, z (latitude, longitude, elevation) scatter set consisting of 181,974 data points with the elevation values referenced to MSL 1912 and the horizontal position referenced to the North American Datum of 1983 (NAD 83). These data were then imported into a geographic information system (GIS) database for further analysis.

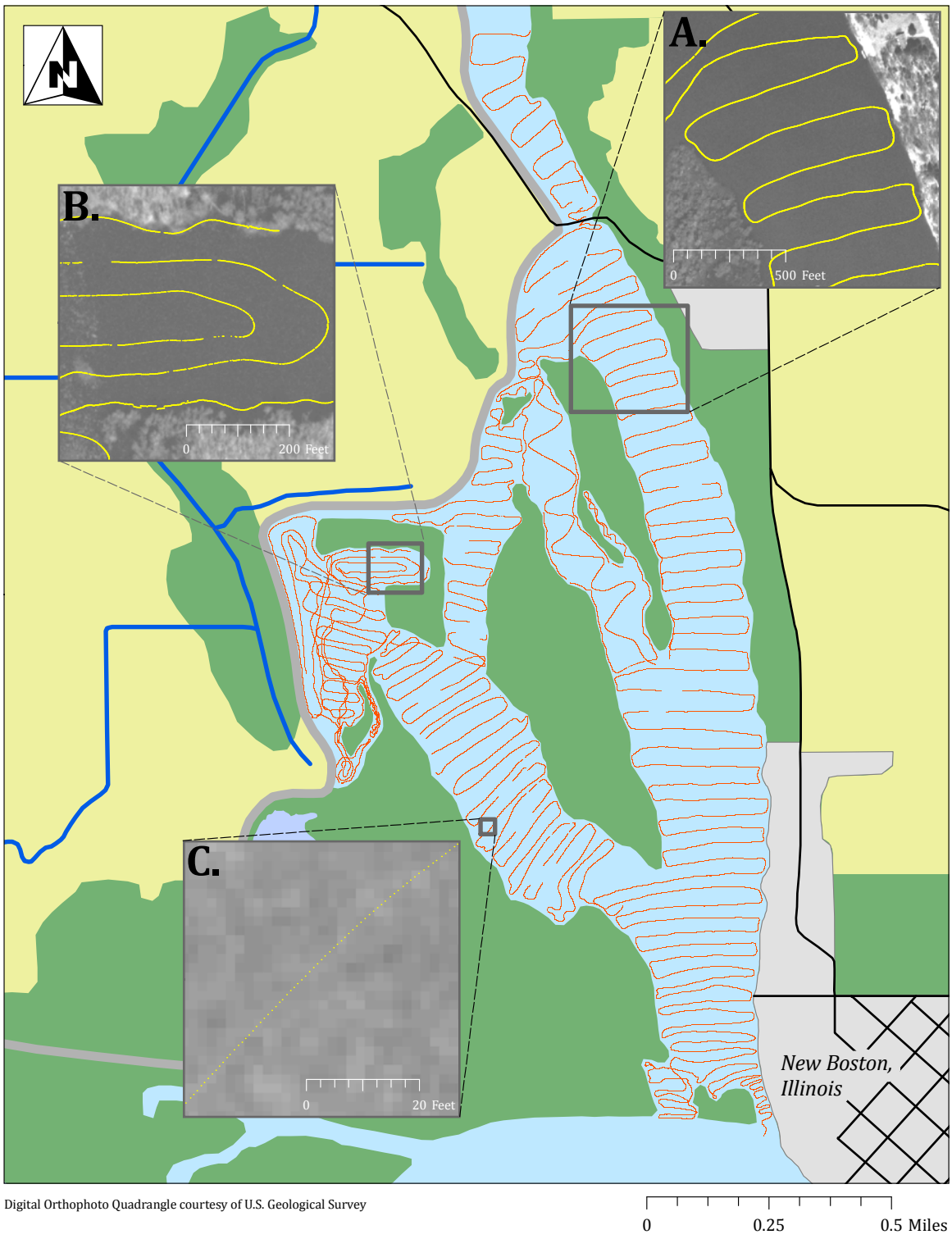

Figure 25: Bathymetric survey data (red/yellow) collected along transects spaced roughly 150 ft apart (A). In areas of higher interest, including 'Bell's Pocket,' transects were spaced much more closely (B). Individual data points were separated by 0.90 ft depending on the boat speed and echo-sound frequency (C).

4.2.2 – Data Processing

Raw, geo-referenced bathymetry data are edited to remove any spurious data including points that are much higher or lower than nearby points, errors resulting from boat pitch and roll, or data points that may have been affected by submerged vegetation or objects that obstruct the bed material from the transducer. This is most easily achieved by displaying transect data plots of bed elevation as a function of distance along a given transect (White and Hodges, 2005; White, et al, 2006; Furnans and Austin, 2008; Mastin and Fosness, 2009). Points that are obviously in error are removed from the data set (Figure 26).

The edited scatter set is then displayed in a GIS with an aerial photo of the study area to help define the survey boundary. Delineation of the boundary was performed using Aquaveo's, Surface Water Modeling System (SMS) resulting in a polygon shapefile of the extent of the bathymetry survey. This extent polygon was then converted to a two-dimensional hybrid mesh consisting of 49,493 nodes and 85,543 elements. The elevation (z) values from the scatter set are interpolated to the mesh using inverse distance weighting, creating a three-dimensional surface of the bed of Boston Bay. Further discussion of the details of mesh generation can be found in the following chapter regarding construction of the numerical model.

Elevation and horizontal position data from the center of each mesh element are exported into Environmental Systems Research Institute's (ESRI) ArcGIS, a collection of GIS software packages that allows data editing and attribution, review and display of data, generation of interpolated data and map creation (Wilson and Richards, 2006; ESRI, 2009). These data were used to create a triangular irregular network model (TIN) of Boston Bay using the 3D Analyst tool in ArcGIS. A TIN is a collection of triangular elements generated using the data points as the corners forming a continuous, faceted surface much like a jewel (Wilson and Richards, 2006).

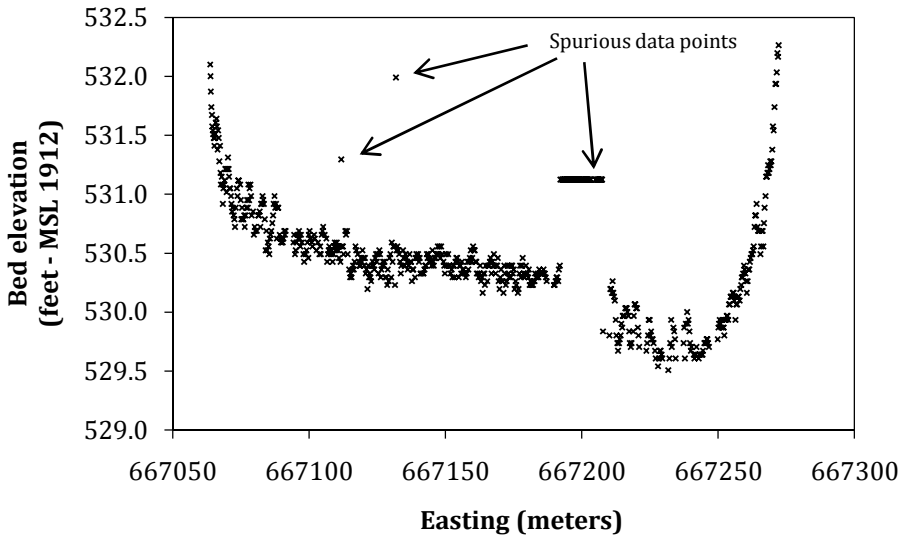

A. Raw bathymetry data.

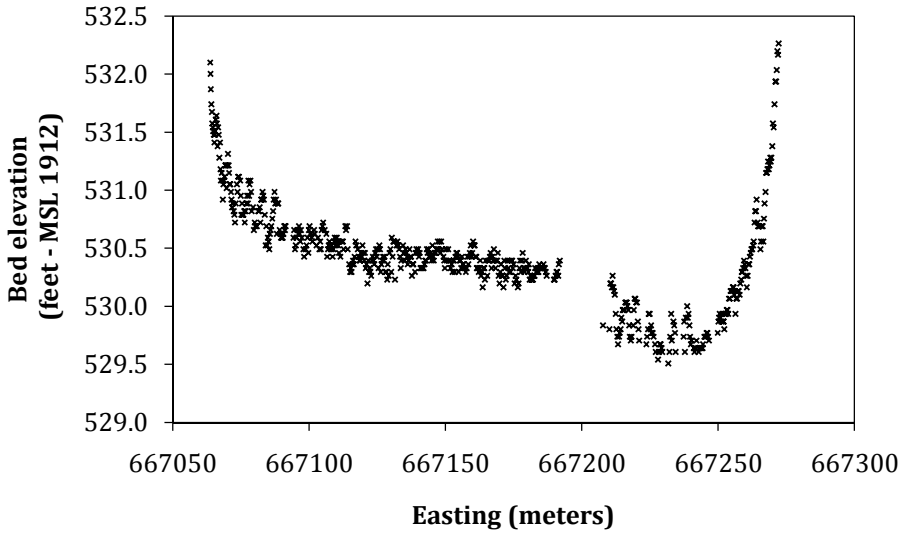

B. Edited bathymetry data with spurious points removed.

Figure 26: Raw bathymetric survey data (A) can be easily edited and erroneous data points removed (B) by plotting transect data with bed elevation on the y-axis and longitude (Easting) on the x-axis.

If raw bathymetric data are used for this process, the TIN surfaces are created from many long, skinny triangles between transect data points. While surfaces generated with these types of triangles are not ideal, the method of data collection forces the creation of such triangles (Wilson and Richards, 2006). However, the intermediate step involving the formation of a hybrid mesh and the generation of a secondary scatter set consisting of points from the center of each mesh element results in a much better coverage of data points, and could help to eliminate the potential errors which may be caused by TIN surface generation using long triangles (Figure 27). The TIN surface is then converted to a raster data set and contoured using a 2 ft contour interval with the Spatial Analyst tool package in ArcGIS.

4.3 – Analysis and Results

The resulting contoured surfaces are layered over a digital orthophoto quadrangle (DOQ) of the region surrounding the survey area and displayed as a series of bathymetric maps of Boston Bay (Figures 28 – 33). Close inspection of these figures reveals that Boston Bay exhibits little topographic relief, with much of the project area lying in a range of elevations between 530 and 532 ft above sea level, and an average elevation of 531.903 ft. The lowest point of elevation within the boundaries of the survey is 507.067 ft and is found in the pond where the pipes from the Bay Island Drainage and Levee District discharge into Boston Bay (Figure 31). The highest elevation measured during the survey had a value of 539.974 feet and also located near the discharge pond.

'Bells Pocket,' a popular location for recreational fishing shows significant changes in topography relative to the rest of the study area, with the deepest portions existing in a range of elevations from 508 and 510 ft above sea level (MSL)

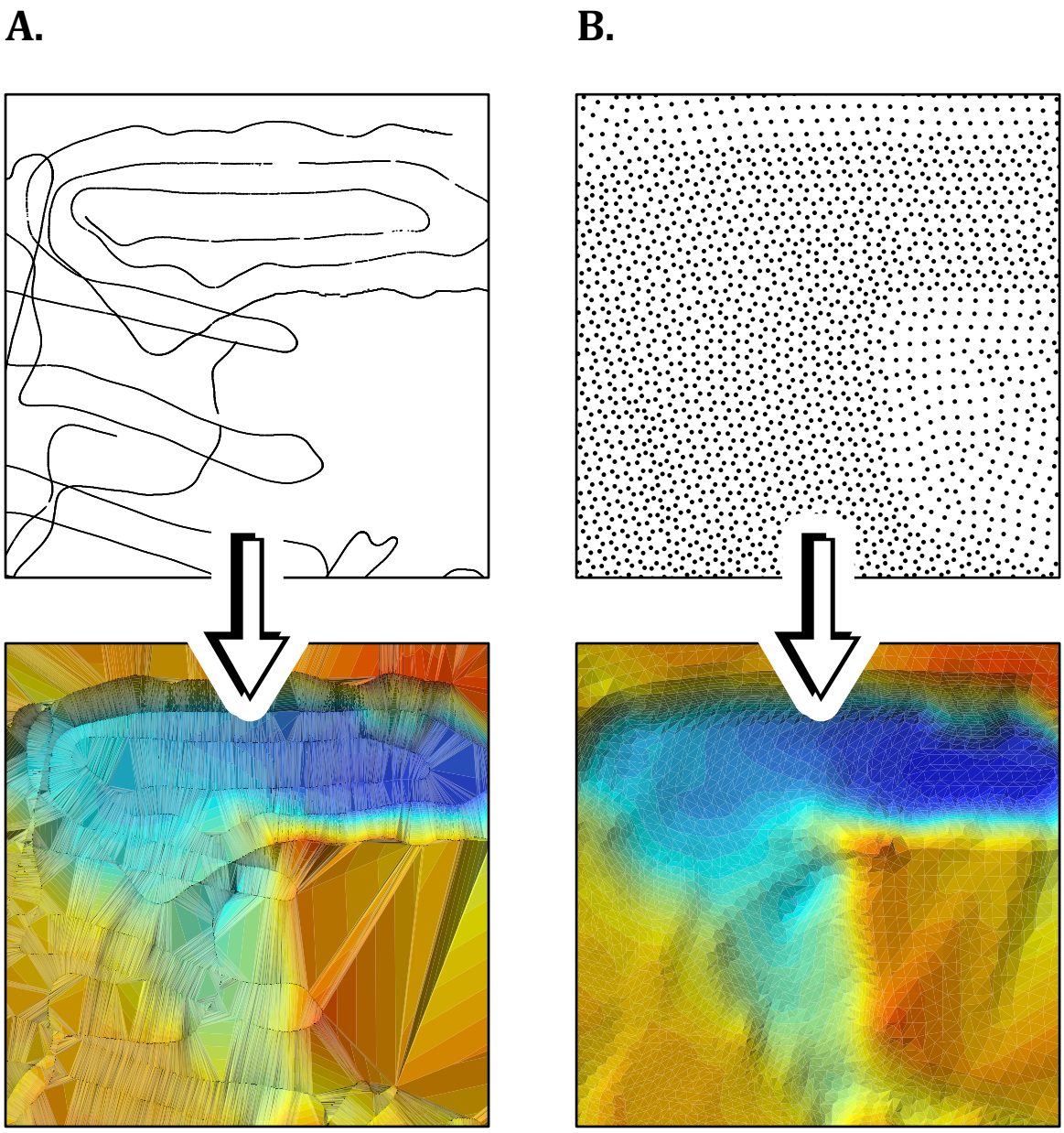

Figure 27: Raw bathymetric data is used to generate a triangular irregular network (TIN) of 'Bell's Pocket' made out of long, skinny triangles (A). Processsed data points corresponding to the center of each element from the mesh created from the bathymetry data results in a TIN with much smaller triangles (B) and may help eliminate associated errors.

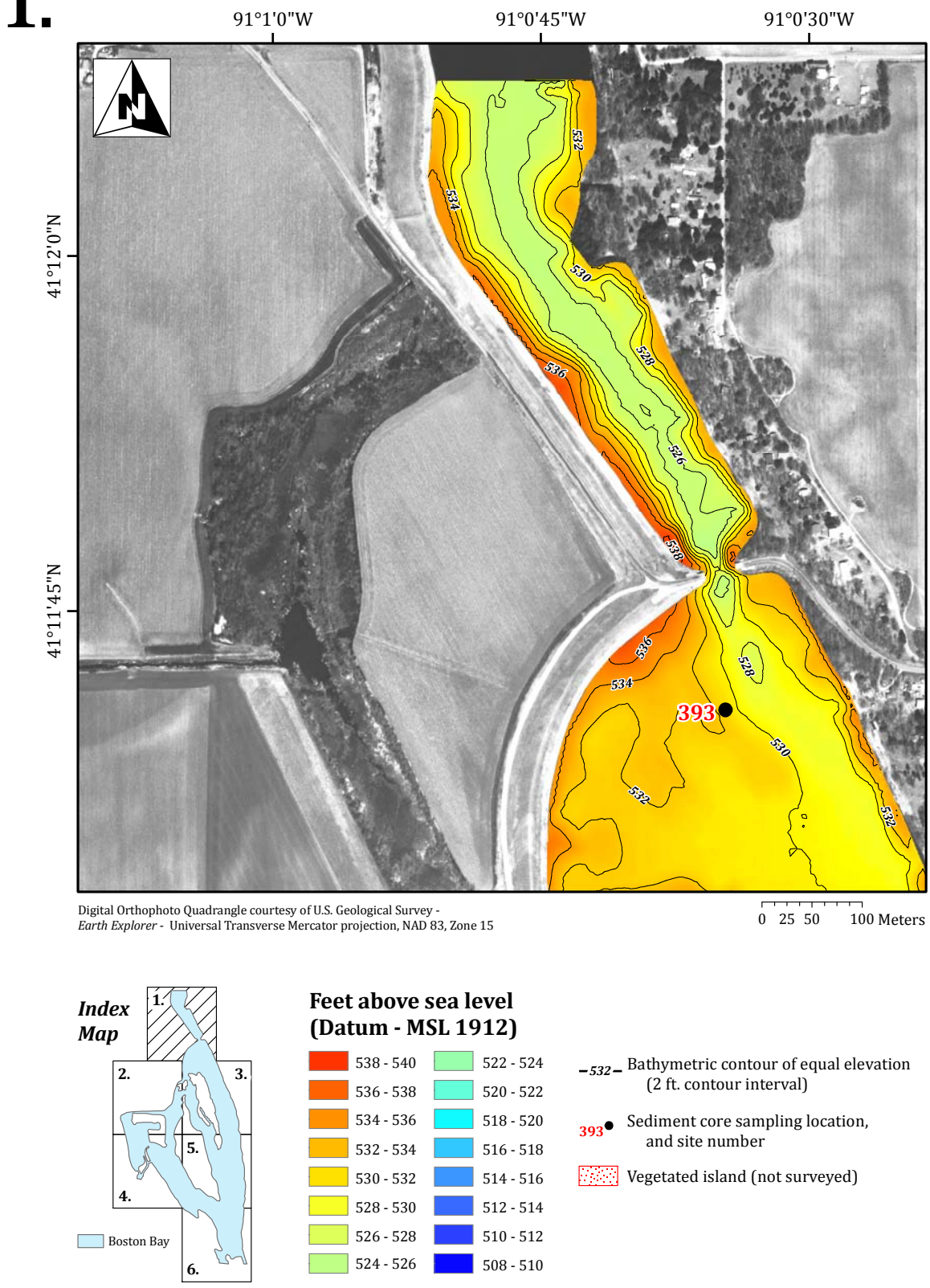

Figure 28: Bathymetry for upstream reach of Boston Bay.

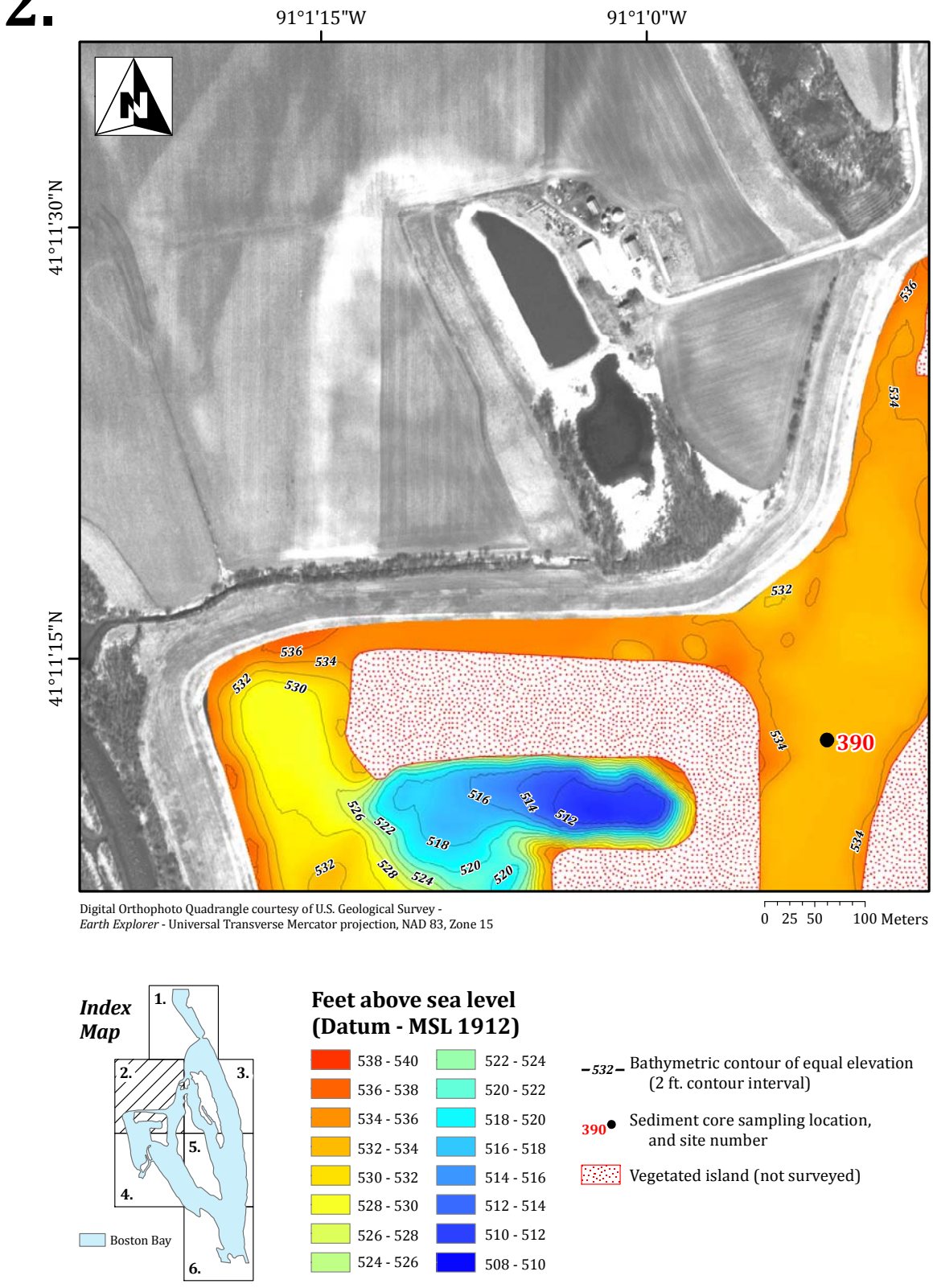

Figure 29: Bathymetry for northwest reach of Boston Bay.

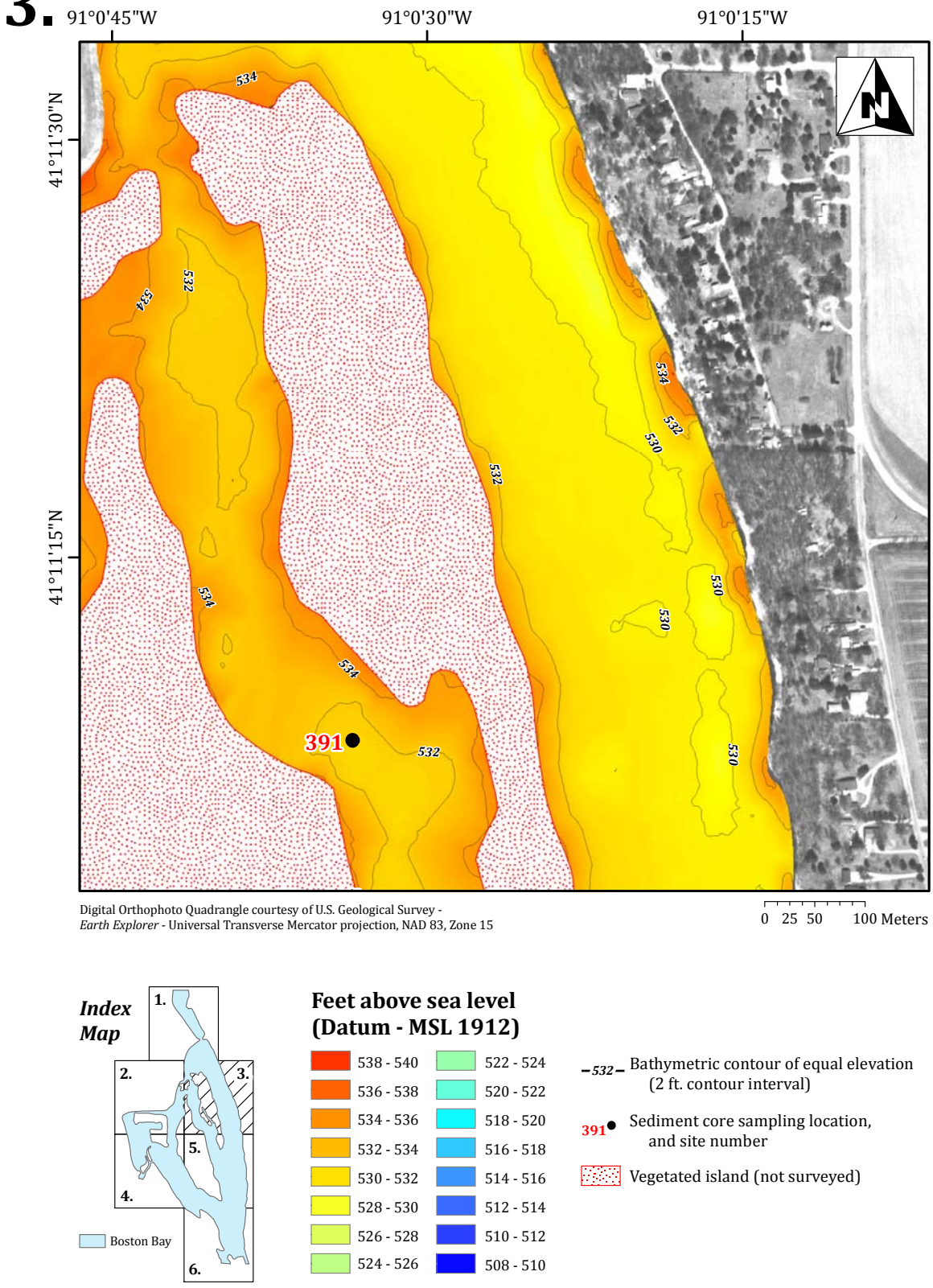

Figure 30: Bathymetry for northeast reach of Boston Bay.

4.

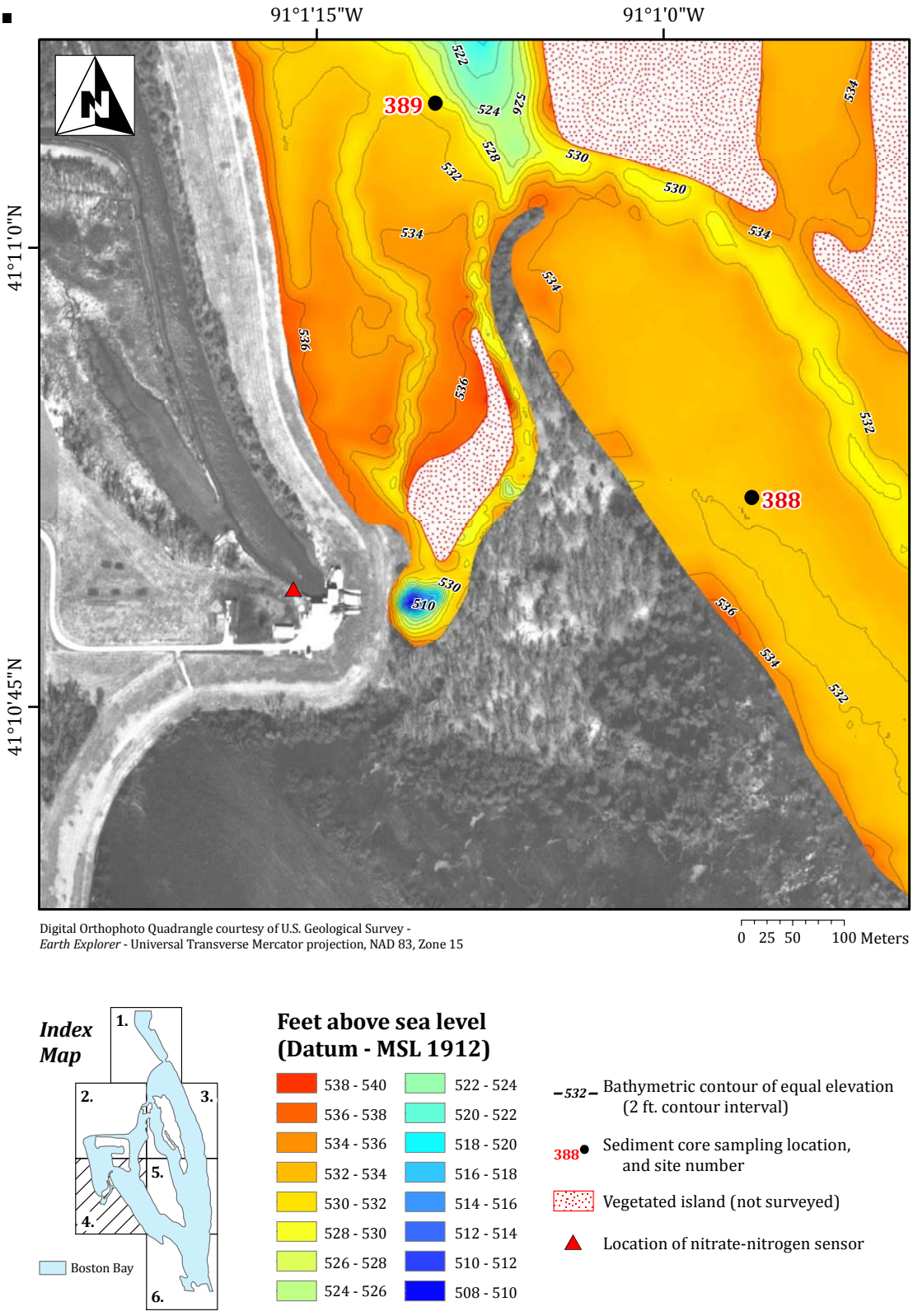

Figure 31: Bathymetry for southwest reach of Boston Bay.

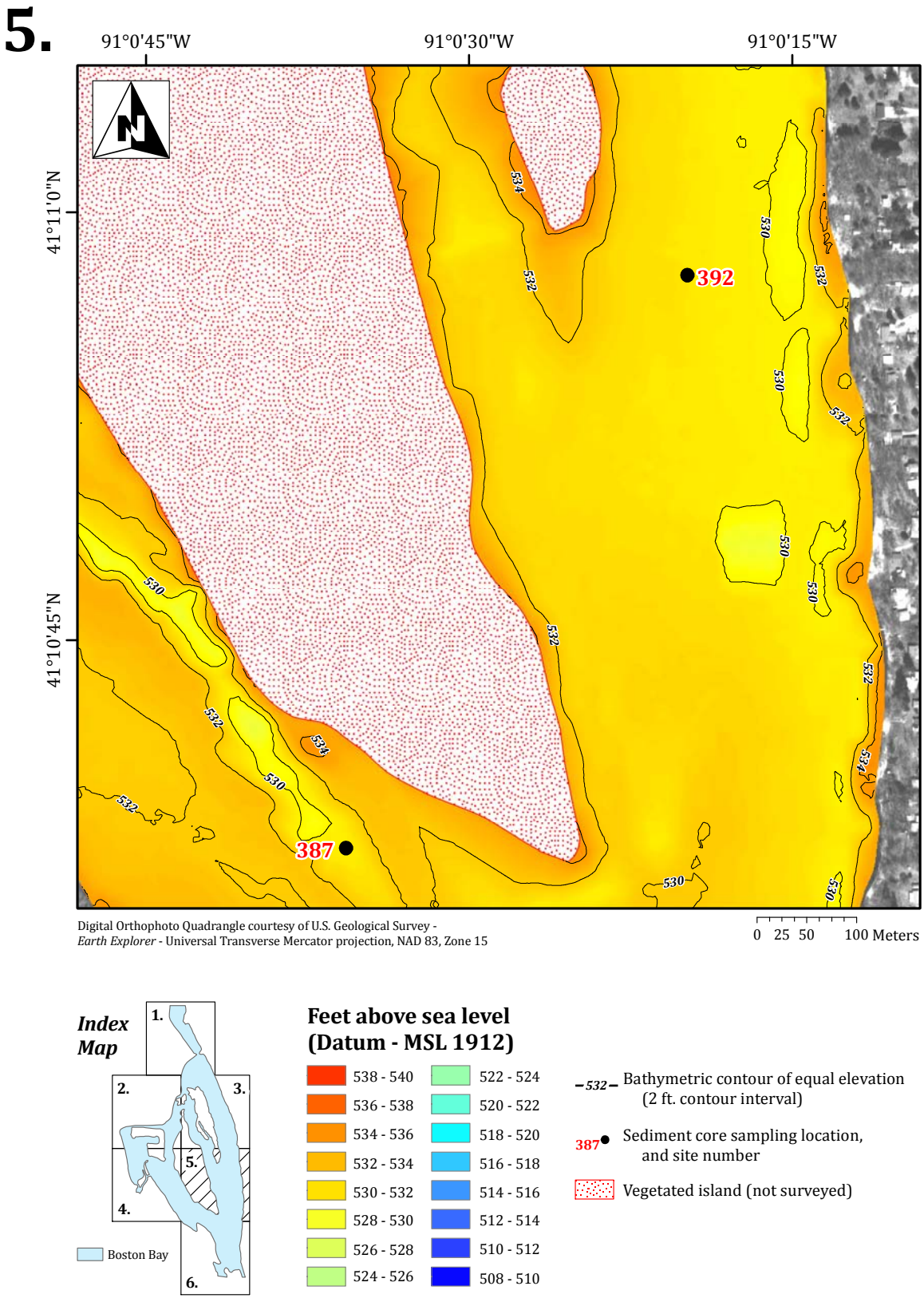

Figure 32: Bathymetry for southeast reach of Boston Bay.

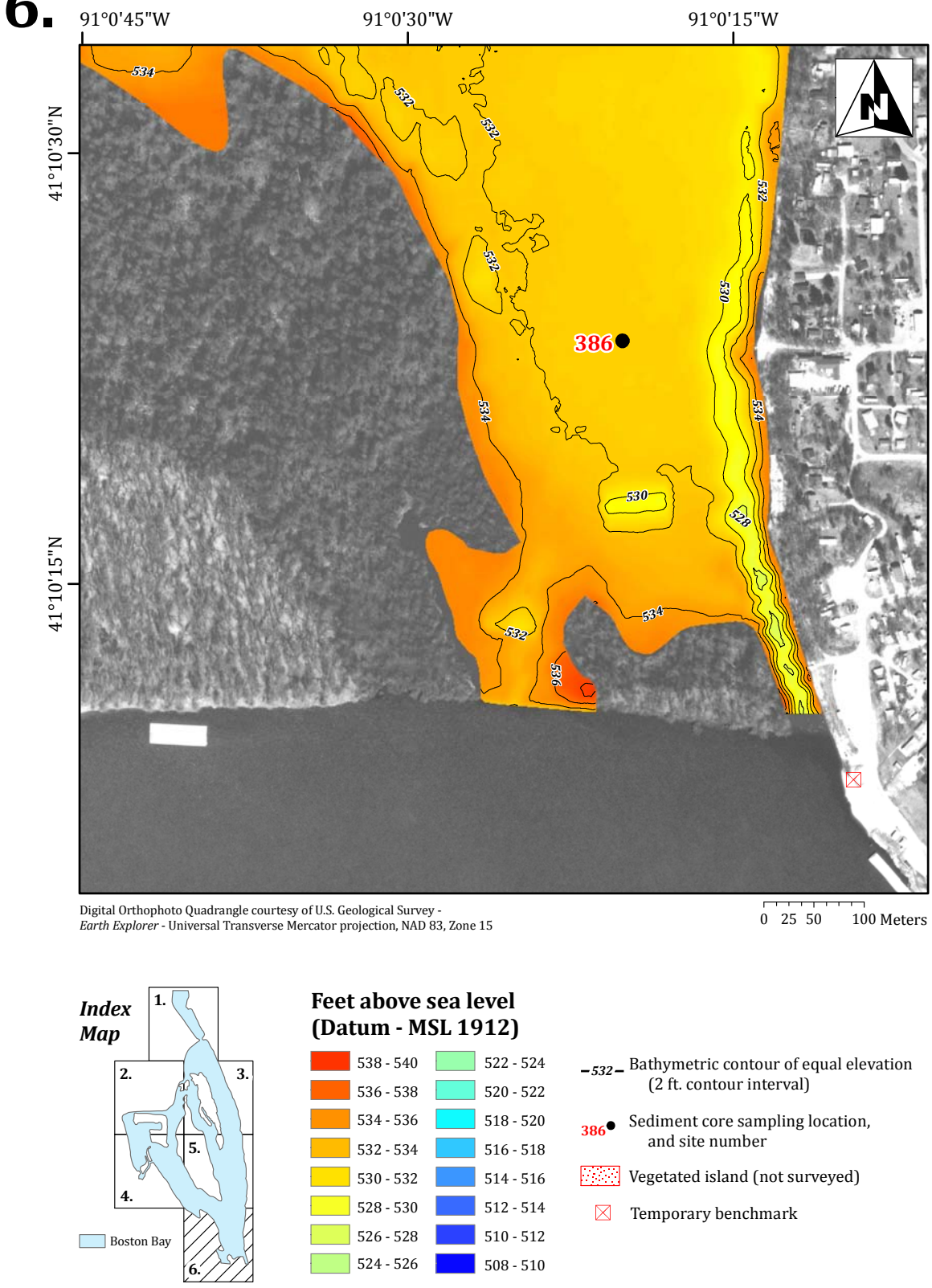

Figure 33: Bathymetry for downstream reach of Boston Bay.

(Figure 29). Knowing this ahead of time, survey data points were collected at a much higher density in this area, when compared to the 150 ft spacing between transects employed throughout the rest of the project area (Figure 25). It is thought that bathymetric maps generated from closely spaced transects of data points are more accurate than those created using a lower density of survey data, which tend to lose information about the topography of the study area (Haag, et al., 2005). The Bells Pocket region owes its topographic diversity to the removal of material from the area to assist with the construction of the adjacent levee in the 1960's (Marston, 2009), as shown by a comparison of the aerial photos displayed in Figure 5.

4.4 – Discussion

While bathymetric data from a survey of Boston Bay conducted by the USACE in August of 2008 exists, differences in data collection techniques limits comparison of the results from the two surveys to qualitatively studies only (Rogala, 2009). The two studies both reveal that the Boston Bay study area is generally flat, with little topographic relief. Both surveys show that the deepest regions of Boston Bay exist in the Bells Pocket region and in the drainage districts discharge pond. Quantitative comparison of the two surveys could shed light on the sedimentation patterns that exist in the study area.

It should also be mentioned that prior to the survey conducted in March of 2009, IIHR staff also attempted to perform a bathymetric survey of Boston Bay in August, 2008. Unfortunately, the low flow conditions that exist in the study area during the summer months placed serious limitations on where the survey vessel was able to navigate during this study. Water depths became so low that the echo-sound equipment became buried in the bed material, and the boat ran aground on several occasions. Given that the echo-sound equipment is only accurate in depths

greater than 19 inches (Odom Hydrographic Systems, 2007) the quality of the data collected during this study should be called in to question. However, a comparison of the extent of the two surveys conducted by IIHR sheds significant light on the extreme changes in water surface elevation existing in the Boston Bay study area throughout the course of a year.

While such comparative studies may be of some use, the real value of the data collected during this survey will be measured when interested parties use these results to assist in determining the amount of sediment that will need to be dredged in order to meet project objectives, and calculate the associated costs. Likewise, the data collected during this study will be used to aid in the construction of a numerical model of Boston Bay that is able to simulate the proposed dredging, the details of which are discussed in greater depth in the following chapter.

CHAPTER 5 – TWO-DIMENSIONAL HYDRODYNAMIC MODEL

5.1 – Background

It has been shown that numerical modeling can be an effective tool when predicting ecological response to varying hydrologic conditions and physical changes while also providing guidance for riverine and estuarine restoration projects (Roman, et al., 1995; Boumans, et al., 2002; Silvestri et al., 2005; Yang, et al, 2009). Traditionally, one-dimensional (1D) hydraulic modeling has been the most accepted approach when simulating fluvial systems (Huizinga, 2007; Tayefi, et al, 2007). Unfortunately such models are incapable of reproducing the hydrodynamic characteristics required to fully understand different river phenomenon which are generally two-dimensional (2D) and often-times three-dimensional (3D) in nature (Crowder and Diplas, 2000; Wagner, 2007).

One-dimensional hydrodynamic models are limited in several ways including their ability to fully represent the detailed bathymetry affecting river processes, accurately depict extreme flooding events and simulate complex systems such as braided streams and rivers (Merwade, et al, 2008). In an attempt to better understand riverine environments, researchers have begun replacing traditional 1D modeling methods with 2D and 3D hydrodynamic models (Leclerc, et al, 1995; Bates and De Roo, 2000; Martini, et al, 2004; Carrivick, 2006; Crowder and Diplas, 2006; Dutta, et al, 2007).

Until recently the use and development of 2D models required extensive field data collection, significant computer resources and increased man-power when compared with traditional 1D methods. Readily available high-resolution topographic data, the growing use of graphical user interfaces for 2D modeling software, and continued improvements in computer hardware have resulted in

major advances in the applicability of 2D models to practical problems (Huizinga, 2007; Merwade, et al, 2008). Given the recent growth in the field, 2D modeling is now commonly used to assist with various efforts which include, but are not limited to, flood inundation mapping (Dutta, et al, 2007; Tayefi, et al, 2007; Musser, 2008), analysis of flow conditions near intake structures (Holtschlag and Koschik, 2001; Shelton, 2009), determining habitat suitability characteristics (Crowder and Diplas, 2000; Wagner, 2003), studying the impact of scour on bridge piers (Huizinga, 2007; Wagner, 2007; Brabets and Conaway, 2009), development of sediment budgets (McDonald, et al, 2005) and providing guidance for environmental restoration efforts (Cavagnero and Revelli, 2009; Yang, et al, 2009).

To help gain a better understanding of how the proposed restoration of Boston Bay would influence the existing hydrologic conditions, SHR-W, the 2D hydraulic model designed by the Sediment and River Hydraulics group at the U.S. Bureau of Reclamation, along with Aquaveo's Surface Water Modeling System (SMS) were used to construct a model of the Boston Bay study area capable of simulating the prescribed dredging activity and the associated environmental impacts.

Field data collection including the bathymetric survey described in the previous chapter as well as discharge measurements from upstream inlets, readings of water-surface elevation at the downstream outlet and values of Manning's roughness (n) for the different regions of Boston Bay are required to sufficiently generate a simplified surface of the study area, define boundary conditions and calibrate a 2D hydrodynamic model (Wagner, 2007; Thompson, et al, 2008; Brabets and Conaway, 2009). Several different scenarios involving various combinations of inlet discharge, outlet water-surface elevation and Manning's roughness were modeled in an attempt to re-create the full range of flow conditions that exist throughout Boston Bay over the course of a year. The resulting output files from each simulation are edited and displayed using a GIS for comparison of the results.

Special attention was paid to how flow conditions in the vicinity of the proposed dredging locations and near 'Bells Pocket,' the deepest region of the study area, would change in response to the proposed restoration.

5.2 – Methods

5.2.1 – Data Collection

As mentioned above, successfully generating a 2D model of the hydrodynamic properties of Boston Bay requires collection of elevation data through a bathymetric survey, as outlined in the previous chapter. This data defines the topography for the simulation solution and availability of such data is essential to developing reliable hydraulic models (Wagner, 2007). In addition to elevation data, boundary conditions for the model including water-surface elevation at the outlet of Boston Bay and discharge into the study area from Eliza Creek and the Bay Island pumping station need to be defined through field data collection.

5.2.1.1 – Discharge from Eliza Creek

Eliza Creek empties into Boston Bay from the north and serves as the main drainage outlet for a watershed of roughly 37 square miles (USGS, 2009) (Figure 4). Like many small streams in the upper Midwest, the flow conditions of Eliza Creek are not continuously monitored. In order to accurately define the discharge of Eliza Creek into the bay as a boundary condition, flow measurements were taken using Teledyne RDI's StreamPro ADCP, capable of determining the velocity and discharge of shallow, slow-moving bodies of water (Teledyne RD Instruments, 2006).

Twelve transects of Eliza Creek were taken on June 3, 2009 with the ADCP and averaged using Teledyne RDI's WinRiver software to give the best possible value of stream discharge. Transects which resulted in discharge values not within

5% of mean value were discarded, as described by Herschey (2009), in order to arrive at an acceptable discharge measurement. The results indicate that on the day measurements were taken, Eliza Creek had a discharge of 33.65 ft^3/sec. It is assumed that this value is representative of low-flow conditions in Eliza Creek, as flows on that day were well below bank-full and data was gathered after a long period with little rainfall. Data collection at Eliza Creek was limited to one day thus requiring average- and high-flow conditions to be estimated, as will be discussed in greater detail below.

5.2.1.2 – Discharge from Bay Island Pumping Station

As described in earlier sections, detailed operation and maintenance log sheets are available from the Bay Island Drainage and Levee District and indicate when the pumps are turned 'On' and 'Off,' along with the speed at which each pump is operating. Given the maximum discharge a pump is capable of producing, and at what speed, one can easily determine pump discharge at other speeds using the pump affinity law (Equation 4).

5.2.1.3 – Water-Surface Elevation at Outlet

Measurements of the water-surface elevation at the outlet of Boston Bay were not taken concurrently with data collected at Eliza Creek and the pumping station, requiring that the value of this boundary condition be estimated. Lock and Dam #17, located four miles upstream from the outlet of Boston Bay (Figure 1) continuously monitors pool level, and stage elevation which is typically kept between 530 and 540 ft above sea level (MSL 1912) with the exception of extreme flooding events like those which occurred in 1993 and 2008 (USACE, 2009). Similarly, the pool level at Lock and Dam #18, 22 miles downstream from the study area, is generally maintained at an elevation of 528 ft above sea level (MSL 1912),

allowing for the range of water-surface elevation values near the outlet of the bay to be easily estimated.

5.2.2 – Data Processing

5.2.2.1 – Mesh Generation

After sufficient collection of field data, the next step in the numerical modeling process consists of developing a description of the continuous and irregular geometry of the Boston Bay study area in order to simplify the calculations of hydrodynamic quantities. This representation, known as a 'finite element network' or 'mesh,' is a surface consisting of a collection of contiguous elements which are typically quadrilateral or triangular in shape (Conaway and Moran, 2004; Musser, 2008; Cavagnero and Ravelli, 2009).

Creating a continuous surface involves interpolating point measurements or linear cross-sections using GIS interpolation techniques to a conceptual model describing the geometry and boundaries of the study area developed within the 'Map' module in SMS using feature objects (Holtschlag and Koschik, 2001; Merwade, et al, 2008). Nodes and arcs form polygons which and are used to delineate the domain of the study area with the assistance of digital orthophotography, and the data collected during the aforementioned bathymetric survey.

Polygons are assigned a material type defined by a value of Manning's *n*, a unitless parameter describing the roughness of the river channel or floodplain material (Jain, 2001). Tables like those published by the U.S. Geological Survey (Barnes, 1967) list values of *n* for different material types and land cover. After further review of aerial photographs and observations made during field visits, it was decided that the polygons defining the densely vegetated islands would be assigned an *n* value of 0.20, while the remainder of the study area would be given a value of 0.08. Simulations of flow conditions after the proposed restoration

required that those locations where dredging occurred be assigned an *n* value of 0.03 (Figure 34).

Once the study area is properly delineated and roughness values assigned to all of the polygons, the conceptual model is converted a finite element mesh using the 'Map to 2D Mesh' command in the 'Map' module of SMS. The hybrid mesh, containing a combination of quadrilateral and triangular elements, was chosen as it achieves the best compromise between computing demand, and solution accuracy (Lai, 2008). The individual mesh elements provide a location where the 2D, depth-averaged dynamic wave equations (St. Venant equations) can be defined. For this study, the typical triangular element comprising the majority of the mesh is on the order of 20 feet per side, resulting in an area of 86 ft^2. This value is dependent upon location within the study area as certain regions of interest, including the locations where the proposed dredging and berm construction will occur required a more detailed mesh, with triangular elements of only 22 ft^2 in area (Figure 35).

Data gathered during the bathymetric survey was imported into SMS as a xyz scatter set and interpolated to the hybrid mesh using inverse distance weighting (IDW). Node-strings are created in the 'Mesh' module of SMS, each one corresponding to a boundary segment of the finite element mesh. In addition, node-strings provide a location where boundary conditions are applied, representing inlet discharges and outlet water surface elevations.

The resulting mesh consisted of 73,622 triangular elements, 11,921 quadrilateral elements, and 49,433 nodes. The maximum and minimum elevation values contained within the mesh are 539.92 and 508.84 ft, respectively. To simulate the proposed dredging of the study area, the mesh generated using the existing bathymetry was altered to reflect the dredging activity prescribed by Living Lands & Waters (Figure 36). This was easily achieved by selecting mesh nodes

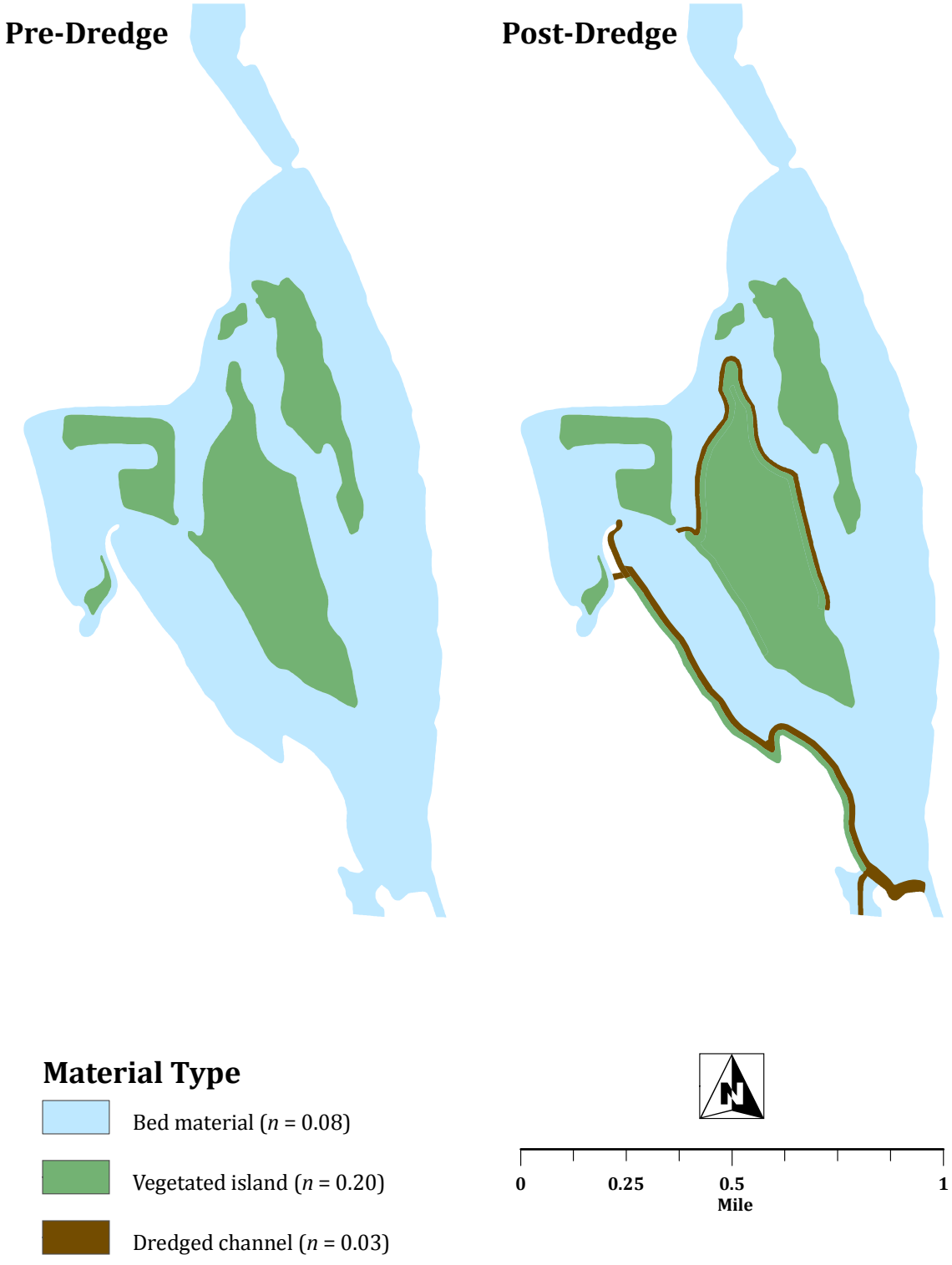

Figure 34: Material types and corresponding values of Manning's roughness coefficient (*n*) for different regions of the Boston Bay study area.

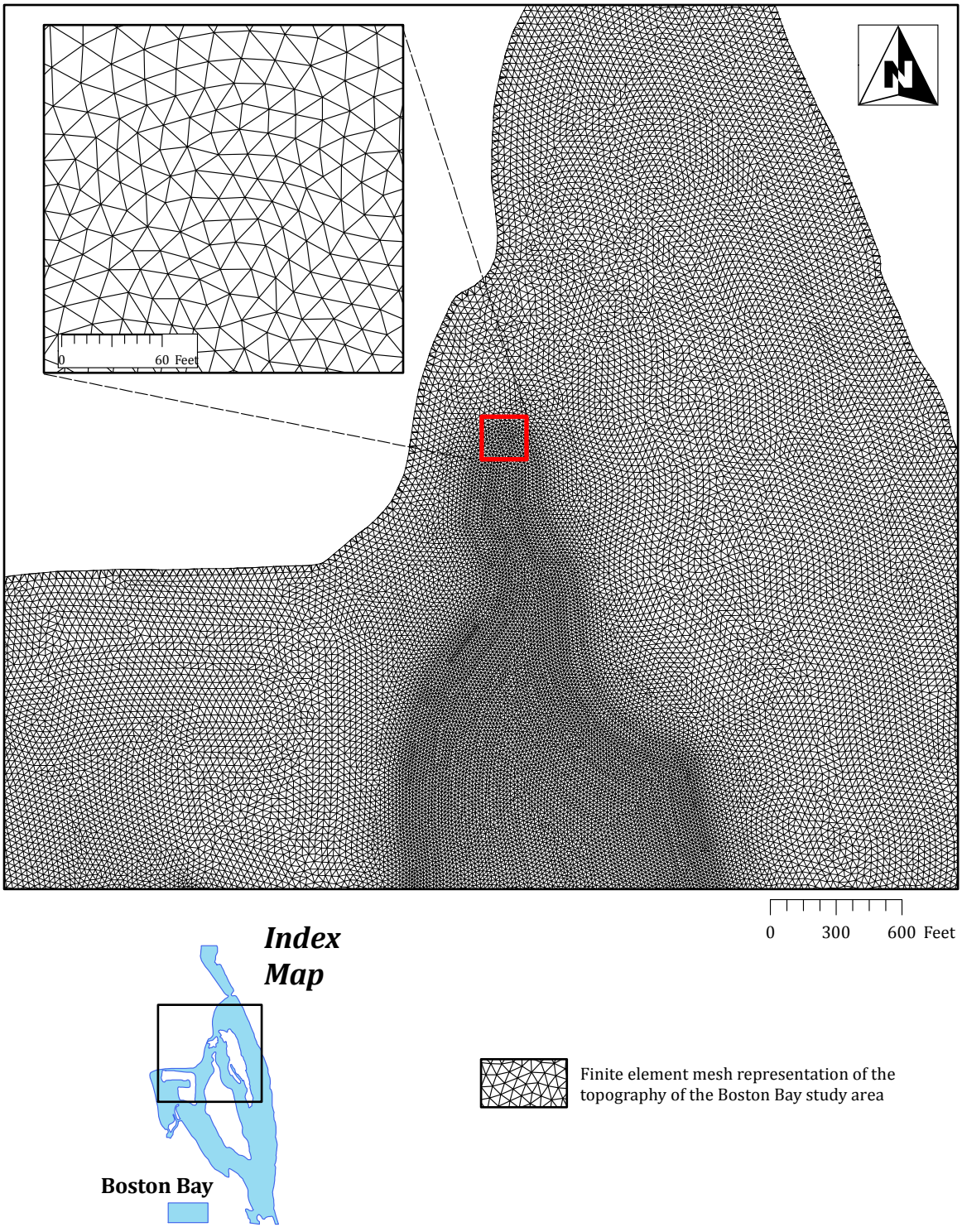

Figure 35: Portion of finite element mesh used to simplify the irregular bathymetry and geometry of the Boston Bay study area. Inest map shows area of higher density mesh in the location of proposed dredging and berm construction.

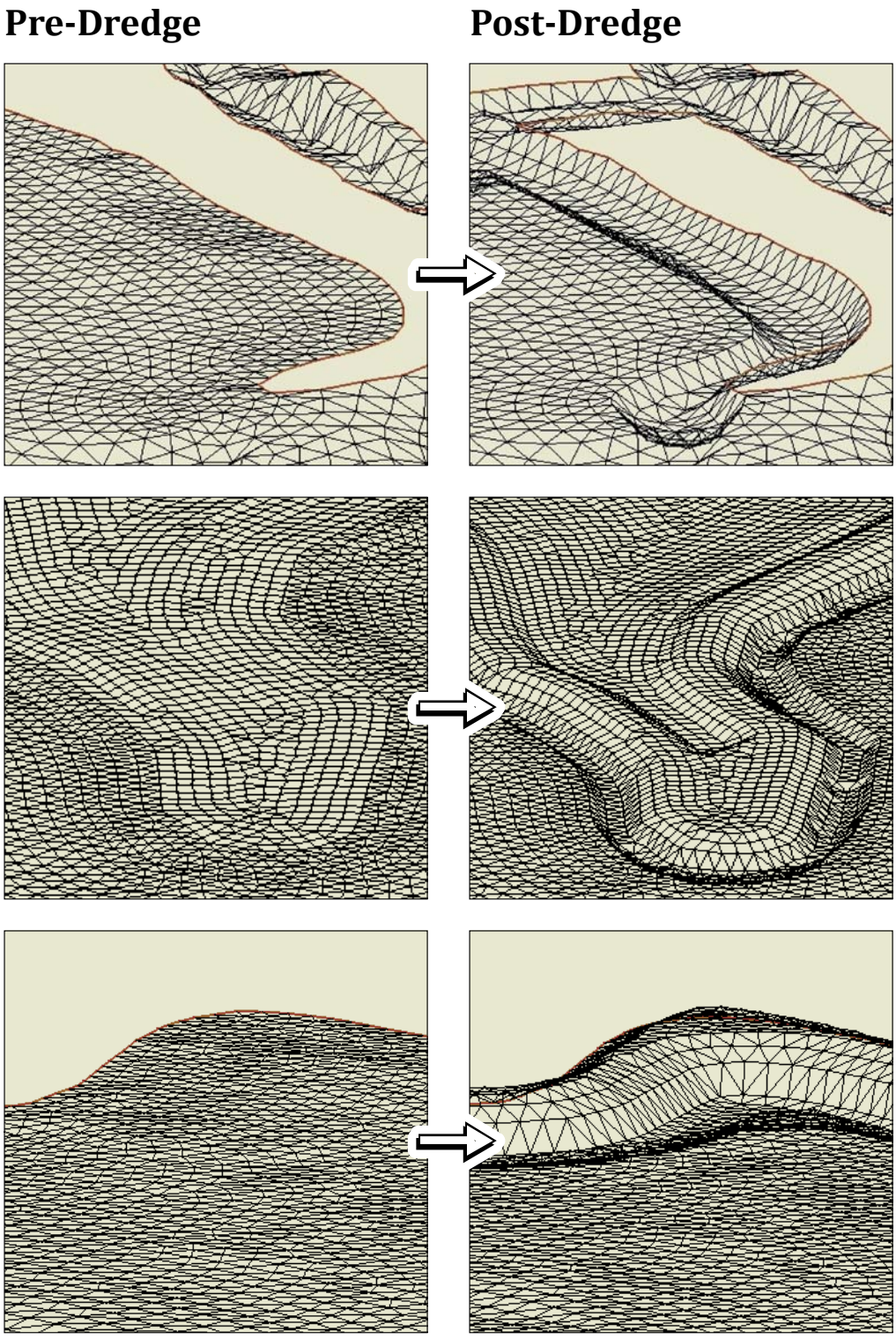

Figure 36: Screenshots from Aquaveo's Surface Modeling Software (SMS) displaying different views of the mesh generated using the existing bathymetry on the left (Pre-Dredge) and the mesh used to describe the study area after the proposed dredging, on the right (Post-Dredge).

contained within the assigned dredging location, and changing the elevation values (z) to mimic what the bathymetry would look like after dredging has occurred. It should be mentioned that unlike Figure 35 which features a portion of the mesh in a two-dimensional plan view, the screenshots from SMS shown in Figure 36 display the mesh at an angle which helps to highlight the three-dimensional nature of the study area and emphasizes the changes to the existing topography resulting from the proposed dredging and berm construction. The final mesh generated from the existing bathymetry will be used for the 'Pre-Dredge' numerical simulations, while the mesh altered to mimic the proposed restoration will help simulate the 'Post-Dredge' scenarios as will be discussed in further detail below.

5.2.2.2 – Boundary Conditions and Simulation Scenarios

As mentioned earlier, several different scenarios were simulated in an attempt to cover the full range of flow conditions that exist in Boston Bay throughout the course of a year. However, before these scenarios could be properly defined, values for boundary conditions that were not directly measured in the field need to be estimated. As previously mentioned, the discharge measurement collected at Eliza Creek on June 3, 2009 was representative of a low-flow scenario. Discharge values that represent average- and high- flow boundary conditions need to be assumed and were given values of 66 and 100 ft^3/sec, respectively. This assumption is based on a comparison of photographs taken at the location where discharge data was collected with photos taken at the same location on March 16, 2009. During periods of high flow, the banks of Eliza Creek are easily breached as evidenced by the flattened appearance of bank vegetation and ponding of water several feet from the banks of the creek (Figure 37).

Figure 37: Photos taken of Eliza Creek upstream from the Bay Island Road Bridge taken on March 16, 2009 (left) and June 3, 2009 (right). Ponding of water several meters from the banks of the creek indicate that the creek is easily breached during high flows.

The boundary condition represented by the discharge from the Bay Island pumping station was assigned values of 200, 450 and 590 ft^3/sec for the low-, medium- and high-flow scenarios. Low-flow conditions result when pump #2 operates at 90% capacity and discharges 200 ft^3/sec, while pumps #1 and #3 are not in operation. Average flows, which are modeled with a discharge of 450 ft^3/sec occur when pump #1 and #2 are running at full capacity, while pump #3 is turned 'Off.' High-flow conditions are achieved when all three pumps run at full capacity resulting in a discharge of 590 ft^3/sec (Marston, 2009).

Finally, values of water-surface elevation at the outlet of the study area also needed to be estimated to define the downstream boundary condition. Given the range of measured stage elevations at Lock and Dam #17 (530 ft – 540 ft) it was decided that low-flow scenarios would be modeled using a value of 530 ft for the downstream outlet, while average- and high-flow scenarios were assigned water-surface elevation values of 535 and 540 ft, respectively. These values are

appropriate and correspond closely with the values of water-surface elevation measured during the two bathymetric surveys conducted by IIHR. During the August, 2008 survey a water surface elevation of 531 ft was measured near the outlet of Boston Bay whereas the survey conducted during high flows in March of 2009 reported the water surface elevation at the same location to be 542 ft.

Each of these scenarios were simulated twice; once using the mesh generated from the existing topography of the study area ('Pre-Dredge'), and again using the mesh that had been altered to reflect the proposed dredging ('Post-Dredge'). The various simulation scenarios have been summarized in Table 10.

Flow Scenario	Eliza Creek discharge (ft^3/s)	Pump station discharge (ft^3/s)	Water-surface elevation (ft)
Low	33	200	530
Medium	66	450	535
High	100	590	540

Table 12: Summary of flow scenarios and their corresponding boundary condition values.

5.2.2.3 – Main Solver Execution

Once the mesh has been generated and boundary conditions determined the preprocessor is used to generate the input file used to run the simulation. SRH-W contains a built-in preprocessor which comes in the form of a text-based user interface that assists in setting up the simulation parameters including boundary conditions, material types, number of time steps, output format and simulation

duration and is designed so that the user is not required to memorize input commands, or lines of code (Lai, 2006). Following preprocessor execution, a data file is produced which serves as the input for the main solver.

The input file is read into the main solver which applies the depth-averaged, 2D wave equations to each element contained within the mesh. As is the case with many open-channel environments, flows in Boston Bay are slow and shallow, with negligible vertical motions. Therefore the most general flow equations (Navier-Stokes) can be vertically averaged to obtain the set of depth-averaged two dimensional equations (Lai, 2006), resulting in the 2D St. Venant equations

$$\frac{\partial h}{\partial t} + \frac{\partial hU}{\partial x} + \frac{\partial hV}{\partial y} = e \qquad (7)$$

$$\frac{\partial hU}{\partial t} + \frac{\partial hUU}{\partial x} + \frac{\partial hVU}{\partial y} = \frac{\partial hT_{xx}}{\partial x} + \frac{\partial hT_{xy}}{\partial y} - gh\frac{\partial z}{\partial x} - \frac{\tau_{bx}}{\rho} + D_{xx} + D_{xy} \qquad (8)$$

$$\frac{\partial hV}{\partial t} + \frac{\partial hUV}{\partial x} + \frac{\partial hVV}{\partial y} = \frac{\partial hT_{xy}}{\partial x} + \frac{\partial hT_{yy}}{\partial y} - gh\frac{\partial z}{\partial y} - \frac{\tau_{by}}{\rho} + D_{yx} + D_{yy} \qquad (9)$$

Here, h is the water depth, g is acceleration due to gravity, t is time, and x and y are the horizontal Cartesian coordinates. U and V are the depth-averaged velocity components in the x and y direction respectively, e is excess rainfall rate, T_{xx} , T_{xy} and T_{yy} are depth-averaged turbulent stresses, D_{xx}, D_{xy}, D_{yx} and D_{yy} are dispersion due to depth averaging. z_b is bed elevation, and $z = z_b+h$ is the water surface elevation. Water density is represented by ρ. The bed shear stress, τ_{bx}, τ_{by} are calculated using Mannings' roughness equation

$$\begin{pmatrix}\tau_{bx}\\ \tau_{by}\end{pmatrix} = \rho C_f \begin{pmatrix}U\\ V\end{pmatrix}\sqrt{U^2+V^2}\ ;\ \ C_f = \frac{gn^2}{h^{1/3}} \qquad (10)$$

Where n is Manning's roughness coefficient. This set of equations is solved during each time step of the simulation at the center of each mesh element (Lai, 2006).

5.3 – Analysis and Results

5.3.1 – Model Output

Traditionally, 2D modeling efforts have employed a method of calibration where values of roughness coefficient (n) are adjusted through an iterative process so that model results closely match measured values of water-surface elevation and velocity (Conaway and Moran, 2004; Huizinga, 2008). However it has been shown that such methods can oftentimes result in nonsensical n values which may act to obscure larger-scale flow patterns (Crowder and Diplas, 2000). This, taken with the lack of available water-surface and velocity data against which model results could be compared led to the decision to forego model calibration altogether.

During model development it was decided that it would be sufficient to assign appropriate roughness coefficients to the study area consistent with regions with dense willows ($n = 0.20$), sluggish reaches with some weeds and deep pools which dominate the study area ($n = 0.08$) and clean, recently completed dredged channels ($n = 0.03$) (Figure 34) (Mays, 2005). After changes were made to the model of existing conditions to reflect the proposed dredging and berm construction, the resulting model output was used to assess how such features influence the flow conditions of Boston Bay. Given the fact that 80% of the ability to accurately construct 2D hydrodynamic models lies in the use of appropriate bathymetry, quality mesh design and properly defined boundary conditions (USACE,

1996), the model results should be representative of how the study area (and other, similar areas) would react to the proposed changes to the existing topography.

The resulting output files from the main simulation solver provide information about flow velocity, water surface elevation, water depth, Froude number, and bed shear-stress at the center of each mesh element. Output files are easily displayed as xyz scatter sets in SMS or ArcGIS (Figure 38 - 42). For this particular study, attention was focused on how water depth would change as a result of the proposed dredging, especially in the deepest region of the study area, 'Bells Pocket' (Figure 38). Initial results indicate that the water depth in this portion of the bay during low-flow conditions would drop by just over 1 ft following the proposed restoration, decreasing from 26.195 ft to 25.165 ft (Figure 38 a and d). Other portions of the study area also appear to experience a change in depth, given that a noticeably smaller portion of Boston Bay appears to be inundated once the dredging has been completed.

During average-flow scenarios, it also appears that a smaller portion of the study area is inundated following dredging and berm construction, with total area of inundation decreasing by 65 acres. In particular, the region behind the constructed berm would appear to provide additional habitat for hardwood tree species. The areas that remain inundated exhibit generally higher water depths throughout. Like the low-flow simulations, water depths in the vicinity of 'Bells Pocket' decrease from 27.561 ft to 26.900 ft following the proposed dredging of the study area (Figure 38 b and e). It is unsure how much can be learned from the results of the high-flow scenarios due to the lack of topographic data in the region just west of the study area which is commonly inundated with water during high flows (Figure 3) and it is therefore assumed that the resulting water-depth values are overestimated (Figure 38 c and f).

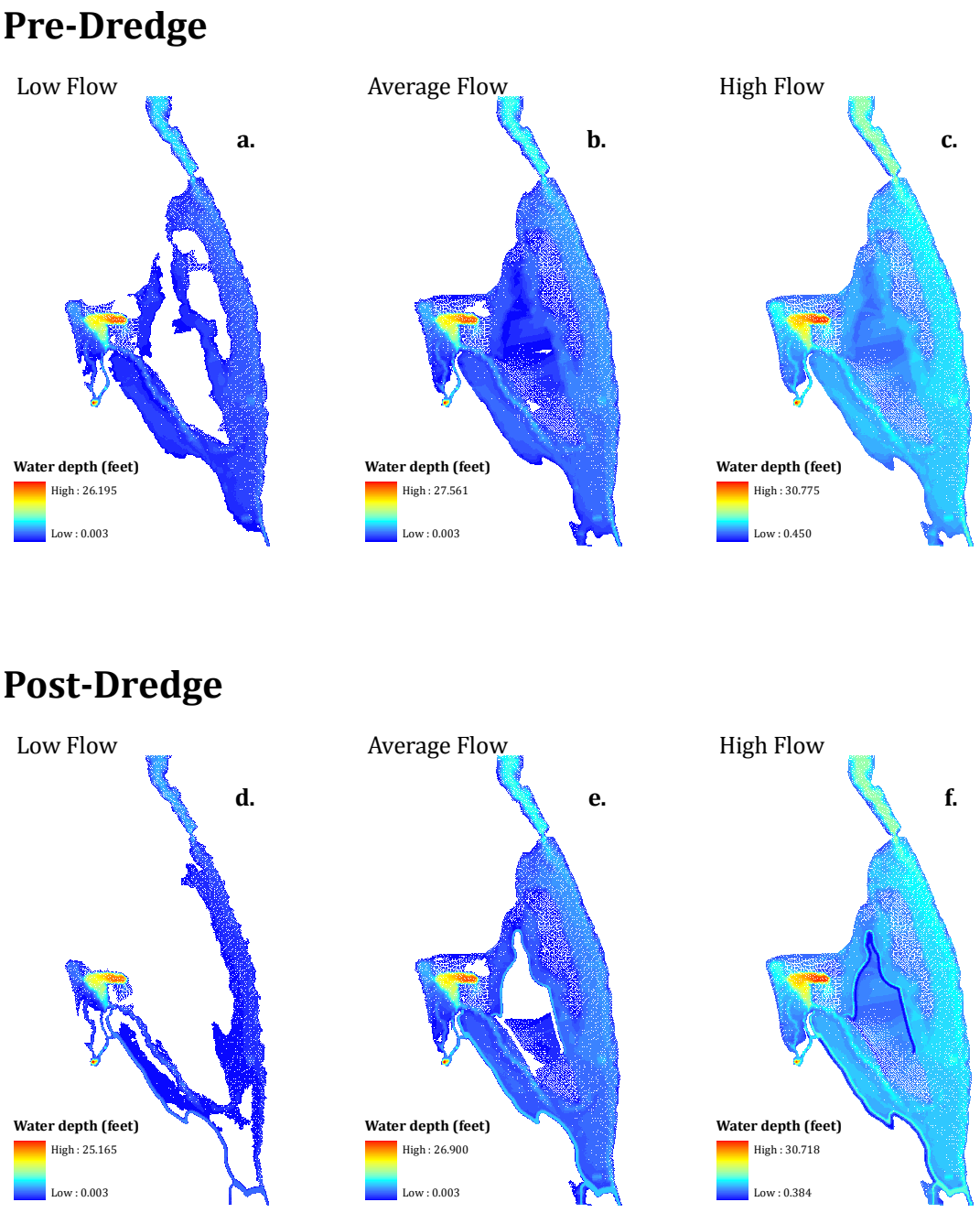

Figure 38: Resulting output from SRH-W main solver displaying values of water depth (measured in feet) for different flow scenarios (High, Medium, Low) simulated with the mesh created from the existing bathymetry (Pre-Dredge) and the mesh representative of the study area following the proposed dredging (Post-Dredge).

In addition to reporting values of water depth, the numerical model is also capable of solving for other parameters of interest including velocity magnitude (Figure 39), water-surface elevation (Figure 40), bed shear-stress (Figure 41) and Froude number (Figure 42). Close observation of Figure 39 reveals that flow velocity is highest near the inlet where the BIDLD discharges into the study area as well as the downstream outlet where Boston Bay merges with the main channel of the Mississippi River. These heightened values may be the result of the models difficulty in accurately simulating the flows coming from the BIDLD pumping station as well as its inability to account for over-bank flows. During low-flow conditions it appears that following restoration the flow velocity in the vicinity of the dredged channels increases as compared with the current flow conditions (Figure 39 a and d).

Figure 40 displays simulated values of water-surface elevation for the various flow scenarios modeled during this study. One's attention is immediately drawn to the significant increase in water-surface elevation that occurs between the downstream outlet and the upstream inlet of the BIDLD during low-flows under the current conditions (Figure 40a). According to the results of the model, water-surface elevation increases from just over 531 ft at the downstream outlet to just over 535 ft at the BIDLD inlet over a distance of roughly 1 mile. This seems unrealistic and may be due to limitations in the models ability to simulate flows coming from the BIDLD and insufficient topographic data necessary to completely describe the study area. Rapid changes in water-surface elevation near the BIDLD inlet during high flows following the proposed dredging (Figure 40f) may be indicative of hydraulic jumps or other rapidly-varied flow conditions existing in the study area.

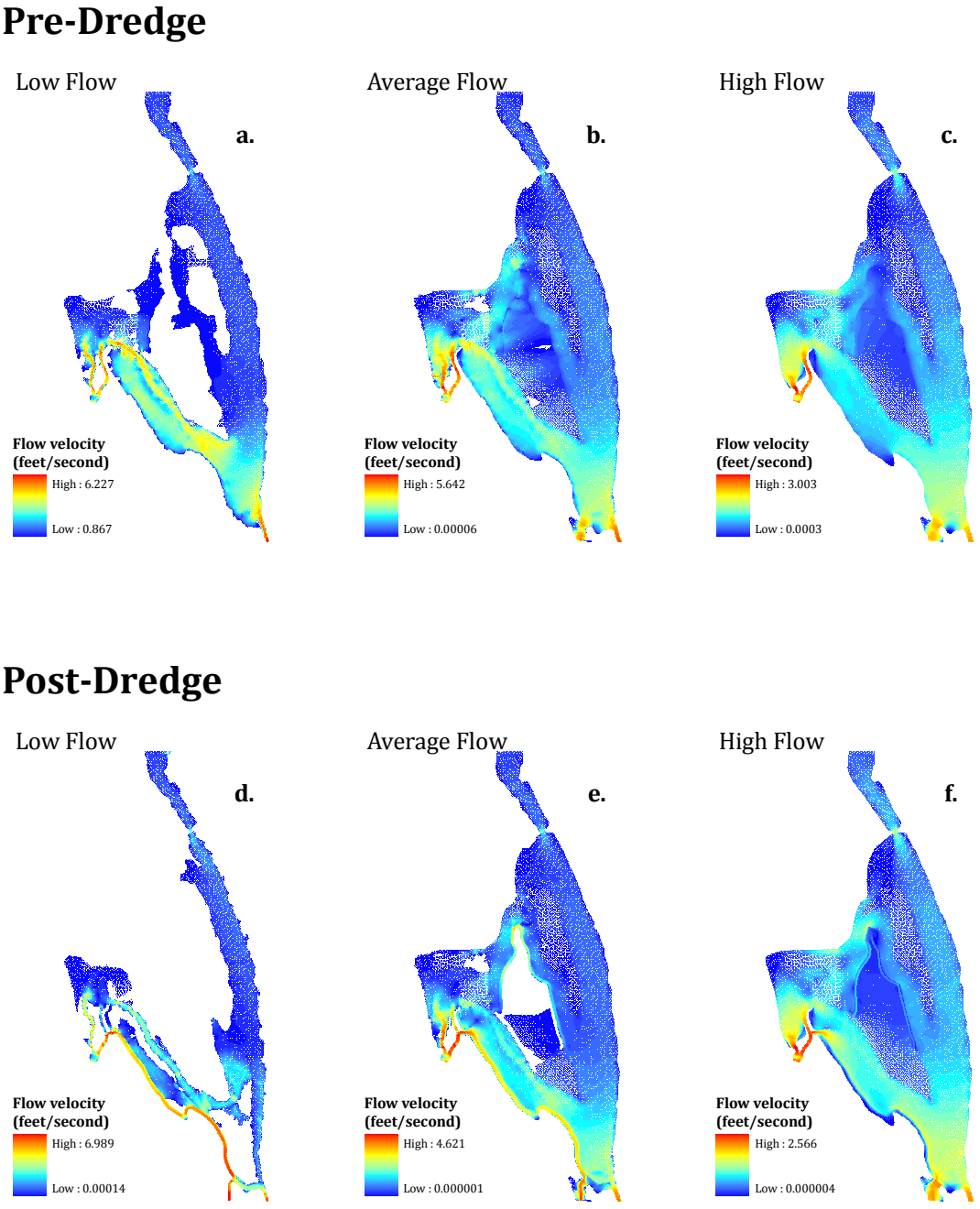

Figure 39: Resulting output from SRH-W main solver displaying flow velocity magnitude (measured in feet/second) for different flow scenarios (High, Medium, Low) simulated with the mesh created from the existing bathymetry (Pre-Dredge) and the mesh representative of the study area following the proposed dredging (Post-Dredge).

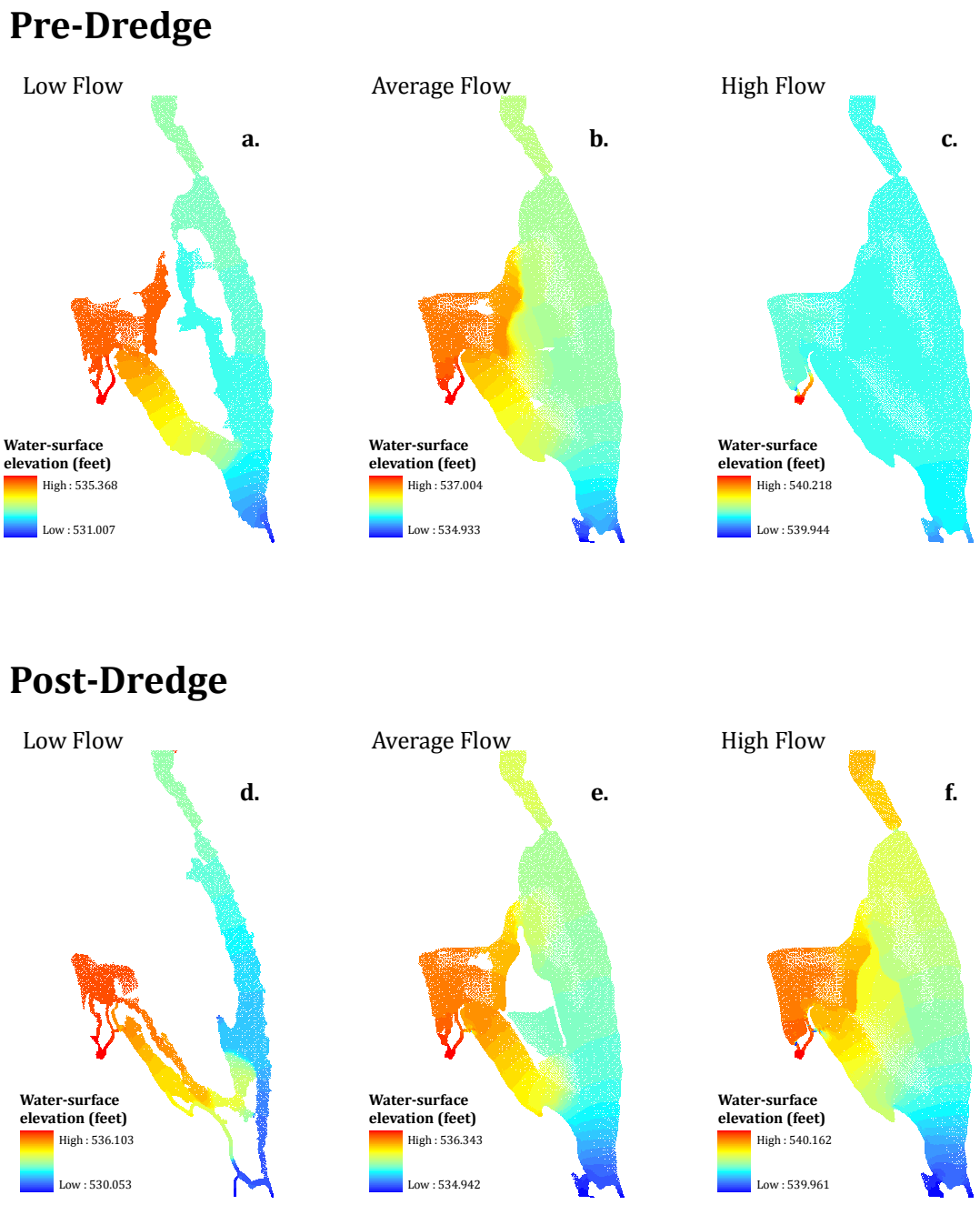

Figure 40: Resulting output from SRH-W main solver displaying values of water-surface elevation (measured in feet above MSL 1912) for different flow scenarios (High, Medium, Low) simulated with the mesh created from the existing bathymetry (Pre-Dredge) and the mesh representative of the study area following the proposed dredging (Post-Dredge).

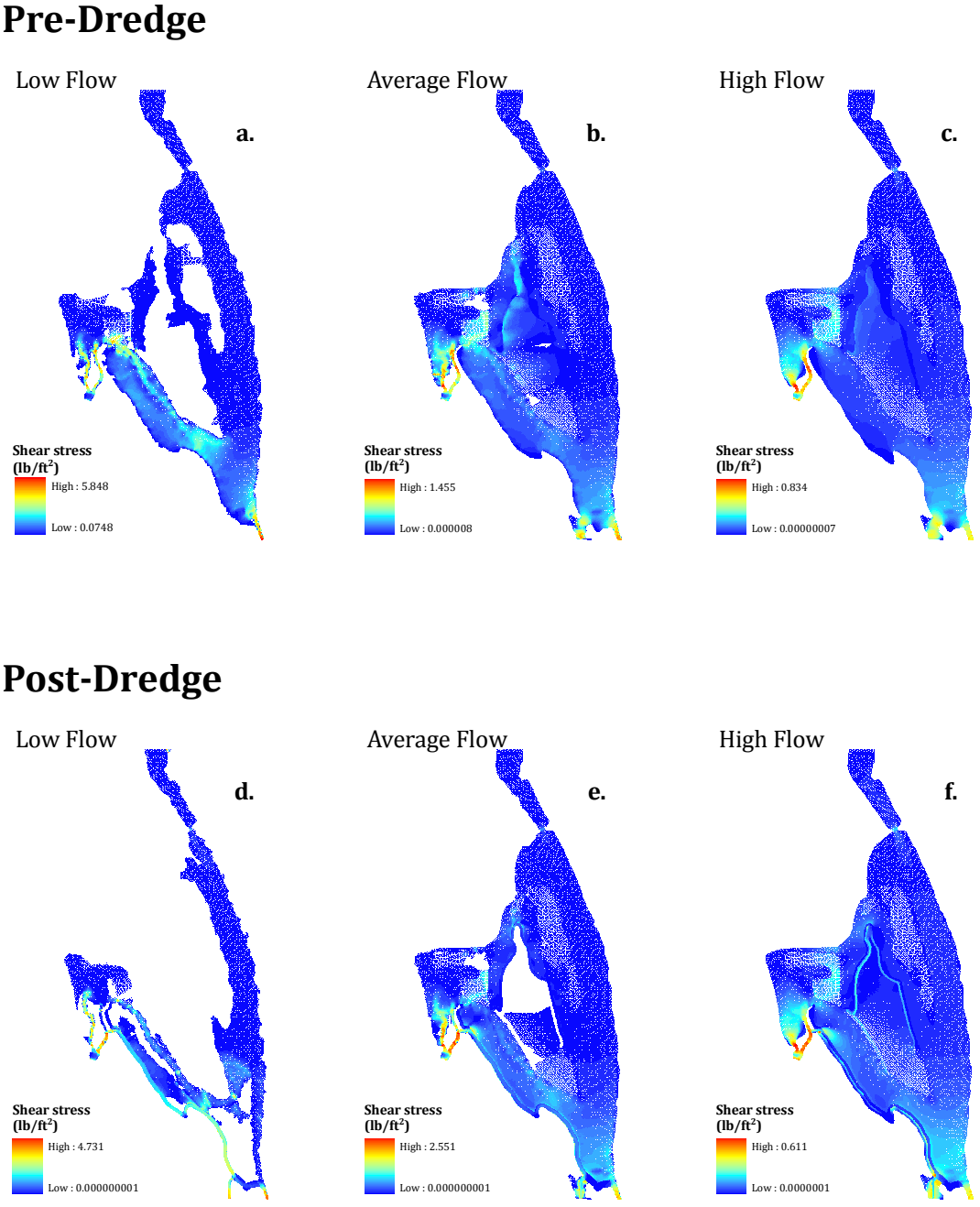

Figure 41: Resulting output from SRH-W main solver displaying values of bed shear-stress (measured in pounds per square foot) for different flow scenarios (High, Medium, Low) simulated with the mesh created from the existing bathymetry (Pre-Dredge) and the mesh representative of the study area following the proposed dredging (Post-Dredge).

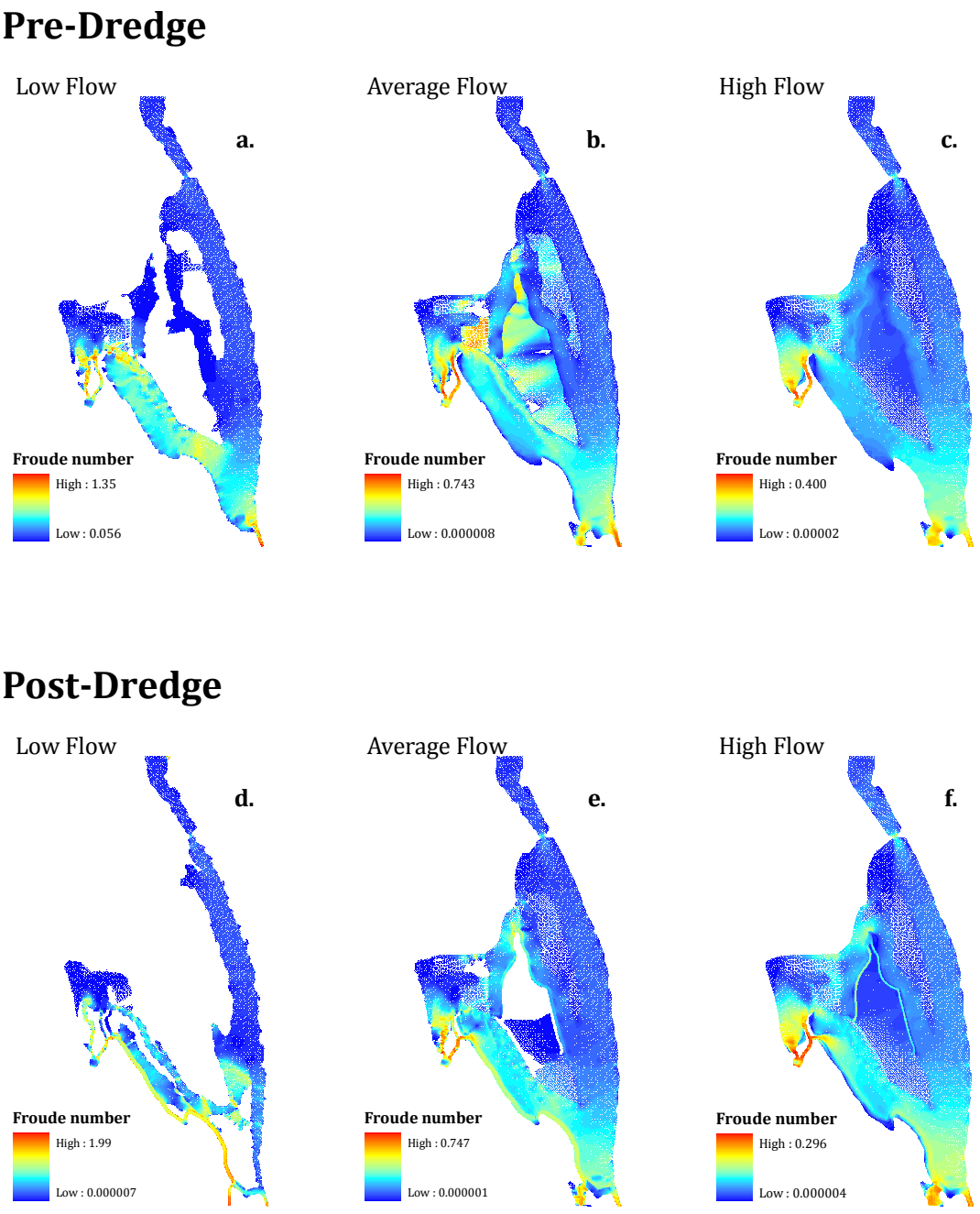

Figure 42: Resulting output from SRH-W main solver displaying values of Froude number for different flow scenarios (High, Medium, Low) simulated with the mesh created from the existing bathymetry (Pre-Dredge) and the mesh representative of the study area following the proposed dredging (Post-Dredge).

Focusing our attention on the output values of water depth and flow velocity (Figures 38 and 39) we see that much of the study area exhibits shallow depths and slow moving flows. These observations are perhaps made more evident by examining a set of histograms displaying water depth and flow velocity for the pre- and post-dredge scenarios for the average flow conditions (Figure 43). Here, one can clearly see that the majority of the water depths fall within the 0.001 – 6.0 ft range, with a slight increase following dredging. Similarly, much of the flow velocities are found to be within 0.00006 – 0.5 ft/sec.

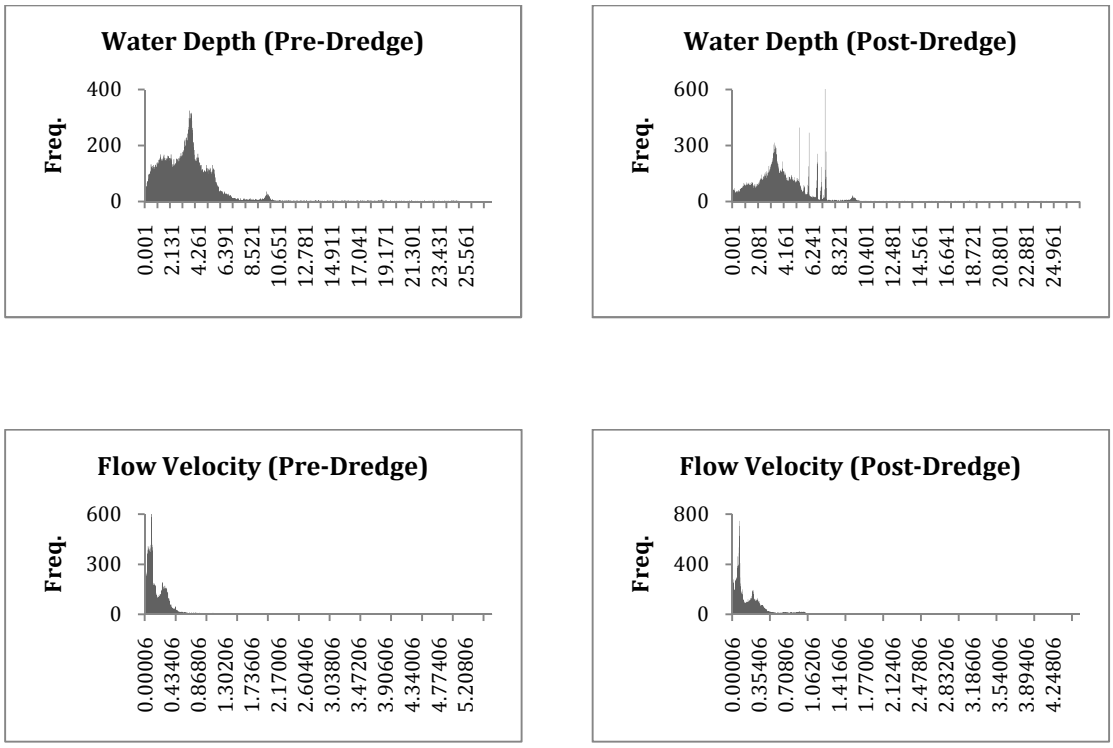

Figure 43: Histograms showing the distributions of water depth and flow velocity for the pre- and post-dredge scenarios using the average flow conditions.

5.3.2 – Sensitivity Analysis

To determine the degree to which model results are sensitive to certain independent variables, simulations of average-flow conditions were repeated using different values of Manning's roughness coefficient (*n*). Two additional simulations of the average-flow scenario were run; once using *n* values that were twice the original values ('large n') and again using *n* values one-half of the original values ('small n'). Simulations run using the originally assigned values of Manning's roughness coefficient are referred to as 'average n.' Using the resulting output files from each simulation, paths were traced from the downstream outlet of the study area to the upstream inlets of Eliza Creek and the Bay Island pumping station, with readings of water-surface elevation recorded for each point along the path. The values of Manning's n assigned to each material type for these simulations are summarized in Table 13.

	Values of Manning's *n* for different scenarios		
Material Type	**Small n**	**Average n**	**Large n**
Bed Material	0.04	0.08	0.16
Vegetated Island	0.1	0.2	0.4
Dredged Channel	0.015	0.03	0.06

Table 13: Values of Manning's roughness coefficient (n) assigned to the differentmaterial types that exist within the study area. Sensitivity of the model to roughness values can be determined by varying the input values of n and repeating the simulation while holding all other variables constant.

The resulting plots clearly show a direct relationship between the assigned values of Manning's roughness and the reported values of water-surface elevation (Figure 45 and 46). Similarly, the model results do not appear to be highly sensitive

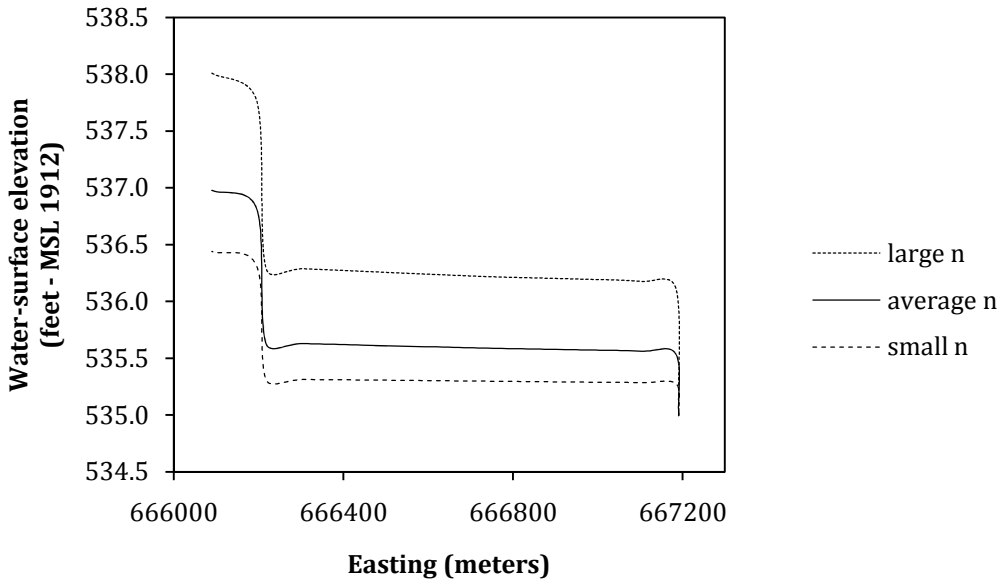

Figure 44: Values of water-surface elevation for different points falling on a line extending from the downstream outlet of Boston Bay and the upstream inlet of the BIDLD pumping station different values of Manning's roughness (*n*).

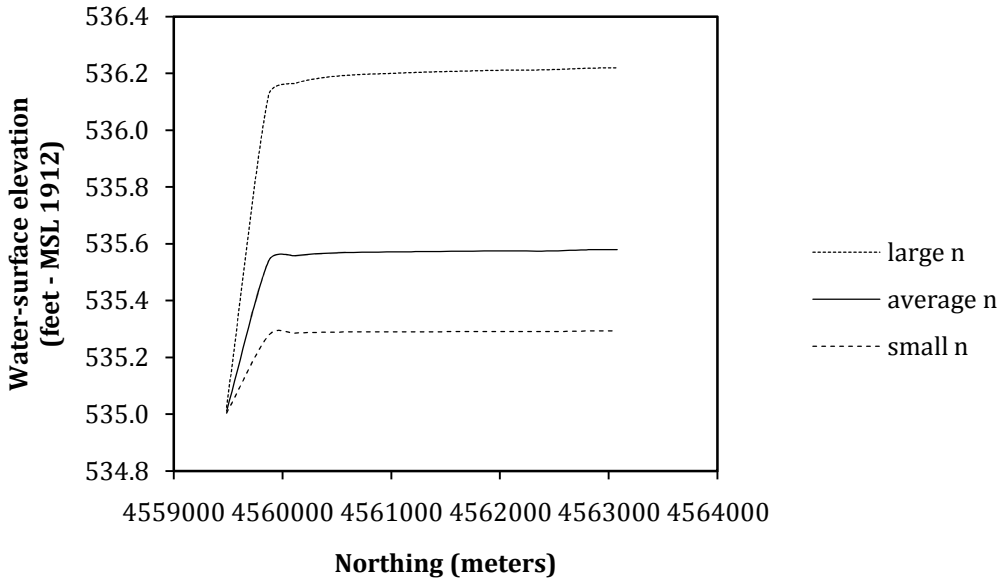

Figure 45: Values of water-surface elevation for different points falling on a line extending from the downstream outlet of Boston Bay and the upstream inlet from Eliza Creek for different values of Manning's roughness (*n*).

to input values of Manning's roughness coefficient. Water-surface elevation is roughly 1 ft greater at the upstream inlet of the BIDLD pumping station for simulations using *n* values that are twice the originally assigned value ('large n') when compared to the original simulation results ('average n') (Figure 45). The upstream inlet of Eliza Creek experiences a 0.6 ft increase in water-surface elevation values when n values are doubled (Figure 46). Similar arguments hold when comparing water-surface elevation values from the original simulations with the results from the simulations using *n* values that were one-half of the original value ('small n').

5.4 – Discussion

While the majority of the model results appear to make physical sense, there is some concern over the accuracy of those results obtained during high flow scenarios. This uncertainty stems from evidence obtained through analysis of aerial photos of Boston Bay during a spring time flood event (Figure 3), which indicates that the solution domain needs to be expanded to account for increased inundation of upland areas during high flows. Figure 3 clearly indicates that the boundary defined by the mesh generation process is not sufficient to handle the high flow conditions that exist in the area of Boston Bay during flood events, and is likely a source of error for the results from the high-flow simulations. However, given that the difficulty with navigation experienced during low-flow is not seen under high-flow scenarios, such errors are of little concern for this study.

Limited funding did not allow for further field data collection necessary to validate results from the various simulation scenarios. Ideally, flow velocity and water-surface elevation data should be collected concurrently with bathymetry and discharge measurements to accurately calibrate and validate a 2D hydrodynamic

model (Conaway and Moran, 2004; Huizinga, 2007). Despite such limitations, initial results from the 2D modeling of Boston Bay indicate that the proposed dredging activity will not significantly impact the existing flow conditions in the bay, with water depths in the deepest regions of the study area remaining mostly unchanged following the proposed dredging (Figure 38). While results from this study should not be used during the design phase of the proposed restoration, they do shed light on areas where further research and data collection are required to fully model and understand the flow characteristics of the Boston Bay study area.

CHAPTER 6 – CONCLUSION

The study into the potential restoration of Boston Bay adopted a multidisciplinary approach involving various methods which included sediment-size analysis of the material to be dredged, monitoring of nitrate-nitrogen concentrations of agricultural runoff water being pumped into the study area, mapping of the existing bathymetry and development of a two-dimensional hydrodynamic model capable of simulating the proposed dredging and berm construction. Taken together, the results of each study will assist interested parties as the restoration of Boston Bay moves forward.

Results from sediment-size analysis reveal that the material contained within the study area is primarily silt- and clay-sized consisting of particles with diameters in the range of 2 to 50 microns. The hydrometer method of sedimentation determined that seven of the 28 sediment samples contained greater than 50% sand. These samples were further analyzed using traditional sieving techniques and it was determined that the majority of sand found within the study is considered to be 'fine sand' as defined by the USDA (Table 6).

The findings from this study into the physical characteristics of the sediment to be dredged closely match results from a field study conducted by the USDA in 2004, which determined that much of the sediment located in the study area would qualify as 'Fluvaquents,' 'Beaucoup silty clay loam,' and 'Coloma sand' (Figure 14). While the fact that results from the two studies agree with one another is indeed reassuring, the USDA states that such soils present severe limitations when used to construct berms, embankments and levees. This may be cause for some concern for those parties interested in using the sediment dredged from Boston Bay to design berms and ridges. Further analysis of the engineering properties of this material should be conducted before dredging begins.

The data obtained from the nitrate-nitrogen sensor is easily displayed as a series of plots of nitrate concentration versus time as shown in Figures 15 through 21. One can immediately observe a direct relationship between measured concentration of nitrate-nitrogen and precipitation events as indicated by abrupt spikes in the data set (see May). Averages for each full month that the nitrate sensor was deployed in the field have been displayed in Table 10. May exhibited the highest average nitrate concentration of 10.271 mg/L while November experienced the lowest concentration with 2.867 mg/L. Nitrate concentration of agricultural runoff water entering Boston Bay from the Bay Island Drainage and Levee District (BIDLD) was observed to be much lower on average during late fall and winter when compared to the concentrations measured during spring. The highest measured nitrate concentrations occurred during the spring, with a maximum value of 20.738 mg/L in early May of 2009. This is nearly twice the 10 mg/L maximum contaminant level defined by the Environmental Protection Agency and could be harmful for livestock and humans (Bruning-Fann and Kaneene, 1993; Knobeloch, et al, 2000; Sturgul and Kelling, 2003).

These data were coupled with the daily operation and maintenance logs from the BIDLD pumping station in an attempt to estimate the total load of nitrate-nitrogen entering the study area via the drainage district. According to the pumping stations daily maintenance logs, the BIDLD pumped over 7,800,000,000 gallons of in nearly 4,300 hours of operating time. Using Equation 5 it was determined that nearly 800 tons of nitrate-nitrogen was pumped into Boston Bay via the neighboring drainage district.

This study points to many valuable applications for monitoring nitrate-nitrogen levels of artificially drained farm runoff. If other drainage districts in the Upper Mississippi River basin adopted similar monitoring practices, it would be a much easier task to identify those watersheds that would benefit the most from best

management practices (BMPs) to help reduce nitrate loading. Carefully targeting programs to areas of higher pollutant loadings could help conservation programs designed to reduce nitrate. Targeting USDA conservation programs to areas of higher nutrient and sediment loadings can lead to BMPs for control of runoff containing sediment and nutrients being implemented on lands that are the primary sources of nonpoint pollutants and major contributors to the hypoxic conditions existing in the Gulf of Mexico.

The situation involving the BIDLD and Boston Bay, presents a unique opportunity to effectively treat nonpoint pollution before entering the Mississippi River. The drainage district and its pumping station could technically be viewed as a point-source polluter, and could be dealt with using 'end-of-pipe' treatment methods to help reduce concentrations of nitrate-nitrogen in the waters of Boston Bay before they join the flows of the Mississippi River and eventually the Gulf of Mexico.

The bathymetric survey of Boston Bay resulted in over 180,000 data points with the elevation values referenced to MSL 1912 and the horizontal position referenced to the North American Datum of 1983 (NAD 83). Using a GIS these data were used to generate the resulting contoured surfaces were layered onto aerial photography of the study area and displayed as a series of bathymetric maps (Figures 28 – 33). These figures reveal that Boston Bay exhibits little topographic relief, with much of the project area lying in a range of elevations between 530 and 532 ft above sea level, and an average elevation of 531.903 ft. The lowest point of elevation within the boundaries of the survey is 507.067 ft and is located near the pond where the pipes from the BIDLD (Figure 31). The highest elevation measured during the survey had a value of 539.974 feet and also located near the discharge pond. 'Bells Pocket,' a popular location for recreational fishing shows significant changes in topography relative to the rest of the study area, with the deepest

portions existing in a range of elevations from 508 and 510 ft above sea level (Figure 29).

Constructing a 2D hydrodynamic model of the Boston Bay study area required that a mesh consisting of 73,622 triangular elements, 11,921 quadrilateral elements, and 49,433 nodes be generated using the data collected during the aforementioned bathymetric survey. The maximum and minimum elevation values contained within the mesh are 539.92 and 508.84 ft, respectively. To simulate the proposed dredging of the study area, the mesh generated using the existing bathymetry was altered to reflect the dredging activity prescribed by Living Lands & Waters (Figure 36). This was easily achieved by selecting mesh nodes contained within the assigned dredging location, and changing the elevation values (z) to mimic what the bathymetry would look like after dredging has occurred. Boundary conditions are applied to different node-strings of the mesh to signify values of inlet discharge and outlet water-surface elevation.

The resulting output files from the numerical simulation provide information about flow velocity, water surface elevation, water depth, Froude number, and bed shear-stress at the center of each mesh element and can be easily displayed as xyz scatter sets in SMS or ArcGIS (Figure 38 - 42). Initial results indicate that the water depth in the 'Bell's Pocket' area would drop by just over 1 ft following the proposed restoration, decreasing from 26.195 ft to 25.165 ft during low-flow conditions (Figure 38 a and d). It also appears that a smaller portion of Boston Bay remains inundated once the dredging has been completed.

Average-flow scenarios reveal that a smaller portion of the study area is inundated following dredging and berm construction. The region behind the constructed berm appears to provide suitable habitat for hardwood tree species. The areas that remain inundated exhibit generally higher water depths throughout. Like the low-flow simulations, water depths in the vicinity of 'Bells Pocket' also

experience a decrease following the proposed dredging of the study area (Figure 38 b and e). Results from the high-flow scenarios are likely inaccurate due to insufficient topographic data required to model the portions of the study area that are inundated during high-flows. However, this is of little concern as the navigation difficulties suffered during low-flows do not exist during high-flow conditions. Output values of water depth and flow velocity magnitude were also compared to determine how the proposed dredging would impact the existing hydrology of the study area (Figure 39 and 40).

Limited funding meant that the model designed during this study could not be validated with field data. Regardless, the initial results from the numerical simulation indicate that the proposed dredging will not have a significant impact on the deepest portions of the study area, including 'Bell's Pocket.' The areas closest to the proposed dredging do appear to experience significant shifts from the existing hydrology as would be expected. And, while these results should not be used during the design phase of the restoration of Boston Bay, they do point to other areas where further research should be conducted to accurately model flow conditions of the study area.

Collectively, the results from each study into the proposed restoration of the Boston Bay provide significant information about the relevant physical and chemical characteristics of the study area. Should the dredging and berm construction outlined by Living Lands & Waters proceed as planned, the data obtained during this multidisciplinary study will prove to be useful, serving as a toolbox for decision makers, providing interested parties with a checklist of data that has already been collected and analyzed, helping to cut down on redundancy while also shedding light on areas that still need to be researched in greater detail.

APPENDIX A – SOIL CHEMISTRY RESULTS

What follows is a summary of the results from chemical analysis conducted on the sediment core samples removed from the Boston Bay study area on April 9, 2008. Analysis was conducted at the TestAmerica laboratory, located in Chicago, Illinois on May 2, 2008. Samples were analyzed for total cyanide, pH, percent solids and the presence of the following selected metals, organochlorine pesticides and PCB's (Table A1). Several semivolatile compounds were tested for (Table A2). Original test results can be made available by contacting Living Lands & Waters (17624 Rt. 84, East Moline, IL, 61244).

Metals	Organochlorine Pesticides	PCB's
Aluminum	4,4'-DDD	PCB-1260
Antimony	4,4'-DDE	PCB-1254
Arsenic	4,4'-DDT	PCB-1221
Barium	Aldrin	PCB-1232
Beryllium	alpha-BHC	PCB-1248
Cadmium	alpha-Chlordane	PCB-1016
Calcium	Atrazine	PCB-1242
Chromium	beta-BHC	
Cobalt	delta-BHC	
Copper	Dieldrin	
Iron	Endosulfan I	
Lead	Endosulfan II	
Magnesium	Endosulfan sulfate	
Manganese	Endrin	
Mercury	Endrin aldehyde	
Molybdenum	Endrin ketone	
Nickel	gamma-BHC (Lindane)	
Potassium	gamma-Chlordane	
Selenium	Heptachlor	
Silver	Heptachlor epoxide	
Sodium	Methoxychlor	
Thallium	Toxaphene	
Vanadium		
Zinc		

Table A1: Selected metals, organochlorine pesticides and PCB's tested for during the chemical analysis of sediment core samples from the Boston Bay study area.

1,1'-Biphenyl	4-Chloro-3-methylphenol	Dibenz(a,h)anthracene
1,2,4,5-Tetrachlorobenzene	4-Chloroaniline	Dibenzofuran
1,2,4-Trichlorobenzene	4-Chlorophenyl phenyl ether	Diethyl phthalate
1,2-Dichlorobenzene	4-Nitroaniline	Dimethyl phthalate
1,3-Dichlorobenzene	4-Nitrophenol	Di-n-butyl phthalate
1,4-Dichlorobenzene	Acenaphthene	Di-n-octyl phthalate
2,2'-oxybis[1-chloropropane]	Acenaphthylene	Fluoranthene
2,4,5-Trichlorophenol	Acetophenone	Fluorene
2,4,6-Trichlorophenol	Anthracene	Hexachlorobenzene
2,4-Dichlorophenol	Benzaldehyde	Hexachlorobutadiene
2,4-Dimethylphenol	Benzidine	Hexachlorocyclopentadiene
2,4-Dinitrophenol	Benzo[a]anthracene	Hexachloroethane
2,4-Dinitrotoluene	Benzo[a]pyrene	Indeno[1,2,3-cd]pyrene
2,6-Dinitrotoluene	Benzo[b]fluoranthene	Isophorone
2-Chloronaphthalene	Benzo[g,h,i]perylene	Naphthalene
2-Chlorophenol	Benzo[k]fluoranthene	Nitrobenzene
2-Methylnaphthalene	Benzoic acid	N-Nitrosodi-n-propylamine
2-Methylphenol	Benzyl alcohol	N-Nitrosodiphenylamine
2-Nitroaniline	Bis(2-chloroethoxy)methane	Pentachlorophenol
2-Nitrophenol	Bis(2-chloroethyl)ether	Phenanthrene
3 & 4 Methylphenol	Bis(2-ethylhexyl) phthalate	Phenol
3,3'-Dichlorobenzidine	Butyl benzyl phthalate	Pyrene
3-Nitroaniline	Caprolactam	
4,6-Dinitro-2-methylphenol	Carbazole	
4-Bromophenyl phenyl ether	Chrysene	

Table A2: Selected semivolatile compounds tested for during the chemical analysis of sediment core samples from the Boston Bay study area.

Description	Lab Location	Method	Preparation Method
Matrix: Solid			
Semivolatile Compounds by Gas Chromatography/Mass Spectrometry (GC/MS)	TAL CHI	SW846 8270C	
Ultrasonic Extraction	TAL CHI		SW846 3550B
Organochlorine Pesticides by Gas Chromatography	TAL CHI	SW846 8081A	
Automated Soxhlet Extraction	TAL CHI		SW846 3541
Polychlorinated Biphenyls (PCBs) by Gas Chromatography	TAL CHI	SW846 8082	
Automated Soxhlet Extraction	TAL CHI		SW846 3541
Inductively Coupled Plasma - Atomic Emission Spectrometry	TAL CHI	SW846 6010B	
Acid Digestion of Sediments, Sludges, and Soils	TAL CHI		SW846 3050B
Mercury in Solid or Semisolid Waste (Manual Cold Vapor Technique)	TAL CHI	SW846 7471A	
Mercury in Solid or Semi-Solid Waste (Manual Cold	TAL CHI		SW846 7471A
Titrimetric and Manual Spectrophotometric Determinative Methods for Cyanide	TAL CHI	SW846 9014	
Cyanide Distillation	TAL CHI		SW846 9010B
Soil and Waste pH	TAL CHI	SW846 9045C	

Lab References:

TAL CHI = TestAmerica Chicago

Method References:

SW846 = "Test Methods For Evaluating Solid Waste, Physical/Chemical Methods", Third Edition, November 1986 And Its Updates.

Table A3: Summary of the methods used for chemical analysis of sediment core samples from the Boston Bay study area.

Lab Section	Qualifier	Description
GC/MS Semi VOA		
	F	MS or MSD exceeds the control limits
	J	Result is less than the RL but greater than or equal to the MDL and the concentration is an approximate value.
GC Semi VOA		
	J	Result is less than the RL but greater than or equal to the MDL and the concentration is an approximate value.
	H	Sample was prepped or analyzed beyond the specified holding time
Metals		
	B	Compound was found in the blank and sample.
	F	MS or MSD exceeds the control limits
	4	MS, MSD: The analyte present in the original sample is 4 times greater than the matrix spike concentration; therefore, control limits are not applicable.
	J	Result is less than the RL but greater than or equal to the MDL and the concentration is an approximate value.
	V	Serial Dilution exceeds the control limits
General Chemistry		
	F	MS or MSD exceeds the control limits
	J	Result is less than the RL but greater than or equal to the MDL and the concentration is an approximate value.
	F	RPD of the MS and MSD exceeds the control limits

Table A4: Data reporting qualifiers used for chemical analysis of sediment core samples from the Boston Bay study area.

Lab Sample ID / Analyte	Client Sample ID	Result / Qualifier		Reporting Limit	Units	Method
500-10601-1	**386.333**					
Phenanthrene		16	J	33	ug/Kg	8270C
Fluoranthene		44		33	ug/Kg	8270C
Pyrene		62		33	ug/Kg	8270C
Benzo[a]anthracene		33		33	ug/Kg	8270C
Chrysene		37		33	ug/Kg	8270C
Benzo[b]fluoranthene		30	J	33	ug/Kg	8270C
Benzo[k]fluoranthene		36		33	ug/Kg	8270C
Benzo[a]pyrene		26	J	33	ug/Kg	8270C
Indeno[1,2,3-cd]pyrene		23	J	33	ug/Kg	8270C
Dibenz(a,h)anthracene		12	J	33	ug/Kg	8270C
Benzo[g,h,i]perylene		31	J	33	ug/Kg	8270C
PCB-1254		22	J	25	ug/Kg	8082
PCB-1260		13	J	25	ug/Kg	8082
Aluminum		17000	B	35	mg/Kg	6010B
Arsenic		6.0		1.8	mg/Kg	6010B
Barium		210		1.8	mg/Kg	6010B
Beryllium		0.81		0.71	mg/Kg	6010B
Cadmium		1.0		0.35	mg/Kg	6010B
Calcium		22000	B	18	mg/Kg	6010B
Chromium		30		1.8	mg/Kg	6010B
Cobalt		9.8		0.89	mg/Kg	6010B
Copper		23		1.8	mg/Kg	6010B
Iron		29000	B	18	mg/Kg	6010B
Lead		24		0.89	mg/Kg	6010B
Magnesium		5800		18	mg/Kg	6010B
Manganese		1100		1.8	mg/Kg	6010B
Nickel		24		1.8	mg/Kg	6010B
Potassium		1800		89	mg/Kg	6010B
Sodium		120	J	180	mg/Kg	6010B
Vanadium		37		0.89	mg/Kg	6010B
Zinc		110		3.5	mg/Kg	6010B
Mercury		0.088		0.033	mg/Kg	7471A
Cyanide, Total		0.24	J	0.79	mg/Kg	9014
pH		7.40		0.200	SU	9045C
Percent Moisture		50		0.10	%	PercentMoisture
Percent Solids		50		0.10	%	PercentMoisture

Table A5: Results from chemical analysis of sediment core number 386.333.

Lab Sample ID / Analyte	Client Sample ID	Result / Qualifier		Reporting Limit	Units	Method
500-10601-2	**386.555**					
Acenaphthylene		11	J	30	ug/Kg	8270C
Phenanthrene		14	J	30	ug/Kg	8270C
Fluoranthene		49		30	ug/Kg	8270C
Pyrene		61		30	ug/Kg	8270C
Benzo[a]anthracene		34		30	ug/Kg	8270C
Chrysene		40		30	ug/Kg	8270C
Bis(2-ethylhexyl) phthalate		390		150	ug/Kg	8270C
Benzo[b]fluoranthene		28	J	30	ug/Kg	8270C
Benzo[k]fluoranthene		29	J	30	ug/Kg	8270C
Benzo[a]pyrene		36		30	ug/Kg	8270C
Indeno[1,2,3-cd]pyrene		20	J	30	ug/Kg	8270C
Dibenz(a,h)anthracene		13	J	30	ug/Kg	8270C
Benzo[g,h,i]perylene		28	J	30	ug/Kg	8270C
PCB-1254		8.0	J	22	ug/Kg	8082
Aluminum		20000	B	34	mg/Kg	6010B
Arsenic		7.4		1.7	mg/Kg	6010B
Barium		220		1.7	mg/Kg	6010B
Beryllium		0.97		0.68	mg/Kg	6010B
Cadmium		0.77		0.34	mg/Kg	6010B
Calcium		8800	B	17	mg/Kg	6010B
Chromium		31		1.7	mg/Kg	6010B
Cobalt		11		0.85	mg/Kg	6010B
Copper		25		1.7	mg/Kg	6010B
Iron		30000	B	17	mg/Kg	6010B
Lead		27		0.85	mg/Kg	6010B
Magnesium		5300		17	mg/Kg	6010B
Manganese		820		1.7	mg/Kg	6010B
Nickel		28		1.7	mg/Kg	6010B
Potassium		2000		85	mg/Kg	6010B
Sodium		88	J	170	mg/Kg	6010B
Vanadium		43		0.85	mg/Kg	6010B
Zinc		120		3.4	mg/Kg	6010B
Mercury		0.080		0.030	mg/Kg	7471A
Cyanide, Total		0.21	J	0.76	mg/Kg	9014
pH		7.42		0.200	SU	9045C
Percent Moisture		45		0.10	%	PercentMoisture
Percent Solids		55		0.10	%	PercentMoisture

Table A6: Results from chemical analysis of sediment core number 386.555.

Lab Sample ID / Analyte	Client Sample ID	Result / Qualifier		Reporting Limit	Units	Method
500-10601-3	**386.777**					
Acenaphthylene		7.9	J	28	ug/Kg	8270C
Phenanthrene		28		28	ug/Kg	8270C
Anthracene		13	J	28	ug/Kg	8270C
Fluoranthene		81		28	ug/Kg	8270C
Pyrene		92		28	ug/Kg	8270C
Benzo[a]anthracene		46		28	ug/Kg	8270C
Chrysene		50		28	ug/Kg	8270C
Bis(2-ethylhexyl) phthalate		380		140	ug/Kg	8270C
Benzo[b]fluoranthene		35		28	ug/Kg	8270C
Benzo[k]fluoranthene		36		28	ug/Kg	8270C
Benzo[a]pyrene		52		28	ug/Kg	8270C
Indeno[1,2,3-cd]pyrene		26	J	28	ug/Kg	8270C
Dibenz(a,h)anthracene		13	J	28	ug/Kg	8270C
Benzo[g,h,i]perylene		35		28	ug/Kg	8270C
Aluminum		18000	B	30	mg/Kg	6010B
Arsenic		6.2		1.5	mg/Kg	6010B
Barium		190		1.5	mg/Kg	6010B
Beryllium		0.88		0.59	mg/Kg	6010B
Cadmium		0.37		0.30	mg/Kg	6010B
Calcium		8000	B	15	mg/Kg	6010B
Chromium		27		1.5	mg/Kg	6010B
Cobalt		10		0.74	mg/Kg	6010B
Copper		20		1.5	mg/Kg	6010B
Iron		27000	B	15	mg/Kg	6010B
Lead		23		0.74	mg/Kg	6010B
Magnesium		5100		15	mg/Kg	6010B
Manganese		660		1.5	mg/Kg	6010B
Nickel		24		1.5	mg/Kg	6010B
Potassium		1800		74	mg/Kg	6010B
Selenium		0.59	J	1.5	mg/Kg	6010B
Sodium		82	J	150	mg/Kg	6010B
Vanadium		42		0.74	mg/Kg	6010B
Zinc		95		3.0	mg/Kg	6010B
Mercury		0.074		0.029	mg/Kg	7471A
Cyanide, Total		0.25	J	0.76	mg/Kg	9014
pH		7.37		0.200	SU	9045C
Percent Moisture		42		0.10	%	PercentMoisture
Percent Solids		58		0.10	%	PercentMoisture

Table A7: Results from chemical analysis of sediment core number 386.777.

Lab Sample ID / Analyte	Client Sample ID	Result / Qualifier		Reporting Limit	Units	Method
500-10601-4	**387**					
Phenanthrene		11	J	30	ug/Kg	8270C
Fluoranthene		25	J	30	ug/Kg	8270C
Pyrene		38		30	ug/Kg	8270C
Benzo[a]anthracene		17	J	30	ug/Kg	8270C
Chrysene		17	J	30	ug/Kg	8270C
Benzo[b]fluoranthene		21	J	30	ug/Kg	8270C
Benzo[a]pyrene		18	J	30	ug/Kg	8270C
Indeno[1,2,3-cd]pyrene		10	J	30	ug/Kg	8270C
Benzo[g,h,i]perylene		15	J	30	ug/Kg	8270C
Aluminum		20000	B	37	mg/Kg	6010B
Arsenic		6.6		1.8	mg/Kg	6010B
Barium		220		1.8	mg/Kg	6010B
Beryllium		0.97	V	0.73	mg/Kg	6010B
Cadmium		0.50		0.37	mg/Kg	6010B
Calcium		9200	B	18	mg/Kg	6010B
Chromium		30		1.8	mg/Kg	6010B
Cobalt		11		0.92	mg/Kg	6010B
Copper		23		1.8	mg/Kg	6010B
Iron		32000	B	18	mg/Kg	6010B
Lead		23		0.92	mg/Kg	6010B
Magnesium		5300		18	mg/Kg	6010B
Manganese		980		1.8	mg/Kg	6010B
Nickel		26		1.8	mg/Kg	6010B
Potassium		2000		92	mg/Kg	6010B
Sodium		100	J	180	mg/Kg	6010B
Vanadium		45		0.92	mg/Kg	6010B
Zinc		100	V	3.7	mg/Kg	6010B
Mercury		0.071		0.031	mg/Kg	7471A
Cyanide, Total		0.29	J	0.86	mg/Kg	9014
pH		7.39		0.200	SU	9045C
Percent Moisture		46		0.10	%	PercentMoisture
Percent Solids		54		0.10	%	PercentMoisture

Table A8: Results from chemical analysis of sediment core number 387.

Lab Sample ID / Analyte	Client Sample ID	Result / Qualifier		Reporting Limit	Units	Method
500-10601-5	**388**					
Fluoranthene		12	J	27	ug/Kg	8270C
Pyrene		14	J	27	ug/Kg	8270C
Benzo[a]anthracene		10	J	27	ug/Kg	8270C
Chrysene		9.3	J	27	ug/Kg	8270C
Bis(2-ethylhexyl) phthalate		430		140	ug/Kg	8270C
Benzo[b]fluoranthene		12	J	27	ug/Kg	8270C
Benzo[a]pyrene		7.6	J	27	ug/Kg	8270C
Benzo[g,h,i]perylene		10	J	27	ug/Kg	8270C
Aluminum		14000	B	29	mg/Kg	6010B
Arsenic		5.7		1.5	mg/Kg	6010B
Barium		160		1.5	mg/Kg	6010B
Beryllium		0.71		0.59	mg/Kg	6010B
Cadmium		0.37		0.29	mg/Kg	6010B
Calcium		9900	B	15	mg/Kg	6010B
Chromium		22		1.5	mg/Kg	6010B
Cobalt		10		0.74	mg/Kg	6010B
Copper		17		1.5	mg/Kg	6010B
Iron		25000	B	15	mg/Kg	6010B
Lead		15		0.74	mg/Kg	6010B
Magnesium		4500		15	mg/Kg	6010B
Manganese		730		1.5	mg/Kg	6010B
Nickel		21		1.5	mg/Kg	6010B
Potassium		1400		74	mg/Kg	6010B
Sodium		87	J	150	mg/Kg	6010B
Vanadium		31		0.74	mg/Kg	6010B
Zinc		68		2.9	mg/Kg	6010B
Mercury		0.036		0.028	mg/Kg	7471A
Cyanide, Total		0.17	J	0.65	mg/Kg	9014
pH		7.45		0.200	SU	9045C
Percent Moisture		40		0.10	%	PercentMoisture
Percent Solids		60		0.10	%	PercentMoisture

Table A9: Results from chemical analysis of sediment core number 388.

Lab Sample ID / Analyte	Client Sample ID	Result / Qualifier		Reporting Limit	Units	Method
500-10601-6	**389**					
Phenanthrene		8.2	J	30	ug/Kg	8270C
Fluoranthene		17	J	30	ug/Kg	8270C
Pyrene		21	J	30	ug/Kg	8270C
Benzo[a]anthracene		8.1	J	30	ug/Kg	8270C
Chrysene		15	J	30	ug/Kg	8270C
Benzo[b]fluoranthene		15	J	30	ug/Kg	8270C
Benzo[a]pyrene		7.5	J	30	ug/Kg	8270C
Indeno[1,2,3-cd]pyrene		10	J	30	ug/Kg	8270C
Benzo[g,h,i]perylene		9.4	J	30	ug/Kg	8270C
Aluminum		19000	B	33	mg/Kg	6010B
Arsenic		8.4		1.7	mg/Kg	6010B
Barium		240		1.7	mg/Kg	6010B
Beryllium		0.95		0.66	mg/Kg	6010B
Cadmium		0.43		0.33	mg/Kg	6010B
Calcium		8700	B	17	mg/Kg	6010B
Chromium		28		1.7	mg/Kg	6010B
Cobalt		11		0.83	mg/Kg	6010B
Copper		21		1.7	mg/Kg	6010B
Iron		32000	B	17	mg/Kg	6010B
Lead		18		0.83	mg/Kg	6010B
Magnesium		5100		17	mg/Kg	6010B
Manganese		1100		1.7	mg/Kg	6010B
Nickel		27		1.7	mg/Kg	6010B
Potassium		1900		83	mg/Kg	6010B
Selenium		0.77	J	1.7	mg/Kg	6010B
Sodium		86	J	170	mg/Kg	6010B
Vanadium		43		0.83	mg/Kg	6010B
Zinc		83		3.3	mg/Kg	6010B
Mercury		0.047		0.030	mg/Kg	7471A
Cyanide, Total		0.19	J	0.78	mg/Kg	9014
pH		7.40		0.200	SU	9045C
Percent Moisture		45		0.10	%	PercentMoisture
Percent Solids		55		0.10	%	PercentMoisture

Table A10: Results from chemical analysis of sediment core number 389.

Lab Sample ID / Analyte	Client Sample ID	Result / Qualifier		Reporting Limit	Units	Method
500-10601-7	**390**					
Benzo[b]fluoranthene		7.7	J	25	ug/Kg	8270C
Benzo[a]pyrene		5.3	J	25	ug/Kg	8270C
Aluminum		16000	B	26	mg/Kg	6010B
Arsenic		3.8		1.3	mg/Kg	6010B
Barium		180		1.3	mg/Kg	6010B
Beryllium		0.95		0.52	mg/Kg	6010B
Cadmium		0.42		0.26	mg/Kg	6010B
Calcium		11000	B	13	mg/Kg	6010B
Chromium		26		1.3	mg/Kg	6010B
Cobalt		7.5		0.65	mg/Kg	6010B
Copper		21		1.3	mg/Kg	6010B
Iron		25000	B	13	mg/Kg	6010B
Lead		19		0.65	mg/Kg	6010B
Magnesium		4000		13	mg/Kg	6010B
Manganese		710		1.3	mg/Kg	6010B
Nickel		20		1.3	mg/Kg	6010B
Potassium		1500		65	mg/Kg	6010B
Sodium		84	J	130	mg/Kg	6010B
Thallium		0.49	J	1.3	mg/Kg	6010B
Vanadium		31		0.65	mg/Kg	6010B
Zinc		81		2.6	mg/Kg	6010B
Mercury		0.053		0.025	mg/Kg	7471A
Cyanide, Total		0.19	J	0.66	mg/Kg	9014
pH		8.15		0.200	SU	9045C
Percent Moisture		34		0.10	%	PercentMoisture
Percent Solids		66		0.10	%	PercentMoisture

Table A11: Results from chemical analysis of sediment core number 390.

Lab Sample ID Analyte	Client Sample ID	Result / Qualifier		Reporting Limit	Units	Method
500-10601-8	**391**					
Aluminum		6300	B	26	mg/Kg	6010B
Arsenic		4.1		1.3	mg/Kg	6010B
Barium		60		1.3	mg/Kg	6010B
Beryllium		0.43	J	0.52	mg/Kg	6010B
Cadmium		0.17	J	0.26	mg/Kg	6010B
Calcium		5000	B	13	mg/Kg	6010B
Chromium		13		1.3	mg/Kg	6010B
Cobalt		4.8		0.65	mg/Kg	6010B
Copper		9.3		1.3	mg/Kg	6010B
Iron		13000	B	13	mg/Kg	6010B
Lead		7.1		0.65	mg/Kg	6010B
Magnesium		2400		13	mg/Kg	6010B
Manganese		190		1.3	mg/Kg	6010B
Nickel		11		1.3	mg/Kg	6010B
Potassium		530		65	mg/Kg	6010B
Selenium		0.69	J	1.3	mg/Kg	6010B
Sodium		55	J	130	mg/Kg	6010B
Vanadium		19		0.65	mg/Kg	6010B
Zinc		32		2.6	mg/Kg	6010B
Mercury		0.020	J	0.023	mg/Kg	7471A
pH		7.81		0.200	SU	9045C
Percent Moisture		29		0.10	%	PercentMoisture
Percent Solids		71		0.10	%	PercentMoisture

Table A12: Results from chemical analysis of sediment core number 391.

Lab Sample ID / Analyte	Client Sample ID	Result / Qualifier		Reporting Limit	Units	Method
500-10601-9	**392**					
Fluoranthene		20	J	34	ug/Kg	8270C
Pyrene		26	J	34	ug/Kg	8270C
Benzo[a]anthracene		18	J	34	ug/Kg	8270C
Chrysene		16	J	34	ug/Kg	8270C
Benzo[b]fluoranthene		25	J	34	ug/Kg	8270C
Benzo[a]pyrene		12	J	34	ug/Kg	8270C
Indeno[1,2,3-cd]pyrene		15	J	34	ug/Kg	8270C
Dibenz(a,h)anthracene		8.6	J	34	ug/Kg	8270C
Benzo[g,h,i]perylene		17	J	34	ug/Kg	8270C
Aluminum		15000	B	39	mg/Kg	6010B
Arsenic		4.1		1.9	mg/Kg	6010B
Barium		170		1.9	mg/Kg	6010B
Beryllium		0.77	J	0.78	mg/Kg	6010B
Cadmium		0.55		0.39	mg/Kg	6010B
Calcium		13000	B	19	mg/Kg	6010B
Chromium		27		1.9	mg/Kg	6010B
Cobalt		8.7		0.97	mg/Kg	6010B
Copper		20		1.9	mg/Kg	6010B
Iron		23000	B	19	mg/Kg	6010B
Lead		19		0.97	mg/Kg	6010B
Magnesium		4000		19	mg/Kg	6010B
Manganese		540		1.9	mg/Kg	6010B
Nickel		22		1.9	mg/Kg	6010B
Potassium		1600		97	mg/Kg	6010B
Selenium		0.84	J	1.9	mg/Kg	6010B
Sodium		110	J	190	mg/Kg	6010B
Vanadium		34		0.97	mg/Kg	6010B
Zinc		83		3.9	mg/Kg	6010B
Mercury		0.057		0.035	mg/Kg	7471A
pH		8.12		0.200	SU	9045C
Percent Moisture		52		0.10	%	PercentMoisture
Percent Solids		48		0.10	%	PercentMoisture

Table A13: Results from chemical analysis of sediment core number 392.

Lab Sample ID Analyte	Client Sample ID	Result / Qualifier		Reporting Limit	Units	Method
500-10601-10	**393**					
Aluminum		11000	B	26	mg/Kg	6010B
Arsenic		2.3		1.3	mg/Kg	6010B
Barium		140		1.3	mg/Kg	6010B
Beryllium		0.84		0.52	mg/Kg	6010B
Cadmium		0.30		0.26	mg/Kg	6010B
Calcium		5400	B	13	mg/Kg	6010B
Chromium		21		1.3	mg/Kg	6010B
Cobalt		6.4		0.65	mg/Kg	6010B
Copper		17		1.3	mg/Kg	6010B
Iron		14000	B	13	mg/Kg	6010B
Lead		12		0.65	mg/Kg	6010B
Magnesium		2800		13	mg/Kg	6010B
Manganese		300		1.3	mg/Kg	6010B
Nickel		16		1.3	mg/Kg	6010B
Potassium		570		65	mg/Kg	6010B
Selenium		0.55	J	1.3	mg/Kg	6010B
Sodium		70	J	130	mg/Kg	6010B
Vanadium		26		0.65	mg/Kg	6010B
Zinc		38		2.6	mg/Kg	6010B
Mercury		0.038		0.024	mg/Kg	7471A
pH		8.14		0.200	SU	9045C
Percent Moisture		30		0.10	%	PercentMoisture
Percent Solids		70		0.10	%	PercentMoisture

Table A14: Results from chemical analysis of sediment core number 393.

APPENDIX B – ESTIMATE OF NITRATE-NITROGEN LOAD

From the output file taken from the data logger, we know that on November 3, 2008 at 5:00 AM, the concentration of nitrate-nitrogen at the location of the nutrient monitor was 2.201 mg/L. Since data is only recorded once every half-hour, one must assume that the concentration of nitrate-nitrogen remains constant during the time between data recordings. While this assumption is not completely valid, it is reasonable to assume that the concentration does not change significantly enough to impact the overall calculation.

From the pumping station log sheets, we also know that pump #1 was turned 'on' at the very same time (5:00 AM), and allowed to run at 1,210 rpm, resulting in a discharge of 100,000 gal/min. If this discharge is multiplied by the amount of time the pump is allowed to run (in this case, 30 minutes), one can calculate the volume of water being pumped

$$100{,}000\,\frac{gal}{min} \times 30\ min = 3{,}000{,}000\ gallons$$

which can easily be converted into liters

$$3{,}000{,}000\ gal \times 3.785\,\frac{liters}{gal} = 11{,}355{,}000\ liters$$

If this value is multiplied by the nitrate-nitrogen concentration, the mass of nitrate-nitrogen is quickly obtained

$$11{,}355{,}000\ liters \times 2.201\,\frac{mg}{liter} = 24{,}992{,}355\ mg_{NO3-}$$

This process was repeated for each time step that the pumps were in operation, allowing for an estimate of the total load of nitrate-nitrogen being pumped into Boston Bay from the Bay Island drainage district. This value comes out to be 7.2×10^{11} mg (~800 tons) of nitrate-nitrogen.

REFERENCES

108th Congress, 1986. The Water Resources Development Act.

Alexander, R. B., Smith, R. A., Schwarz, G. E., Boyer, E. W., Nolan, J. V., Brakebill, J. W., 2008. Differences in Phosphorous and Nitrogen Delivery to the Gulf of Mexico from the Mississippi River Basin. *Environmental Science & Technology*, Vol. 42, p. 822-830.

Armentrout, D., 2009. Resident of New Boston, Illinois. Personal Contact.

Bates, P. D., De Roo, A. P. J., 2000. A simple raster-based model for flood inundation simulation. *Journal of Hydrology*, Vol. 236, p. 54-77.

Barnes, H. H. Jr., 1967. U.S. Geological Survey, Water Supply Paper 1849. *Roughness characteristics of natural channels*.

Bartos, M. J., 1977. *Classification and Engineering Properties of Dredged Material*. Dredged Material Research Program, Technical Report D-77-18, U.S. Army Engineers Waterway Experiment Station

Beecher, K. D., Kalkhoff, S. J., Schnoebelen, J. D., Barnes, K. K., Miller, V. E., 2001. U.S. Geologic Survey Water-Resources Investigation Report 01-4175. *Water-Quality Assessment of the Eastern-Iowa Basins – Nitrogen, Phosphorous, Suspended Sediment and Organic Carbon in Surface Water, 1996-98*.

Berry, R. F., and D. D. Anderson. 1986. Habitat development applications: lower Pool 5 channel maintenance/Weaver Bottoms rehabilitation plan. Pages 134-139 in M. C. Landin and H. K. Smith, eds. *Beneficial Uses of Dredged Material.* Proceedings of the First Interagency Workshop. Technical Report D-87-1, U.S. Army Engineer Waterways Experiment Station, Vicksburg, MS.

Bhowmik, N. G., Demissie, M., 1989. Sedimentation in the Illinois River Valley and Backwater Lakes. *Journal of Hydrology*, Vol. 105, p. 187-195.

Booth, M. S., Campbell, C., 2007. Spring Nitrate Flux in the Mississippi River Basin: A Landscape Model with Conservation Applications. *Environmental Science & Technology*, Vol. 41, p. 5410-5418.

Boumans, R. M. J., Burdick, D. M., Dionne, M., 2002. Modeling habitat change in salt marshes after tidal restoration. *Restoration Ecology*, Vol. 10 (3), p. 543-555.

Bouyoucos, G. J., 1926. Estimation of the colloidal material in soils. *Science*, New Series, Vol. 64, No. 1658, p. 362.

Brabets, T. P., Conaway, J. S., 2009. U.S. Geological Survey Open-File Report 2009-1237. *Application of the multi-dimensional surface water modeling system at Bridge 339, Copper River Highway, Alaska.*

Brandon, D. L., Lee, C. R., Simmers, J. W., 1996. Environmental Effects of Dredging, *Update: Evaluating Ecosystem Development at Contaminated Dredged Material Placement Sites.* US Army Corps of Engineers, Waterways Experimental Station, Vol. D-96-2, June 1996.

Bray, R. N., 2008. *Environmental Aspects of Dredging*. Taylor & Francis. The Netherlands.

Bruning-Fann, C. S., Kaneene, J. B., 1993. The Effects of Nitrate, Nitrite, and N-Nitroso Compounds on Animal Health. *Veterinary and Human Toxicology*, Vol. 35 (3), p. 237-253.

Bukaveckas, P. A., 2007. Effects of Channel Restoration on Water Velocity, Transient Storage and Nutrient Uptake in a Channelized Stream. *Environmental Science & Technology,* Vol. 41, p. 1570-1576.

Carrivick, J. L., 2006. 2D modeling of high-magnitude outbursts floods: An example from Kverkfjöll, Iceland. *Journal of Hydrology*, Vol. 321, p. 187-199.

Castillo, M. M., Allan, J. D., Brunzell, S., 2000. Nutrient Concentrations and Discharges in a Midwestern Agricultural Catchment. *Journal of Environmental Quality*, Vol. 29, p. 1142-1151.

Cavagnero, P., Revelli, R., 2009. Numerical model application for the restoration of the Racconigi Royal Park (CN, Italy). *Journal of Cultural Heritage*, Vol. 10, p. 514-519.

Chen, Y. H., Simons, D. B., 1986. Hydrology, Hydraulics, and Geomorphology of the Upper Mississippi River System. *Hydrobiologia*, Vol. 136, p. 5-20.

Conaway, J. S., Moran, E. H., 2004. U.S. Geological Survey Open-File Report 2004-1225. *Development and Calibration of a two-dimensional hydrodynamic model of the Tanana River near Tok, Alaska*.

Conley, D. J., Paerl, H. W., Howarth, R. W., Boesch, D. F., Seitzinger, S. P., Havens, K. E., Lancelot, C., Likens, G. E., 2009. Controlling Eutrophication: Nitrogen and Phosphorous. *Science*, Vol. 323, p. 1014-1015.

Crowder, D. W., Diplas, P., 2000. Using two-dimensional hydrodynamic models at scales of ecological importance. *Journal of Hydrology*, Vol. 230, p. 172-191.

Crowder, D. W., Diplas, P., 2006. Applying spatial hydraulic principles to quantify stream habitat. *River Research and Applications*, Vol. 22, p. 79-89.

Damberg, C., Davis, M. M., 1994. Weaver Bottoms Wildlife Habitat Restoration: A Case Study. *WRP Technical Note FW-RS 7.1, May 1994.*

Day, P. R., 1965. Particle Fractionation and Particle-Size Analysis. *In* Methods of Soil Analysis, Part 1. Physical and Mineralogical Properties, Including Statistics of Measurement and Sampling, No. 9 in the Series, Agronomy.

DeWitt, N. T., Flocks, J. G., Reynolds, B. J., 2007. Methods and Data Report: U.S. Geological Survey Data Series 312. *Bathymetric Survey of the Nearshore from Belle Pass to Caminada Pass, Louisiana.*

Dister, E., Gomer, D., Obrdlik, P., Petermann, P., Schneider, E., 1990. Water Management and Ecological Perspectives of the Upper Rhine's Floodplains. *Regulated Rivers: Research & Management,* Vol. 5, p. 1-15.

Doonze, M., 1990. *Shaping the Environment: Pollution and Dredging in the European Community*. DELWEL. The Hague, The Netherlands.

Dutta, D., Alam, J., Umeda, K., Hayashi, M., Hironaka, S., 2007. A two-dimensional hydrodynamic model for flood inundation simulation: A case study in the lower Mekong river basin. *Hydrological Processes,* Vol. 21, p. 1223-1237.

Environmental Systems Research Institute, 2009.

Foyle, A. M., Norton, K. P., 2006. Sediment Loading During the 20th Century in Presque Isle Bay, Lake Erie, Pennsylvania. *Journal of Great Lakes Research,* Vol. 32, p. 697-711.

Fredette, T. J., French, G. T., 2004., Understanding the Environmental Consequences of Dredged Material Disposal: History in New England and Current Perspectives. *Marine Pollution Bulletin*, Vol. 49, p. 93-102.

Furnans, J., Austin, B., 2008. Hydrographic Survey Methods for Determining Reservoir Volume. *Environmental Modelling & Software*, Vol. 23, p. 139-146.

Gayman, W., 1978. Offshore Dredging Study: Environmental Ecological Report. *Ocean Management*, Vol. 4, p. 51-104.

Goolsby, D. A., Battaglin, W. A., Lawrence, G. B., Artz, R. S., Aulenbach, B. T., Hooper, R. P., Keeney, D. R., and Gary J. Stensland, G. J., 1999. *Flux and Sources of Nutrients in the Mississippi–Atchafalaya River Basin: Topic 3 Report for the Integrated Assessment on Hypoxia in the Gulf of Mexico.* NOAA Coastal Ocean Program Decision Analysis Series No. 17. NOAA Coastal Ocean Program, Silver Spring, MD.

Goolsby, D. A., Battaglin, W. A., 2000. U.S. Geologic Survey Fact Sheet 135-00, *Nitrogen in the Mississippi Basin – Estimating Sources and Predicting Flux to the Gulf of Mexico*.

Gore, J. A, Shields Jr., F. D., 1995. Can Large Rives be Restored? *BioScience*, Vol. 45 (3), p. 142-152.

Haag, K. H., Lee, T. M., Herndon, D. C., 2005. U.S. Geological Survey Scientific Investigations Report 2005-5109. *Bathymetry and Vegetation in Isolated Marsh and Cypress Wetlands in the Northern Tampa Bay Area, 2000-2004.*

Herbich, J., 2000. Handbook of Dredging Engineering, 2nd Ed., McGraw Hill, New York, NY.
Herschy, R. W., 2009. Streamflow Measurement 3rd Ed., Taylor & Francis, New York.

Hickman, S., 1994. Improvement of Habitat Quality for Nesting and Migrating Birds at the Des Plaines River Wetlands Demonstration Project. *Ecological Engineering*, Vol. 3, p. 485-494.

Holcombe, T. L., Warren, J. S., Taylor, L. A., Reid, D. F., Herdendorf, C. E., 1997. Lakefloor Geomorphology of Western Lake Erie. *Journal of Great Lakes Research*, Vol. 23, p. 190-201.

Holtschlag, D. J., Koschik, J. A., 2001. U.S. Geological Survey Water-Resources Investigations Report, 01-4236. *A two-dimensional hydrodynamic model of the St. Clair-Detroit river waterway in the Great Lakes basin.*

Hornewer, N. J., Flynn, M. E., 2008. U.S. Geological Survey Open-File Report 2008-1098. *Bathymetric Survey and Storage Capacity of Upper Lake Mary near Flagstaff, Arizona.*

Horng-Guang, L., Chaio-Fuei, O., Jua-Lang, S., 1996. Effects of Flow Velocity Changes on Nitrogen Transport and Conversion in an Open Channel Flow. *Water Research,* Vol. 30, p. 2065-2071.

Huizinga, R. J., 2007. U.S. Geological Survey Scientific Investigations Report 2007-5230. *Two-dimensional simulation of flow and evaluation of bridge scour at structure A-1700 on Interstate 155 over the Mississippi River near Caruthersville, Missouri.*

Huizinga, R. J., 2008. U.S. Geological Surveys Scientific Investigations Report 2008-5194. *Hydrologic analysis and two-dimensional simulation of flow at State Highway 17 crossing the Gasconade River near Waynesville, Missouri.*

Iowa Department of Natural Resources, 2009.

Isenhart, T. M., Crumpton, W. G., 1989. Transformation and Loss of Nitrate in an Agricultural Stream. *Journal of Freshwater Ecology*, Vol. 5 (2), p. 123-129.

Jain, S., 2001. *Open-Channel Flow*. John Wiley & Sons, Inc. New York.

James, W. F., Richardson, W. B., Soballe, D. M., 2008a. Contribution of Sediment Fluxes and Transformations to the Summer Nitrogen Budget of an Upper Mississippi River Backwater System. *Hydrobiologia*, Vol. 598 (1), p. 95-107.

James, W. F., Richardson, W. B., Soballe, D. M., 2008b. Effects of Residence Time on Summer Nitrate Uptake in Mississippi River Flow-Regulated Backwaters. *River Research and Applications,* Vol. 24, p. 1206-1217.

Kalkhoff, S. J., Barnes, K. K., Beecher, K. D., Savoca, M. E., Schnoebelen, D. J., Sardof, E. M., Porter, S. D., Sullivan, D. J., 2000. U.S. Geologic Survey Circular 1210. *Water Quality in the Eastern Iowa Basins, Iowa and Minnesota, 1996-98.*

Karr, J. R. and E. W. Chu, 1999. *Restoring Life in Running Waters: Better Biological Monitoring*, Island, Washington D.C.

Keefe, L., 2005. Earth Building: Methods and Materials, Repair and Conservation.

Keeney, D. R., 2002. Reducing Nonpoint Nitrogen to Acceptable Levels with Emphasis on the Upper Mississippi River Basin. *Estuaries*, Vol. 25 (4b), p. 862-868.

Kemp, J., Brampton, A., 2007. The Development of a Time Trend Analysis Tool for GIS and its Application in the Assessment of Nash Bank, South Wales. *Journal of Hydroinformatics*, Vol. 9, p. 193-201.

Knobeloch, L., Salna, B., Hogan, A., Postle, J., Anderson, H., 2000. Blue Babies and Nitrate-Contaminated Well Water. *Environmental Health Perspectives*, Vol. 108 (7), p. 675-678.

Kress, W. H., Sebree, S. K., Littin, G. R., Drain, M. A., Kling, M. E., 2005. U.S. Geologic Survey Scientific Investigations Report 2005-5040. *Comparison of Preconstruction and 2003 Bathymetric and Topographic Surveys of Lake McConaughy, Nebraska.*

Lai, Y., 2006. *Theory and user manual for SRH-W version 1.1.* Sediment and River Hydraulics – Watershed model, U.S. Bureau of Reclamation.

Laine, A. O., Andersin, A. B., Leiniö, S., Zuur, A. F., 2006. Stratification-Induced Hypoxia as a Structuring Factor of Macrozoobenthos in the Open Gulf of Finland (Baltic Sea). *Journal of Sea Research*, Vol. 57 (1), p. 65-77.

Landers, J., 2008. Halting Hypoxia. *Civil Engineering*, Vol. 78 (6), p. 54-65.

Lane, R. R., Mashriqui, H. S., Kemp, G. P., Day, J. W., Day, J. N., Hamilton, A., 2003. Potential Nitrate Removal from a River Diversion into a Mississippi Delta Forested Wetland. *Ecological Engineering*, Vol. 20, p. 237-249.

Leclerc, M., Boudreault, A., Bechara, J. A., Corfa, G., 1995. 2-Dimensional hydrodynamic modeling – A neglected tool in the instream flow incremental methodology. *Transactions of the American Fisheries Society*, Vol. 124 (5), p. 645-662.

Leming, T. D., Stuntz, W. E., 1984. Zones of Coastal Hypoxia Revealed by Satellite Scanning Have Implications for Strategic Fishing. *Nature*, Vol. 310, p. 136-138.

Lepland, Ai., Bøe, R., Lepland, Aa., Oddbjørn, T., 2009. Monitoring the Volume and Lateral Spread of Disposed Sediments by Acoustic Methods, Olso Harbor, Norway. *Journal of Environmental Management*, Vol. 90, p. 3589-3598.

Linhart, S. M., Lund, K. D., 2008. U.S. Geological Survey Scientific Investigations Map 3051. *Bathymetric Contour Maps for Lakes Surveyed in Iowa in 2006.*

Machesky, M. L., Slowikowski, J. A., Cahill, R. A., Bogner, W. C., Marlin, J. C., Holm, T. R., Darmody, R. G., 2005. Sediment Quality and Quantity Issues Related to the Restoration of Backwater Lakes Along the Illinois River Waterway. *Aquatic Ecosystem Health & Management*, Vol. 8 (1), p. 33-40.

Maa, J. P.-Y., Hobbs, C. H., III, Hardaway, C. S., 2001. A Criterion for Determining the Impact on Shorelines Caused by Altering Wave Transformation. *Journal of Coastal Research*, Vol. 17, p. 107-113.

Marston, J., 2009. Engineer - Bay Island Drainage & Levee District, New Boston, Illinois. Personal Contact.

Martini, P., Carniello, L., Avanzi, C., 2004. Two dimensional modeling of flood flows and suspended sediment transport: The case of the Brenta River, Veneto (Italy). *Natural Hazards and Earth Systems Sciences*, Vol. 4, p. 165-181.

Mastin, M. C., Fosness, R. L., 2009. U.S. Geological Survey Data Series 475. *Bathymetry and Near-River Topography of the Naches and Yakima Rivers at Union Gap and Selah Gap, Yakima County, Washington, August 2008.*

Mays, L. W., 2005. Water Resources Engineering. John Wiley & Sons. Hoboken, NJ.

McCoy, J., Johnston, K., 2001. *Using ArcGIS Spatial Analyst*. ESRI, Redlands, CA.

McDonald, R., Nelson, J., Kinzel, P., Conaway, J., 2005. U.S. Geological Survey Fact Sheet 2005-3078. *Modeling surface-water flow and sediment mobility with the Multi-Dimensional Surface-Water Modeling System (MD_SWMS).*

Merwade, V., Cook, A., Coonrod, J., 2008. GIS techniques for creating river terrain models for hydrodynamic modeling and flood inundation mapping. *Environmental Modelling & Software*, Vol. 23, p. 1300-1311.

Minke, G., 2006. Building with Earth: Design and Technology of Sustainable Architecture.

Mississippi River/Gulf of Mexico Watershed Nutrient Task Force, 2001. *Action Plan for Reducing, Mitigating and Controlling Hypoxia in the Northern Gulf of Mexico.* Washington D.C.

Mississippi River/Gulf of Mexico Watershed Nutrient Task Force, 2004. *A Science Strategy to Support Management Decisions Related to Hypoxia in the Northern Gulf of Mexico and Excess Nutrients in the Mississippi River Basin*. Prepared by the Monitoring, Modeling, and Research Workgroup of the Mississippi River/Gulf of Mexico Watershed Nutrient Task Force, U.S. Geological Survey Circular 1270.

Mississippi River/Gulf of Mexico Watershed Nutrient Task Force. 2008. *Gulf Hypoxia Action Plan 2008 for Reducing, Mitigating, and Controlling Hypoxia in the Northern Gulf of Mexico and Improving Water Quality in the Mississippi River Basin.* Washington, DC.

Mitsch, W. J., Day, J. W., Gilliam, J. W., Groffman, P. M., Hey, D. L., Randall, G. W., Wang, N., 2001. Reducing Nitrogen Loading to the Gulf of Mexico from the Mississippi River Basin: Strategies to Counter a Persistent Ecological Problem. *BioScience*, Vol. 51 (5), p. 373-388.

Mitsch, W. J., Day, J. W., Zhang, L., Lane, R. R., 2005. Nitrate-nitrogen Retention in Wetlands in the Mississippi River Basin. *Ecological Engineering*, Vol. 24, p. 267-278.

Mitsch, W. J., Day, J. W., 2006. Restoration of Wetlands in the Mississippi-Ohio-Missouri (MOM) River Basin: Experience and Needed Research. *Ecological Engineering*, Vol. 26, p. 55-69.

Murthy, V. N. J., 2003. Geotechnical Engineering: Principles and Practices of Soil Mechanics and Foundation Engineering. Marcel Dekker, Inc. New York, NY.

Musser, J. W., 2008. U.S. Geological Survey Scientific Investigations Report 2008-5223. *Evaluation of floodplain modifications to reduce the effect of floods using a two-dimensional hydrodynamic model of the Flint River at Albany, Georgia.*

National Science and Technology Council Committee on Environmental and Natural Resources, 2000. *Integrated Assessment of Hypoxia in the Gulf of Mexico.*

National Research Council, 2008. Mississippi River Water Quality and the Clean Water Act: Progress, Challenges and Opportunities. National Academies Press, Washington DC.

National Resources Conservation Service, 2009.

Odom Hydrographic Systems, 2007. Hydrotrac Installation and Operation Manual, Ver. 2.23, Odom Hydrographic Systems, Inc. New Orleans, Louisiana.

O'Neal, B. J., Heske, E. J., Stafford, J. D., 2008. Waterbird Response to Wetlands Restored Through the Conservation Reserve Enhancement Program. *Journal of Wildlife Management*. Vol. 72 (3), p. 654-664.

Osterman, L. E., Swarzenski, P. W., Poore, R. Z., 2006. U.S. Geologic Survey Fact Sheet 2006-3005, *Gulf of Mexico Dead Zone – The Last 150 Years*.

Phipps, R. G., Crumpton, W. G., 1994. Factors Affecting Nitrogen Loss in Experimental Wetlands with Different Hydrologic Loads. *Ecological Engineering*. Vol. 3, p. 399-408.

Porter, S. D., Harris, M. A., Kalkhoff, S. J., 2000. U.S. Geological Survey Water-Resources Investigations Report 00-4288. *Influence of Natural Factors on the Quality of Midwestern Streams and Rivers.*

Potash & Phosphate Institute, 1999. News & Views – Multi-region (October, 1999). *Hypoxia in the Gulf of Mexico and Fertilizer Facts*.

Rabalais, N. N., Turner, R. E., Justić, D., Dortch, Q., Wiseman, W. J., Sen Gupta, B. K., 1996. Nutrient Changes in the Mississippi River and System Responses on the Adjacent Continental Shelf. *Estuaries*, Vol. 19 (2B), p. 386-407.

Rabalais, N. N., Turner, R. E., Justić, D., Dortch, Q., Wiseman, W. J., 1999. *Characterization of Hypoxia: Topic 1 Report for the Integrated Assessment on Hypoxia in the Gulf of Mexico.* NOAA Coastal Ocean Program Decision Analysis Series No. 15. NOAA Coastal Ocean Program, Silver Spring, MD.

Rabalais, N. N., Turner, R. E., Scavia, D., 2002. Beyond Science into Policy: Gulf of Mexico Hypoxia and the Mississippi River. *BioScience*, Vol. 52 (2), p. 129-142.
Randall, G. W., Mulla, D. J., 2001. Nitrate Nitrogen in Surface Waters as Influenced by Climatic Conditions and Agricultural Practices. *Journal of Environmental Quality*, Vol. 30, p. 337-344.

Renaud, M., 1986. Hypoxia in Louisiana Coastal Waters During 1983: Implications for Fisheries. *Fisheries Bulletin 84*, p. 19-26.

Ribaudo, M. O., Heimlich, R., Peters, M., 2005. Nitrogen Sources and Gulf Hypoxia: Potential for Environmental Credit Trading. Ecological Economics, Vol. 52, p. 159-168.

Roberts, G., Marsh, T., 1987. The Effects of Agricultural Practices on the Nitrate Concentrations in the Surface Water Domestic Supply Sources of Western Europe. *Water for the Future: Hydrology in Perspective* (Proceedings of the Rome Symposium, April 1987). IAHS Publ. no 164.

Robertson, K. R., 2008. *List of Native Trees for Use Along Roadsides in Illinois.* Developed for the Corridors for Tomorrow Project. (November, 2008).

Rogala, J. T., 2009. U.S. Geologic Survey Upper Midwest Environmental Sciences Center. Personal Contact.

Roman, C. T., Garvine, R. W., Portnoy, J. W., 1995. Hydrological modeling as a predictive basis for ecological restoration of salt marshes. *Environmental Management*, Vol. 19, p. 559-566.

Russell, J., 2009. Former resident of New Boston, Illinois. Personal Contact.

Sarretta, A., Pillon, S., Molinaroli, E., Guerzoni, S., Fontolan, G., 2009. Sediment Budget in the Lagoon of Venice, Italy. *Continental Shelf Research*, Article in Press
Saunders, D. L., Kalff, J., 2001. Denitrification Rates in the Sediments of Lake Memphremagog, Canada-USA. *Water Resources,* Vol. 35, p. 1874-1904.

Sawyer, D. E., Jacoby, R., Flemings, P., and Germaine, J.T., 2008. Data Report: Particle Size Analysis of Sediments in the Ursa Basin, IODP Expedition 308 Sites U1324 and U1322, northern Gulf of Mexico. *In* Flemings, P.B., Behrmann, J.H., John, C.M., and the Expedition 308 Scientists, *Proc. IODP,* 308: College Station, TX.

Schnoebelen, D. J., Beecher, K. D., Bobier, M. W., Wilton, T., 1999. U.S. Geologic Survey Water-Resources Investigations Report 99-4028. *Selected Nutrients and Pesticides in Streams of the Eastern Iowa Basins 1970-95*.

Schnoebelen, D. J., McVay, J. C., Barnes, K. K., Beecher, K. D., 2003. U.S. Geologic Survey Water-Resources Investigations Report 03-4085. *Bathymetric Mapping, Sediment Quality, and Water Quality of Lake Delhi, Iowa 2001-02.*
Schoonover, H., Muller, M., 2002. Institute of Agriculture and Trade Policy (IATP) Fact Sheet – *Hypoxia in the Gulf of Mexico: A Growing Problem.*

Seitzinger, S. P., 1988. Denitrification in Freshwater and Coastal Marine Ecosystems: Ecological and Geochemical Significance. *Limnology and Oceanography,* Vol. **33**, p. 702–724.

Shelton, J. M., 2009. U.S. Geological Survey Data Series 315. *Bathymetric, velocity, streamflow, and dissolved oxygen data on the Pee Dee River near Bostick Boat Landing, Florence County, South Carolina, May – August 2007.*

Sherwood, C. R., Jay, D. A., Harvey, R. B., Hamilton, P., Simenstad, C. A., 1990. Historical Changes in the Columbia River Estuary. *Progress in Oceanography*, Vol. 25, p. 299-352.

Silvestri, S., Defina, A., Marani, M., 2005. Tidal regime, salinity and salt marsh plant zonation. *Estuarine, Coastal Shelf Science*, Vol. 62, p. 119-130.

Smith, D. P., Kvitek, R., Iampietro, P. J., Wong, K., 2007. Twenty-nine Months of Geomorphic Change in Upper Monterey Canyon. *Marine Geology*, Vol. 236, p. 79-94.

Smith, M., Thomas, D., Gattie, D., 2003. Agricultural Runoff: Characteristics *In* Stewart, B. A., Howell, T. A., Encyclopedia of Water Science, 2nd Ed., Marcel Dekker, Inc., New York, NY.

Smith, R., 1995. *Bathymetric and Physical Monitoring of the Pilot Project Dredging Site in Funafuti Atoll, Tuvalu.* SOPAC Technical Report 216.

Smith, R. S., 1925. *University of Illinois Agricultural Experiment Station Soil Report No. 29, Mercer County Soils*. Urbana: University of Illinois, 1925.

Sorenson, S. K., Porter, S. D., Akers, K. K. B., Harris, M. A., Kalkhoff, S. J., Lee, K. E., Roberts, L. R., Terrio, P. J., 1999. U.S. Geologic Survey Open-File Report 99-202. *Water-Quality and Habitat Conditions in Upper Midwest Streams Relative to Riparian Vegetation and Soil Characteristics, August 1997. Study Design, Methods and Data.*

Strauss, E. A., Richardson, W. B., Cavanaugh, J. C., Bartsch, L. A., Kreiling, R. M., Standorf, A. J., 2006. Variability and Regulation of Denitrification in an Upper Mississippi River Backwater. *Journal of the North American Benthological Society*, Vol. 25 (3), p. 596-606.

Sturgul, S. J., Kelling, K. A., 2003. Nutrient Best Management Practices, *In* Stewart, B. A., Howell, T. A., Encyclopedia of Water Science 2nd Ed. Marcel Dekker, Inc., New York, NY.

Tafeyi, V., Lane, S. N., Hardy, R. J., Yu, D., 2007. A Comparison of the One- and Two-Dimensional Approaches to Modelling Flood Inundation over Complex Upland Floodplains. *Hydrological Processes*, Vol. 21, p. 3190-3202.

Teledyne RD Instruments, 2006. *StreamPro Quick Start Guide*

Theiling, C., 1998. Important Milestones in the Human and Ecological History of the Upper Mississippi River System. *In* Ecological Status and Trends of the Upper Mississippi River System – A Report of the Long Term Resource Monitoring Program 1998, United States Geologic Survey.

Thein, S. J., 1979. A Flow Diagram of Teaching Texture by Feel Analysis. *Journal of Agronomic Education*, Vol. 8, p. 54.

Thompson, A., Guo, Y., Moin, S., 2008. Uncertainty analysis of a two-dimensional hydrodynamic model. *Journal of Great Lakes Research*, Vol. 34, p. 472-484.

Tomer, M. D., Meek D.W., Jaynes, D. B., Hatfield, J. L., 2003. Evaluation of Nitrate Nitrogen Fluxes from a Tile-Drained Watershed in Central Iowa. *Journal of Environmental Quality,* Vol. (32), 642-653.

Trimble Navigation Limited, 2009. Trimble R8 GNSS Receiver – Datasheet. Trimble Engineering & Construction Group. Dayton, Ohio.

U.S. Army Corps of Engineers, 1996. Users guide to RMA2, Version 4.3. Waterways Experiment Station Laboratory.

U.S. Army Corps of Engineers, 2004. Engineering Research and Development Center (ERDC), Dredging Operations and Environmental Research (DOER) Technical Note. *Predicting Geotechnical Parameters of Fine-Grained Dredged Materials Using the Slump Test Method and Index Property Correlations.* August, 2004.

U.S. Army Corps of Engineers, 2006a. Upper Mississippi River System Environmental Management Program Design Handbook. Ch. 4 – Dredging.

U.S. Army Corps of Engineers, 2006b. Upper Mississippi River System Environmental Management Program Design Handbook. Ch. 9 – Islands, Appendix A – Physical River Attributes.

U.S. Army Corps of Engineers, 2009.

U.S. Department of Agriculture, 1993. Chapter 3 – Examination and Description of Soils *In* USDA Soil Survey Manual

U.S. Department of Agriculture, 2004. *Soil Survey of Mercer County, Illinois.*

U.S. Environmental Protection Agency, 1986. *Quality Criteria for Water 1986: Report 440/5-86-001*. Washington D.C.
U.S. Fish & Wildlife Service, 2009.

U.S. Geologic Survey, 2009. StreamStats,

Venkatramaiah, C., 2006. Geotechnical Engineering, p. 57. New Age International Publishers, New Delhi.

Vitousek, P. M., Aber, J. D., Howarth, R. W., Likens, G. E., Matson, P. A., Schindler, D. W., Schlesinger, W. H, Tilman, D. G., 1997. Human Alteration of the Global Nitrogen Cycle: Sources and Consequences. *Ecological Applications*, Vol. 7 (3), p. 737-750.

Wagner, C. R., Mueller, D. S., 2001. U.S. Geologic Survey Water-Resources Investigations Report 01-4091. *Calibration and Validation of a Two-Dimensional Hydrodynamic Model of the Ohio River, Jefferson County, Kentucky.*

Wagner, C. R., 2003. U.S. Geological Survey Water-Resources Investigations Report 03-4336. *Results of a two-dimensional hydrodynamic model and sediment-transport model to predict the effects of the phased construction and operation of the Olmstead locks and dam on the Ohio River near Olmstead, Illinois.*

Wagner, C. R., 2007. U.S. Geological Survey Scientific Investigations Report, 2007-5263. *Simulation of water-surface elevations and velocity distributions at the U.S. Highway 13 bridge over the Tar River at Greenville, North Carolina, using one- and two-dimensional steady-state hydraulic models.*

White, L., Hodges, B. R., 2005. Filtering the Signature of Submerged Large Woody Debris from Bathymetry Data. *Journal of Hydrology*, Vol. 309, p. 53-65.

White, L., Hodges, B. R., Austin, B. N., Osting, T. D., 2006. Identification of Large Woody Debris from Single-Beam Echo Soundings. *Journal of Hydroinformatics*, Vol. 8 (1), p. 1-12.

Whol, E., Angermeier, P. L., Bledsoe, B., Kondolf, G. M., MacDonnell, L., Merritt, D. M., Palmer, M. A., Poff, N. L., Tarboton, D., 2005. River Restoration. *Water Resources Research*, Vol. 41.

Wilson, G. L., Richards, J. M., 2006. U.S. Geological Survey Scientific Investigations Report 2006-5208. *Procedural Documentation and Accuracy Assessment of Bathymetric Maps and Area/Capacity Tables for Small Reservoirs.*

Windhorn, R., 2001. Eliza Creek – Investigation Conducted. Eliza Creek Watershed Project, USDA, Illinois NRCS.

Wisconsin Department of Natural Resources, 2009.

Wiseman, W. J., Rabalais, N. N., Turner, R. E., Dinnel, S. P., MacNaughton, A., 1997. Seasonal and Interannual Variability Within the Louisiana Coastal Current: Stratification and Hypoxia. *Journal of Marine Systems*, Vol. 12, p. 237-248.

Withgott, J. H., Brennan, S., 2007. *Environment: The Science Behind the Stories*. Pearson Education Inc., San Francisco, CA.

Yang, Z., Sobocinski, K. L., Heatwole, D., Khangaonkar, T., Thom, R., Fuller, R., 2009. Hydrodynamic and ecological assessment of nearshore restoration: A modeling study. *Ecological Modelling*, doi:10.1016/j.ecolmodel.2009.07.011